The Dissertation Committee for Sung Yul Shin certifies that this is the approved version of the following dissertation:

Towards Better Assessment and Training of Kinematics in Post-Stroke Gait Therapy

Committee:

James Sulzer, Supervisor

Ashish D. Deshpande

Kathleen J. Manella

Richard Neptune

Theresa A. Jones

Towards Better Assessment and Training of Kinematics in Post-Stroke Gait Therapy

by

Sung Yul Shin

Dissertation

Presented to the Faculty of the Graduate School of

The University of Texas at Austin

in Partial Fulfillment

of the Requirements

for the Degree of

DOCTOR OF PHILOSOPHY

The University of Texas at Austin

May 2019

Dedicated to my loving wife, Mihyun and my son Joshua Harang

Acknowledgements

I would like to first acknowledge and thank my advisor Dr. James Sulzer for providing opportunity to pursue my research in Rewire Lab at University of Texas at Austin. Through countless discussions on my research and writing experience on grant proposals and publications, I learned how to establish and solve problems from different perspectives and how to efficiently communicate with other research colleagues. I definitely feel lucky that I had a chance to meet and work with him for my PhD study.

I would also like to thank my dissertation committee members for providing valuable feedback on my research. It was my honor to have Dr. Richard Neptune as my committee member who I have always respected and admired. His comments were critical but very helpful to enriched my research. I also had a great time working as a teaching assistant for his Dynamics course for two semesters in Spring 2015 and Fall 2019. I learned how to be an excellent teacher and mentor as a faculty member from him. I would like to express my deep gratitude to Dr. Ashish Deshpande for his course on robot mechanism design and discussions on robotics theory, which helped to establish foundation for the first aim of my research. I am also grateful to Dr. Kathleen Manella and Dr. Theresa Jones for providing valuable comments and suggestions to improve my research from the viewpoints of physical therapist and neuroscientist.

I would also like to express my special thanks to the members of Rewire Lab, especially initial members, Tunc and Ethan, who have started the lab together from scratch. I enjoyed working and discussing with graduate and undergraduate students and researchers at UT which hugely motivated me throughout my graduate career. Also, I would like to thank the therapists, clinicians, staff members and participants from St.

David's Medical Center, Austin, TX who have supportively helped me to collect data for my research.

And finally, I would like to sincerely appreciate my loving wife and son, Mihyun and Joshua, and all my family members in South Korea. Everything was possible through their constant love, support, encouragement and patience until now.

I would like to reiterate the prayer on the gift from Mrs. Neptune to my wife which engraved in my mind and became the motto of my life:

God, grant me the serenity to accept the things I cannot change,
the courage to change things I can,
and the wisdom to know the difference.

Abstract

Towards Better Assessment and Training of Kinematics in Post-Stroke Gait Therapy

Publication No. _____

Sung Yul Shin, Ph.D.

The University of Texas at Austin, 2019

Supervisor: James Sulzer

Gait impairment is common following neurological injury such as stroke. Therapists train patients based on restoring healthy motions, or kinematics, but evidence for training proper kinematics is not well-established. Because the dosage of therapy has not been well quantified, it is unclear what aspects of gait therapy are important, but simply that more therapy is likely better. However, cost restrictions prevent such intensive therapy, incentivizing value-based care. Robotic gait trainers that repetitively train a specific kinematic walking motions can potentially ease the burden on therapists and allow greater patient throughput, improving the value of therapy. Still, the cost of these trainers is only affordable to the wealthiest clinics, leaving them unavailable to the vast majority of stroke survivors. The overall goal of my research is twofold: to show the role of kinematics in gait recovery following stroke, and how these kinematics can be trained in an economical

manner. My first aim focuses on design of an affordable robotic gait trainer that can adapt to an individual's healthy gait pattern. Such a device could make robotic gait training more accessible to new markets including resource-limited hospitals and even patients' homes. My second aim presents development of an online algorithm for producing speed-dependent reference joint trajectories that can be used for general robotic gait training applications. The goals of my third and fourth aims investigate the importance of gait kinematics using a novel longitudinal cohort approach in subacute stroke patients. I quantified the dosage of therapy using a wearable motion capture to find correlates of functional recovery, defined as gait speed. I then questioned whether gait speed was sufficient to define gait recovery, taking an innovative look at how gait quality during this subacute period changes as gait function improves. I expect these aims will justify the importance of kinematics and suggest that wearable sensors can become a valuable tool for monitoring detailed kinematic motion, providing insight for more effective therapy regimens.

Table of Contents

List of Tables

List of Figures

Chapter 1

Introduction

Gait impairment is common following neurological injury such as stroke. Every year there are 790,000 new strokes in the US and approximately two thirds of the survivors have gait impairment [1]. The financial burden of lost productivity and caretaking is $104 billion and projected to rise 129% by 2030 [2]. Medicare reimbursement threshold for total outpatient therapy is $2,040 for both physical therapy and speech-language therapy per year that requires special coding when exceeded, and services exceeding $3,000 require medical review [3]. However, the median annual cost of outpatient therapy alone was $8,629 during the time period of 2001 to 2005 [4], which includes only 20 sessions of physical therapy. This comes at a time when nearly half of Americans are unable to cover a $400 emergency expense [5] and staggering poverty rates persist among the elderly [6], the most likely population to have a stroke [2]. Indeed, uninsured patients and those of lower socioeconomic status have more severe impairments, suggesting a wealth factor in stroke recovery [7], [8]. There is ample literature that shows those with lower incomes have greater risk of morbidity and mortality [9], [10]. *This financial burden and restrictions on insurance reimbursement are substantial problems and reducing the cost of therapy with effective training regimens is a significant need [2]*.

Kinematics is a branch of mechanics that describes the motion of bodies, including human body motions, without considering the forces that cause the motion [11]. Perhaps

the kinematics would be the most detailed way to represent the human movements including gait motion after stroke. Therefore, the central hypothesis of this dissertation is that the kinematics plays an important role in training and characterizing post-stroke gait recovery.

Recent advances in robotics technology have introduced the electromechanical or robotic gait trainer as a potential solution to reduce the burden on clinicians, quantify training and increase the number of patients treated compared to conventional gait therapy [12]. These trainers guide the legs through repetitive, natural gait kinematic motions by physically interacting with the patient. Consensus evidence suggests that such training improves the chance of achieving independent walking and other functional benefits [13], [14]. While robotic gait trainers reduce the physical burden on therapists and allow greater patient output, there exists no evidence showing how such robotic trainers reduce the cost of therapy. This could be due to the relatively sparse proliferation of the devices due to the high capital expenditure involved. For instance, the most successful commercial robotic trainer costs approximately 20% of a large hospital's annual capital expenditures [15] – unaffordable for the approximately 15,000 outpatient clinics in the US [2]. This means that outpatient clinics, where patients spend most time during the recovery process, cannot afford to provide the most helpful technology.

Providing natural, individualized reference walking patterns to account for changes in speed, body features or therapy strategy is an important factor in robotic gait training. For instance, strategies for encouraging voluntary participation into the training such as patient-cooperative, assist-as-needed, or force-field control have been suggested as a key

principle of neurological recovery than passively guiding fixed walking movements [16]–[18]. While these training strategies are all adaptive by nature and allow spatiotemporal variations in gait patterns, they are based on a fixed reference gait pattern without considering changes in walking speed. A number of approaches for providing reference gait patterns reflecting walking speed were proposed [19], [20], but current methods only allow offline adjustments. Thus, providing an online adjustment of reference gait patterns addressing changes in speed would potentially fill the gap to improve both gait function and quality by training with a more ecological walking experience.

Lack of information on effective therapy regimen is another significant barrier to recovery after neurological injury. For instance, the first months following stroke, known as the subacute stage, are the most critical to sensorimotor recovery [1], [21], but this stage is also the least understood. Despite decades of gait rehabilitation, we are still unsure which methods work best. A major hurdle in characterizing recovery in this early stage is obtaining accurate and quantifiable measurements during therapy, a difficult task that can interfere with the patient care regimen. Perhaps because of the lack of detailed outcomes, meta-analyses have been unable to identify any clear trends describing which methods of physical therapy are most effective. In fact, it has been shown that the best predictor of final level of recovery is simply the initial level of impairment of the patient [22]–[24]. Such a finding casts a shadow over exactly what rehabilitation is doing and why its outcomes are so variable from patient to patient. Understanding exactly what happens during therapy and how patients recover could shine a light on this vexing problem.

Other missing information on gait recovery following stroke would be the importance of gait quality. True gait recovery should involve improvements in both functional ability as well as quality of movement in the form of symmetry or natural gait pattern. However, traditional clinical outcomes for measuring gait are mostly focused on functionality (e.g., gait speed), lacking the information on the gait quality, which may lead towards biased assessment of improvements in gait. While the spatiotemporal symmetry has been commonly reported to quantify gait impairment [25], relatively less attention has been paid to joint kinematics. However, joint kinematics, or joint motions, would perhaps better characterize the disturbances in gait quality [26], [27], arguably with greater sensitivity than the spatiotemporal characteristics, because spatiotemporal measures are composed of a combination of joint kinematics. In recent years, limb kinematics, related to the end-effector (i.e., foot) movement in task space, has also been indicated as an important parameter for locomotor function. For instance, Chang et al. suggested that limb kinematics were preferentially conserved over joint kinematics during walking after peripheral nerve injury in cats [28].

Yet measuring kinematics of patients during their hospital stay is challenging due to the limitations on inpatient accessibility and mobility. Typical motion capture technology using cameras in a fixed environment and a lengthy setup time is not conducive to a therapy setting. However, recent technological advances in sensors have led to the increased use of alternative motion sensors [29], [30]. Inertial measurement units (IMUs) are one of the alternative devices that can track kinematics during therapy sessions to quantify the therapy received (see Fig. 1.1). The advantages of IMUs include portability,

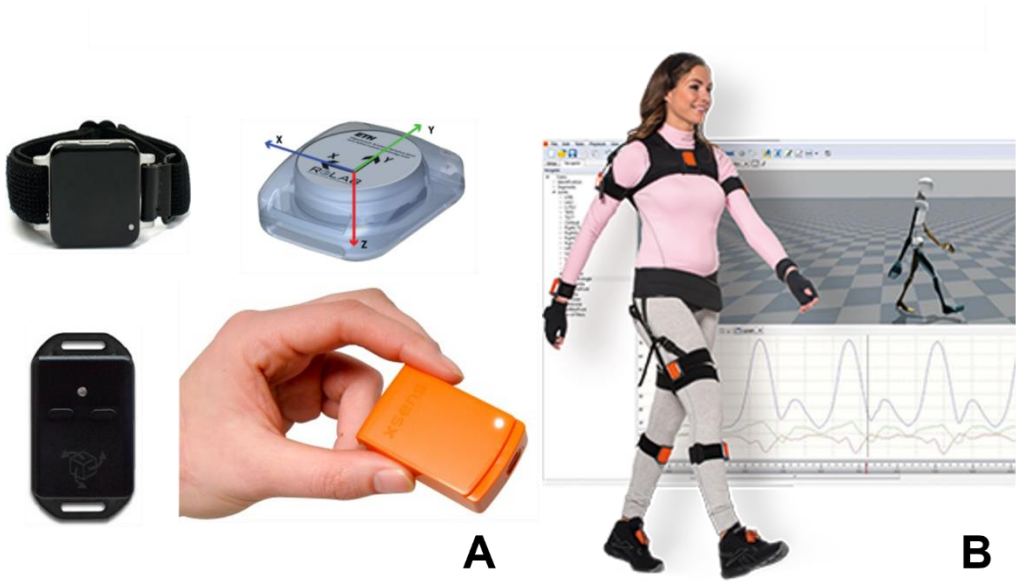

Figure 1.1: Inertial measurement unit (IMU) based motion capture technology. A) Example of commercialized IMU sensor units, B) Capture of a person wearing full body IMU suit with the recording software (XSens, Enschede, The Netherlands). IMUs incorporate accelerometers, gyroscopes and a magnetometer measuring linear acceleration, angular velocity and orientation relative to earth's magnetic field, respectively. By fusing its output, IMUs provide three-dimensional angular motion of individual body segments as well as joint trajectories.

low profile, light weight, and can measure all directions of body segment motions by combining its output of linear accelerations, angular velocities and orientations. Improvements in technology have enabled both research and commercial devices to successfully measure gait kinematics [30]. Using IMUs, we can quantitatively monitor patient activity during therapy unobtrusively with minimal setup time.

My first and second aims focus on further improvement of the currently existing robotic gait trainers in terms of reducing the cost and providing more ecological reference walking experience during the training. The first aim is the design of an affordable, adaptable robotic gait trainer that maintains key therapeutic principles. The second aim is

to establish an online algorithm for producing speed-dependent reference joint trajectories that can be used for general robotic gait training applications. The goals of my third and fourth aims are to explore the importance of gait kinematics in subacute post-stroke recovery. My third aim quantifies the "dosage" of therapy by measuring kinematics and heart rate longitudinally during training in a pilot cohort of subacute stroke patients, correlating these variables with functional gait recovery in the form of gait speed. My fourth aim re-examines this data from the perspective of gait quality to assess the relationship between these gait quality measures and gait speed, and to observe whether these parameters have different recovery timeframes. Here I describe the overview of my specific goals through the following aims:

Aim 1. Design of a single degree-of-freedom, adaptable electromechanical gait trainer for people with neurological injury (Chapter 2)

The cost of therapy is one of the most significant barriers to recovery after neurological injury [2]. Robotic gait trainers move the legs through repetitive, natural motions imitating gait [12]. Recent meta-analyses conclude that such training improves walking function in neurologically impaired individuals [13], [14]. While robotic gait trainers promise to reduce the physical burden on therapists and allow greater patient output, they are prohibitively costly. My novel approach is to design a new single degree-of-freedom (DoF) robotic trainer that maintains the key advantages of the expensive trainers but with a simplified design to reduce cost. My primary design challenge is translating the motion of a single actuator to an array of natural gait trajectories. I address this with an eight-link Jansen mechanism that matches a generalized gait trajectory. I then

optimize the mechanism to match different trajectories through link length adjustment based on nine different gait patterns obtained from gait database of 113 healthy individuals [31]. To physically validate the range in gait patterns produced by the simulation, I tested kinematic accuracy on a motorized wooden proof-of-concept of the gait trainer. The simulation and experimental results suggested that an adjustment of two links can reasonably fit a wide range of gait patterns under typical within-subject variance. I conclude that this design could provide the basis for a low-cost, patient-based electromechanical gait trainer for neurorecovery.

Aim 2. An online transition of speed-dependent reference joint trajectories for robotic gait training (Chapter 3)

Rehabilitation robots reduce the physical burden on therapists, quantify training and allow greater dosage of therapy for individuals with neurological impairments [32], [33]. Robots are also capable of precisely customizing therapy based on the user's physiology and/or needs, for example, customizing a reference trajectory for gait training [19], [20], [31], [34]–[36]. While a number of methods for obtaining reference gait patterns have been proposed, these approaches lack the ability of altering the trajectories according to the varying walking speed in real-time [37]–[39]. The objective of this aim is to develop an online algorithm that can provide a continuous, speed-dependent reference gait pattern for robotic gait training. I employed Fourier series and profile blending methods to generate natural transitions in gait patterns, and synchronized the gait cycle time according to the given arbitrary walking speed. The simulation results suggested that the algorithm can stably change the gait patterns with the given walking speed in a synchronous manner. I

conclude that the method can provide online speed-dependent walking motion that can be used for general robotic gait training applications.

Aim 3. Quantifying dosage of physical therapy using lower body kinematics: a longitudinal pilot study on early post-stroke individuals (Chapter 4)

The first months following neurological injury such as stroke, known as the subacute stage, are the most critical to sensorimotor recovery of locomotor function [1], [21]. Despite the importance of the initial stage, we lack detailed information of the patient experience, likely leading towards sparsely explained variations in outcomes and effects of therapy input. Unlike the pharmacological interventions, the dosage of physical therapy remains unmeasured or unspecified making assessment of its utility exceedingly difficult [23], [40]. While various measurements have been attempted to quantify dosage of therapy [41], kinematics, i.e. joint motions, would be one of the primary indicators of gait impairment arguably with greater sensitivity than traditional clinical outcome measures due to the rich information involved [26], [27]. Here I used a portable, unobtrusive IMU motion capture technology to monitor lower limb joint motions. The objective of this observational pilot study is to examine the role of joint kinematics during therapy over the early stage of recovery. To achieve this, I longitudinally monitored full lower body kinematics and heart rate of six post-stroke individuals from the first inpatient gait therapy session until the 12^{th} week of outpatient therapy. The main functional outcome measure was gait speed recorded during therapy sessions [42]. My main finding indicated that the amount of motion (AoM) extracted from joint kinematics was a better predictor of gait speed than the number of steps, spontaneous recovery (i.e. time), metabolic expenditure

parameterized with heart rate or the types of tasks performed. This result and the additional findings outlined in this study suggest that wearable sensors can become a valuable tool for better understanding dosage of therapy received and the efficacy of rehabilitation training.

Aim 4. Does kinematic gait quality improve with functional gait recovery? A longitudinal pilot study on early post-stroke individuals (Chapter 5)

Gait recovery following neurological injury involves regaining both functional ability as well as quality of movement. However, most clinical outcomes are focused on functional ability such as gait speed [42], timed-up-and-go [43], six minute walk [44], and others. The large focus on functional outcomes may bias therapy towards exaggerating assessments of improvements in gait [41], [45]. Disturbances in gait quality in the form of asymmetry or deviations from a natural gait pattern are major factors in risk of falls [46], greater metabolic expenditure [27], and long term problems such as learned non-use or use-dependent plasticity and pain [47], [48]. However, due to the focus on functional outcomes, there is sparse information characterizing gait quality, and most existing studies report instantaneous measurements on chronic patients; lacking the information of how the gait quality changes over the course of initial recovery. A number of studies have attempted to characterize gait quality after stroke in terms of spatiotemporal characteristics and joint kinematics [27], [49]. In recent years, limb kinematics, related to end-effector movement in task space, are suggested to be an important parameter for locomotor function [28]. The objective of this observational pilot study is to examine changes in gait quality including spatiotemporal, limb and joint kinematic features over the initial stage of recovery by using

portable, unobtrusive IMU motion capture. My first hypothesis is that gait quality will remain asymmetric over the course of early recovery, and the asymmetry will be mainly driven by joint kinematics [27], [28]. Secondly, I expect the impaired side of limb kinematics will preferentially associate with increased gait speed over joint kinematics [28]. This work represents a novel characterization of disturbances in gait quality during the early recovery. The information from this study will justify the importance of gait quality and provide insight for more effective therapy regimens to improve gait quality.

Chapter 2

Design of a single degree-of-freedom, adaptable electromechanical gait trainer for people with neurological injury[1]

2.1 Introduction

The financial burden following neurological injury such as stroke and spinal cord injury is a substantial problem and reducing the cost of therapy is a significant need [2], [4]. Rehabilitation leaders have looked towards robotic technology to help reduce costs, quantify treatment and unload the physical burden to therapists. For instance, the Lokomat, one of the most popular commercialized robotic gait trainers, controls the hip and knee joint motions in the sagittal plane through a pre-specified natural gait trajectory [12]. By attaching to the thigh and shank, the Lokomat, as well as other similar exoskeletal devices (e.g., ALEX, LOPES), use one motor per joint [12], [16], [50]. Other electromechanical gait trainers interact at the foot, similar to an elliptical trainer, known as an end-effector format (e.g., GT I, Haptic Walker, LokoHelp) [51]–[53]. Although not conclusive, a meta-analysis suggested a slight advantage of end-effector based devices over exoskeletons in restoring independent walking after stroke [54].

[1] Portions of this chapter has previously been published in the following article–S. Y. Shin, A. D. Deshpande and J. Sulzer, "Design of a single degree-of-freedom, adaptable electromechanical gait trainer for people with neurological injury," Journal of Mechanisms and Robotics 10(4), 044503, 2018. The author carried out the literature review of the existing robotic gait trainers, and simulated the algorithm and validated with the proof-of-concept model in the cited work.

Robotic gait training has shown significant therapeutic benefits for patients with neurological impairments. For example, improvements have been reported in walking independence and mobility [55], [56], functional walking ability [57], [58], gait speed [59], [60], muscle activation [57], [59] and joint range of motion [60]. Recent meta-analyses on robotic gait training have concluded that it improves the chance of achieving independent walking and locomotor ability after SCI and stroke [13], [14]. Other recent studies indicate that robotic gait trainers are as effective as conventional treadmill training [61]–[63]. However, there exists no evidence showing how such trainers have reduced costs. This could be due to the relatively sparse proliferation of the devices due to the high capital expenditure involved. Specifically, the estimated price of $300,000 for the Lokomat [64] represents up to 20% of the annual capital expenditure of large hospitals [15], meaning that this technology is restricted to only the wealthiest facilities. Given that most of therapy occurs at outpatient clinics without access to such resources, the potential benefits of robotic gait training remain largely unredeemed.

Changes in design can reduce cost. Compared to other movements such as reaching, gait is a highly stereotypical motion that varies between individuals. Instead of multiple actuators, gait motions can be driven by a single actuator. The mechanized gait trainer GT I, one of the pioneering single DoF gait trainers, generates ellipsoid-like movement at the footplate based on a doubled crank and rocker gear system [51]. Another group developed the LokoHelp [53], a single DoF device that moves the ankles, strapped in boots, through a roughly elliptic trajectory. These devices have shown some promising results [58], [65], although they lack ground contact proprioception and a natural gait trajectory. Such

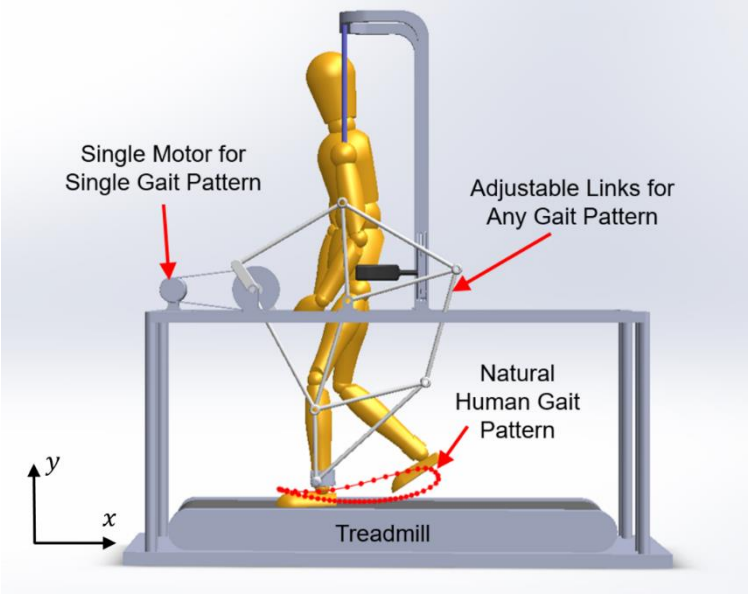

Figure 2.1: Rendering of robotic gait trainer utilizing a single motor to produce a natural gait trajectory. The device can produce adaptable gait patterns by link adjustments.

proprioceptive feedback is fundamental to gait function [66]–[69]. For instance, cutaneous and muscle spindle afferents regulate reflexes and help generate motor output [70]. Thus, reducing cost is important, but should not come at the expense of principles of gait training.

The objective of this work is to design and build an affordable and adaptable end-effector based robotic gait trainer without sacrificing therapeutic benefits of locomotor training. I employ a single actuator to create a natural, individualized gait motion via an innovative mechanical design (see Fig. 2.1). This configuration maintains ground contact offering proprioceptive feedback intended to induce beneficial neuroplastic effects on recovery. The rotation of the actuator is transmitted into a gait-like trajectory using a Jansen mechanism [71], an eight-bar linkage. While this mechanism produces gait-like patterns, they are not individual-specific. The human gait patterns change with different physical

factors such as height, age, speed, and other anthropometric characteristics [19], [31], [72]. An individualized gait trainer must be able to adjust to different gait patterns, and ideally with as few adjustments as possible. I present a solution that minimizes the number of adjusted link lengths to match the different end-effector gait patterns of a database of 113 healthy individuals [31]. I extracted nine canonical gait patterns of different step lengths and determined the minimum number of adjustable links needed to match user trajectories within normal variance. I tested this optimization experimentally using a motorized full-scale model of the trainer. I found that the kinematic accuracy using two link adjustments was sufficient to match these patterns. This design offers the potential for lower-cost, individualized gait training.

2.2. Design

2.2.1. Determination of Reference Gait Pattern

My approach is to generate gait patterns specific to the participant. Gait patterns can vary widely based on factors such as anthropometric characteristics and gait speed [19], [72]. Here I leverage measurements taken from a large database of healthy individuals (113, 63 female) walking at 3.0 km/h on a treadmill [31] to determine the range of gait trajectories that need to be accommodated by the gait trainer. I extracted the sagittal-plane marker position data of the ankle relative to the pelvis, separating into single gait cycles based on heel strike. The single gait cycle trajectories were normalized into 50 time frames and averaged to represent each subject's gait pattern. From all subjects' gait patterns, I

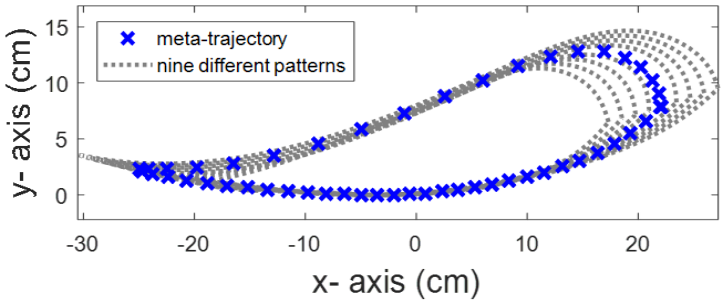

Figure 2.2: Mean of total 113 healthy subjects' gait patterns (meta-trajectory) and total 9 gait patterns with different step lengths in x-y plane (average of 10 subjects for large, medium and small step lengths and their intermediates).

generated the grand mean, called the meta-trajectory, as well as extracted the mean of the 10 individuals with the largest, average and smallest step lengths to represent the range of gait patterns. As the design of the trainer may have non-linearities, I interpolated six additional intermediate patterns to more thoroughly span the manifold, thereby a set of total nine different patterns is determined as reference. Figure 2.2 illustrates the meta-trajectory (blue x) and the nine trajectories (grey dotted lines) calculated from the pool of 113 subjects.

2.2.2 Kinematics

The proposed kinematic solution for reproducing gait patterns at the ankle is based on Jansen mechanism, previously employed in kinetic sculptures [71]. The mechanism (Fig. 2.3) uses eight moving linkages parameterized in 12 different lengths comprising four closed loop components; a pair of upper and lower four-bar mechanisms, $L_1L_2L_3L_4$ and $L_1L_7L_8L_4$, respectively, a coupler, $L_3L_5L_6$, a parallelogram mechanism, $L_6L_8L_9L_{10}$ and a rigid foot-link, $L_9L_{11}L_{12}$. In the application of the gait trainer, my main interest is the end-

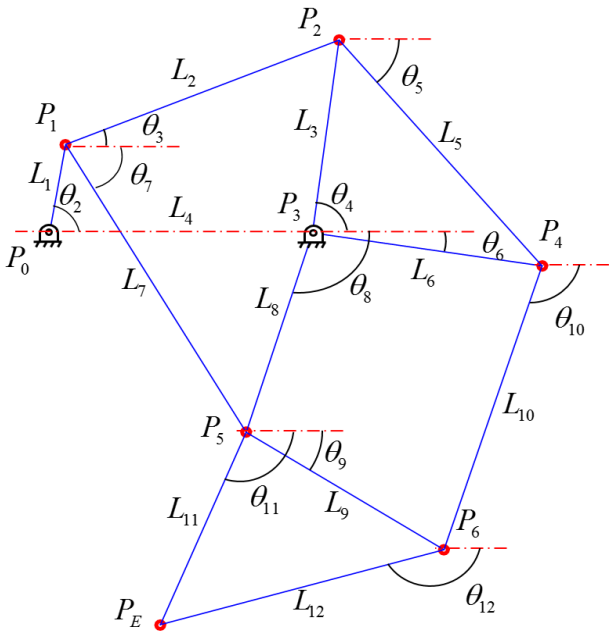

Figure 2.3: Parameterized structure of the proposed mechanism. The end-effector path at P_E is determined based on the angle of the rotary crank, θ_2 and the configuration of 12 links with given lengths.

effector at the rigid foot-link, P_E, the ankle interface (see Fig. 2.1). Motion at P_E can be determined by the configuration of the mechanism with the given input angle of the rotary crank, θ_2 expressed as

$$P_E = f(\theta_2, \Theta, L), \tag{2.1}$$

where $\Theta = [\theta_3, \cdots, \theta_{12}]$ is the vector of unknown joint angles and $L = [l_1, \cdots, l_{12}]$ is the link length vector that incorporates the given 12 lengths of the mechanism.

The vector loop representation, widely used for the motion analysis of mechanisms [73], solves for unknown parameters by creating a vector loop (or loops) around the linkages of the mechanism. With the input angle, θ_2 given at every instant, the end-effector path can be determined by the unknowns solved with the vector loop equations.

2.2.3 Optimization

2.2.3.1 Matching the meta-trajectory

While the motion of the linkage mechanism produces an arbitrary walking pattern, it has not been configured to be a human-like gait pattern. To match the end-effector of the linkage mechanism with natural human gait pattern, I employed optimization technique based on the meta-trajectory. My cost function of the mechanism configuration was formulated as

$$\min_{L} \quad J(L) = \frac{1}{2}\sum_{k=1}^{f}\{p_H(t_k) - p_E(\tau_k, L)\}^2 + |A_H - A_E| \tag{2.2}$$

$$\text{such that } L_{Lower} \leq L \leq L_{upper}$$

where p_H is the reference meta-trajectory, p_E is the end-effector trajectory of the linkage mechanism, A_H and A_E are the area of gait patterns of meta-trajectory and end-effector

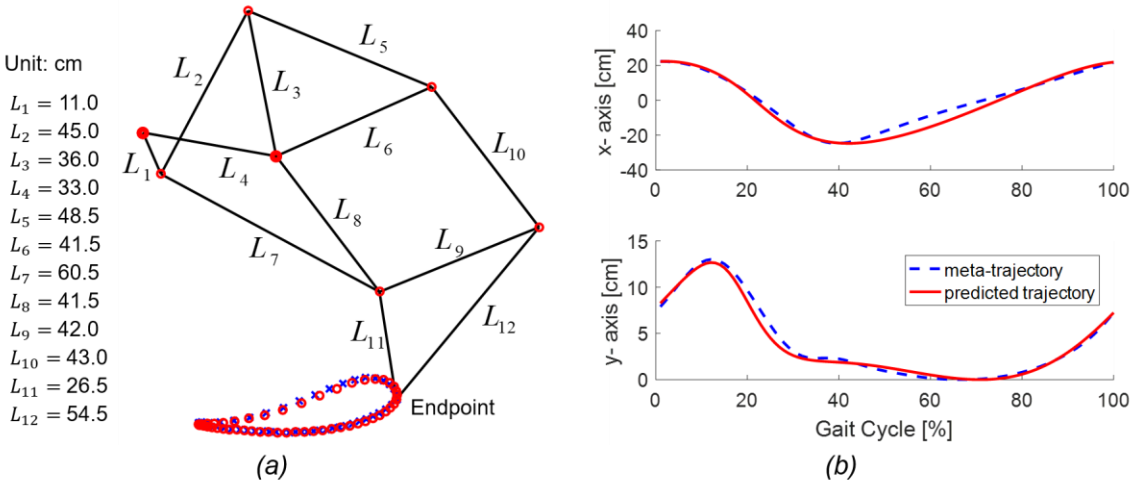

Figure 2.4: Optimized to the meta-trajectory, the structure results in an RMS error of 3.09 cm. *(a)* Blue crosses delineate the meta-trajectory, and red circles show the predicted trajectory. *(b)* Meta-trajectory and predicted endpoint trajectories in gait cycle domain with a constant crank (L_1) input angular velocity.

trajectory in sagittal plane, respectively, L is a link length vector that incorporates all 12 lengths of the mechanism, t_k is the k^{th} time frame and τ_k is the k^{th} time frame that minimizes the error between p_H and p_E. L_{Lower} and L_{Upper} are lower and upper boundary condition vector of the link lengths, respectively.

My goal was to minimize the sum of trajectory and area differences between the reference meta-trajectory and the end-effector of the mechanism within the bounded link lengths, starting from the given initial values. I used Interior point method (IPM) [74] to iteratively perform the optimization as it is one of the most efficient algorithms that solve for linear and nonlinear convex optimization problems. I implemented the IPM approach by using the *fmincon* function in Matlab R2016A (Mathworks Inc., Natick, MA). The resulting configuration is shown in Fig. 2.4.

2.2.3.2 Minimizing link adjustments

The mechanism must not only match an average gait trajectory, but it must also be able to be adjusted to match an array of human gait trajectories. While adjusting all 12 links could flexibly cover the variations in gait patterns, the implementation would be redundant and highly impractical. As such, finding the minimum number of link adjustments will facilitate practical use. Thus, I selected all the combinations among 11 links (except the crank, L_1). For each combination, I optimized for a set of nine different canonical gait patterns (Fig. 2.2) by using the same cost function in Eq. (2.2) based on the three optimized initial estimates (meta-trajectory, largest and smallest patterns, respectively) attempting to scan for the global minima. I calculated the mean root-mean-square-error (RMSE) of nine

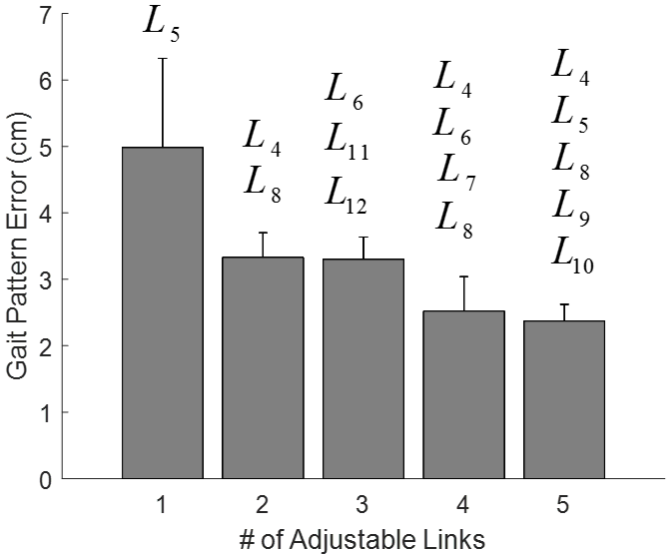

Figure 2.5: Gait pattern error for number of adjustable links. Selected adjustable links are denoted on each bar graph. Adjusting just two links (L_4 and L_8) provides the largest drop in error for the fewest adjustments.

patterns to evaluate each combination. For each set of adjustable links, the error was defined by the minimum value among the mean RMSE of nine different gait patterns of all combinations. Figure 2.5 illustrates the minimum error with selected link combinations resulting from one to five link adjustments. As expected, the results show that the error deceases as number of adjusted links increase. Note that a large drop can be observed at two link adjustments. Although greater error compared to adjustments of more than two links, the data indicate that adjustment of two links at L_4 and L_8 (Fig. 2.3) accounted for approximately 70% of the maximum reduction in trajectory error. Importantly, the average error of 3.33 cm is under typical within-subject variance of 5.02 cm calculated from the gait database. The trajectory error using two link length adjustments is consistent, ranging from an RSME of 2.62 to 3.71 cm in the canonical gait patterns (Fig. 2.6). Thus, the

adjustment of two links (L_4 and L_8) is sufficient to reasonably fit a wide range of gait patterns.

2.3. Evaluation

To physically validate the gait patterns produced by the simulation, I designed and built a motorized proof-of-concept of the gait trainer. I selected three representative gait patterns from the canonical patterns (smallest, average and largest step lengths) and manufactured the linkages based on the output link lengths from the optimization algorithm. Since the primary goal of this work is restricted to kinematic validation of the end-effector path of the device, I determined the required design specification and manufactured the model without considering the dynamic effects of the system and interaction force acting on the device by user.

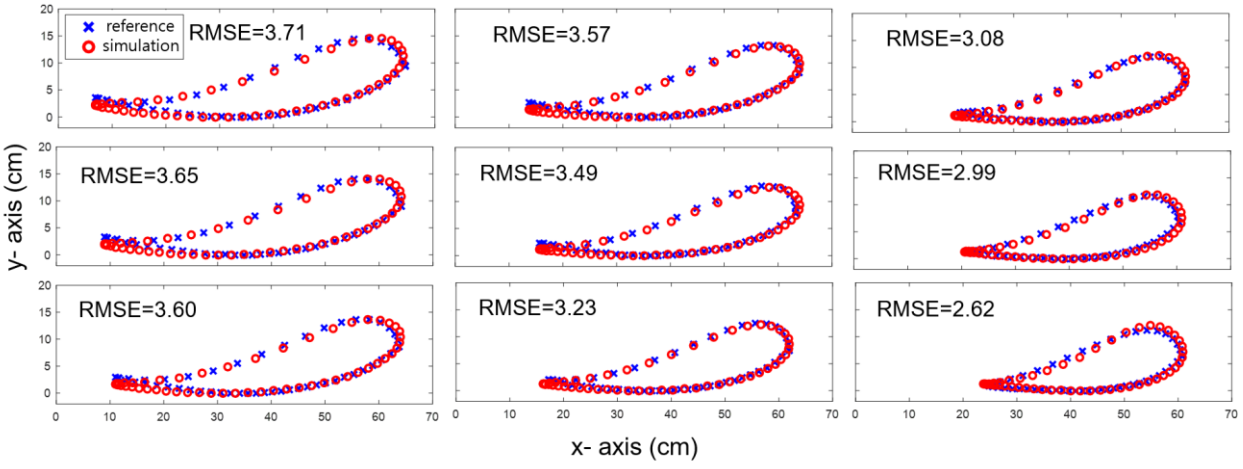

Figure 2.6: The RMS error for each canonical gait pattern given two link adjustments shows consistent performance across patterns, with expectedly larger error in larger gait patterns.

I used a brushless DC servomotor (1.4 kW, Moog Inc., East Aurora, NY) with a gearbox of 5:1 ratio (Apex Dynamics, Inc., Ronkonkoma, NY) and an additional 2:1 gear reduction though a timing belt drive attached to the output shaft. A motor driver (Moog T200) was used to control the motor. A real-time control system, Simulink Realtime, Matlab R2016A and 16-bit data acquisition system (National Instruments, Austin, TX) were used to generate the motor control input at 1kHz. The entire wooden model of the trainer is shown in Fig. 2.7 (left).

A simple velocity feedback controller was achieved with the control input given by

$$u = K(\dot{\theta}_{ref} - \dot{\theta}_a) \tag{2.3}$$

where u is the control input, K is a gain, $\dot{\theta}_{ref}$ is the reference joint velocity input and $\dot{\theta}_a$ is the actual joint velocity of the motor calculated from the encoder. A constant motor velocity (3.1 rad/s) related to the typical gait speed of mildly impaired stroke patients (0.7 m/s) was used as the reference control input. The endpoint path with respect to the world coordinate was recorded with an optical motion capture system in 240Hz (PhaseSpace, Inc., San Leandro, CA). The optical motion capture data was resampled and truncated into a single gait cycle to compare with simulated patterns. Since the purpose of this evaluation was to experimentally validate the kinematic gait patterns from the simulation, I used the simulated patterns as reference and compared with the actual patterns recorded from the model.

Figure 2.7 (right) illustrates the simulation and experimental results of end-effector path for three conditions. The performance of the model well-approximated the simulated gait pattern. It can be seen that the actual gait patterns (black solid line) are qualitatively

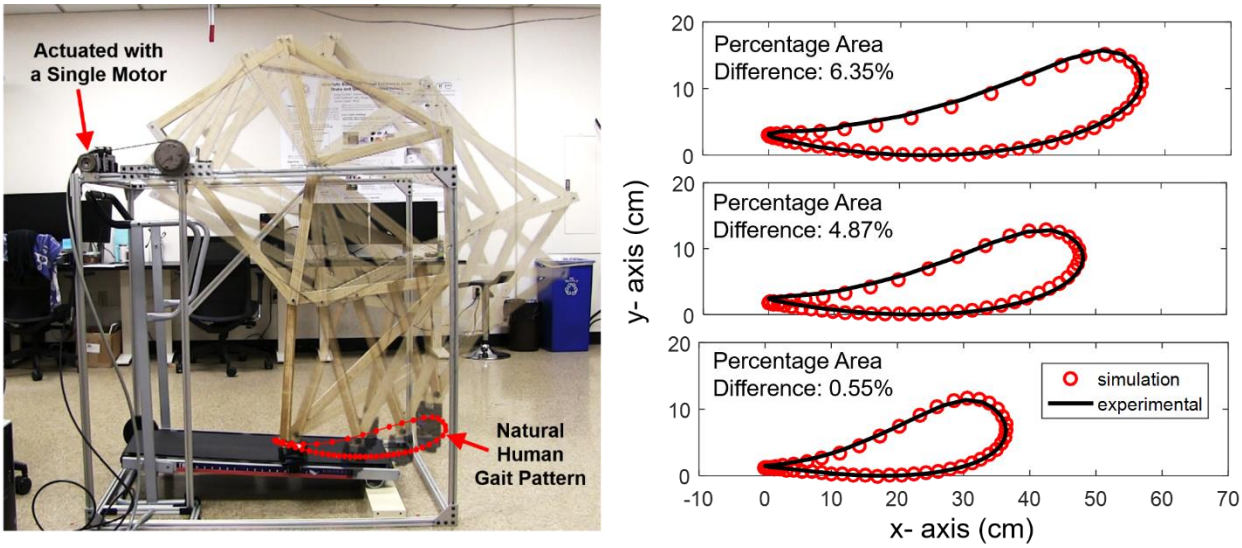

Figure 2.7: (Left) Motorized wooden model of the gait trainer with accompanying range of motion reflecting a natural gait pattern. (Right) Experimental results using optical motion capture system by adjusting link lengths to match with three different step lengths (largest-top, medium-middle and smallest-bottom).

very similar to the reference simulated patterns (red circles) for all three conditions. The spatial pattern at the end-effector (e.g., shape of the gait pattern in x-y plane) is predefined based on the given link lengths. To quantitatively evaluate the spatial accuracy of the gait pattern, I used percentage area difference given by

$$Percentage\ Area\ Difference = \frac{|A_s - A_a|}{A_s} \times 100\% \tag{2.4}$$

where A_s and A_a are the area of simulated and actual gait patterns, respectively. Compared to the reference simulated gait patterns, the percentage area differences translated to 6.35% and 0.55% for the largest and smallest gait patterns, respectively. Ideally, the simulated and actual gait patterns should be exactly the same. However, the experimental error could result from errors in manufacturing. In order to judge the severity of this error, I performed sensitivity analysis by scanning -5 to 5 mm offset from the selected two adjustable link

lengths given by the simulation. Based on the sensitivity analysis, a manufacturing error on both links on the order of ± 1.5 mm would result in 6.35% area difference error, well within manufacturing tolerances of the wooden model.

2.4. Discussion

In this work, I introduced a novel design method for a single DoF, adjustable robotic gait trainer operated by a single actuator. I found that a multi-link planar mechanism can produce natural gait trajectories and with adjusting only two links, the mechanism can fit a wide range of gait patterns. My proof-of-concept full-scale model confirms the results. I conclude that this design is a viable solution towards the ultimate goal of a simplified, patient-based, low-cost gait trainer available to outpatient clinics and possibly at home.

While the Jansen mechanism has been applied to kinetic art, this is the first instance of its use towards human-interactive applications. This linkage has a unique ability to precisely match human gait patterns. I exploited this property and optimized its structure to match a meta-trajectory within the typical variance of gait. However, I do not propose that the Jansen mechanism is the only solution. For example, a recent innovative overground gait trainer uses a single four-bar linkage to induce gait patterns [75]. I compared this design with my own. Compared to the Jansen mechanism, RMSE of the four-bar linkage was substantially larger with two link adjustments (mean RMSE = 6.24 cm compared to 3.33 cm), and this error did not significantly alter with additional link adjustments (minimum RMSE = 5.92 cm). Using inverse kinematics analysis, such error translates to hip and knee angles of approximately 7.1° and 10.6°, respectively, compared

to 2.6° and 3.3° for the Jansen mechanism. Thus, in contrast to the four-bar design, the Jansen-based design produces more accurate gait kinematics, and within normal gait variability.

A key concept introduced with this device is the focus on accurately training natural gait kinematics. While some electromechanical gait trainers with multiple actuated DoF have the ability to match natural gait patterns [12], [16], [76], this functionality is overlooked. The guiding philosophy behind my gait trainer is that inducing proprioceptive input as close as possible to natural gait will be most beneficial for recovery, and there is some evidence to support this sentiment [67], [70]. Thus, training a natural gait trajectory along with inducing ground contact are crucial elements of the design. However, it should be noted that the level of importance in training natural gait trajectories has not yet been systematically investigated. Without this knowledge, therapy could be suboptimal, or even worse, counterproductive, and thus will be the subject of future research.

Another key feature is the projected ease of use. A use case scenario would involve algorithmic estimation of the approximate gait trajectory of the patient based on my gait database, followed by link adjustments by the therapist. Practical use would necessitate the minimum number of adjustments to match a given gait pattern. My challenge was to minimize both, the error in imposed gait pattern and the number of links to adjust. I found that only two links were needed to obtain performance within typical human gait pattern variance. I then confirmed this finding through the development of a full-scale proof-of-concept, which exhibited a maximum pattern error of 6.35%, well within normal gait pattern variance of 15.6% based on my gait database. I believe that adjustment of two links

is a reasonable amount of effort in customizing the device to an individual's gait pattern, and would have a setup time roughly equivalent to other gait trainers.

To drive the wooden model, I used a simple velocity feedback controller without considering any dynamic effects (e.g., gravity, friction) since my primary goal was to merely focus on the kinematic end-effector path of the device as a proof-of-concept. However, the experimental results also showed temporal deviation (Fig. 2.4b). Future optimization could involve taking non-linear dynamics into account, although for this concept I chose to maintain simplicity, and thus my evaluation also used constant velocity. Physical improvements to my model would also help reduce trajectory error, including use of more rigid materials with lower friction bearings.

Maintaining active participation in training is a key tenet of neurological recovery, especially for those further along the recovery spectrum [77]. However, much of the history of robotic gait trainers, including the design in my current form, has focused on trajectory-controlled sagittal plane motion of the hips and knees [12]. As a result, considerable effort has been devoted towards "zero-impedance" controllers [78], [79], pelvic actuation [76], [80], and frontal plane actuation [80], [81]. Similar to other robotic gait trainers such as the Lokomat, my design is limited in its backdrivability due to substantial transmission dynamics. However, efforts can be made to facilitate backdrivability, including mechanical compliance, passive frontal plane DoFs and improved sensing and controls [78]–[80]. Further, due to its end effector-based design, the gait trainer described here does not inhibit pelvic motion. The minimum level of backdrivability necessary for effective training has not yet been effectively identified

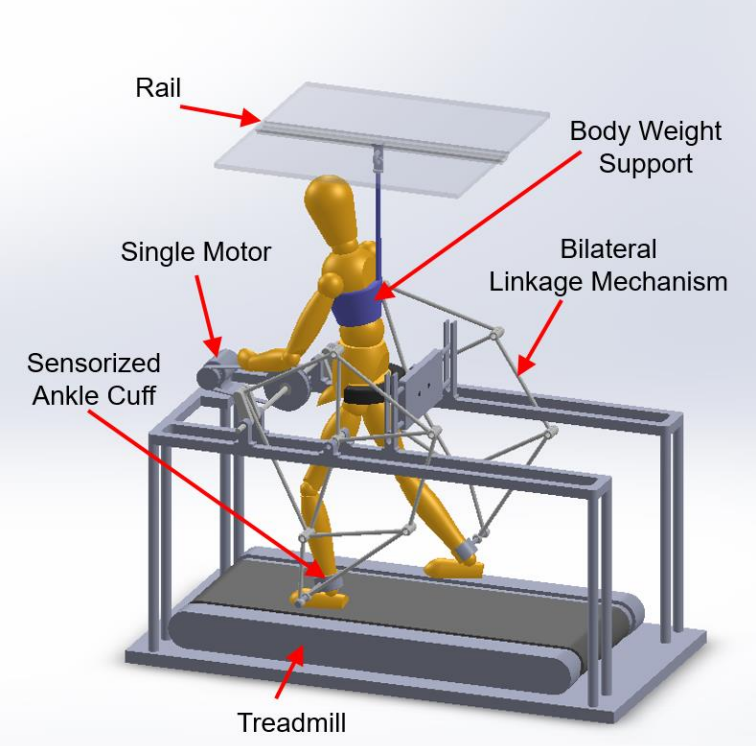

Figure 2.8: Rendering of expected alpha prototype. The design of the gait trainer involves a robust frame with body weight support, a removable pelvic support, a treadmill and the operational linkage mechanism, driven by a DC gearmotor and belt drive.

and likely depends on the patient characteristics such as recovery level and abilities [77]. In summary, the main objective of this work is to make robotic gait training more widely available without reducing the functionality of the current commercial devices. However, future work will continue to make this concept more available to a larger segment of the neurologically-impaired population.

2.5. Conclusions

I have introduced a concept of an individualized electromechanical gait trainer intended to be affordable to outpatient clinics without sacrificing beneficial aspects of gait

training. This concept is enabled by the first human-interactive application of the Jansen mechanism, which uses a single actuator to drive a complex gait trajectory. The optimization of the mechanism additionally provides adaptable gait patterns specific to the user through the adjustments of only two links. This concept will become the basis for a future prototype (Fig. 2.8). The mechanical design of the entire trainer will incorporate components including bilateral linkage mechanism, sensorized ankle cuff interface, removable pelvic support, a single actuator with gear drive and treadmill. I intend on leveraging existing equipment at clinical facilities such as body weight support to avoid redundancy. Future design will facilitate bilateral training using a single DoF through mechanical couplings (e.g. crankshaft) that could be selectively disengaged for unilateral training. An overground, walker-based version is an additional possibility, as illustrated by innovative previous work [75]. Given the relatively large machining tolerances, single actuator and simple control, I intend to further develop a robotic gait trainer that has the potential to be an order of magnitude lower cost than some of the most widely used robotic gait trainers. The reduced cost will make robotic training accessible to new markets including resource-limited hospitals, outpatient clinics, patients' homes and also to many research labs. More access to such beneficial training may result in more intensive therapy and greater compliance with training regimens, ultimately producing better outcomes per patient at lower costs.

Chapter 3

An Online Transition of Speed-dependent Reference Joint Trajectories for Robotic Gait Training

3.1 Introduction

In recent years, robotic gait training has grown in popularity for use on individuals with neurological impairments such as stroke or spinal cord injury [32], [33]. These robotic trainers were developed to reduce burden on therapists, quantify training and increase the number of patients treated compared to conventional gait therapy. For instance, the Lokomat, one of the most popular commercialized trainers, guides repetitive, pre-specified gait motion by physically interacting with the patients [12]. The Lokomat as well as other exoskeletal devices (e.g., ALEX, LOPES) control the hip and knee joint trajectories by attaching to the thigh and shank [12], [16], [50]. Other trainers, known as an end-effector type (e.g., GT I, Haptic Walker, LokoHelp), interact at the foot, similar to an elliptical trainer [51], [52], [65]. Along with the impressive array of robotic devices comes the problem of how to produce natural reference gait patterns for training [19].

Several early methods for obtaining the reference gait patterns include pre-recording trajectories from healthy subjects walking on a treadmill or overground [16], [17], [82], [83], or recording trajectories while walking with the device in a transparent mode [37], [38] or without actuators [12]. Other methods measured patient-specific reference gait patterns by manually assisting patients' legs during walking [37], [38], or

reproduced from the motion of the unaffected limb [39]. Based on the previous findings that the gait parameters are highly associated with walking speed [84], [85], Koopman et al. developed a regression-based algorithm that estimates joint trajectories with the input walking speed and user's height [19]. More recent studies proposed various approaches that predict individual-specific gait patterns by using machine learning techniques based on the gait motion and anthropometric database obtained from healthy individuals [20], [31], [34]–[36].

The ability to smoothly transition to different natural gait patterns online to account for changes in speed or therapy strategy is an important factor in robotic gait training. For instance, evidence suggests that motivating active participation into the training based on the strategies such as patient-cooperative, assist-as-needed, or force field-control is a key tenet of neurological recovery, rather than passively guiding fixed movements with a constant velocity-based control [16]–[18]. While these training strategies are all adaptive by nature and allow online spatial and temporal variations in gait patterns, they were applied on a fixed reference gait pattern without considering changes in walking speed. A number of methods for producing reference gait patterns reflecting walking speed were proposed [19], [20], but current methods only allow offline adjustment of gait patterns. Thus, the addition of an online adjustment for reference gait patterns depending on speed would provide more ecological gait training.

The objective of this paper is to develop an online algorithm that can provide a continuous, speed-dependent reference gait pattern for robotic gait training. My specific target was to smoothly change the reference joint trajectories while synchronizing the

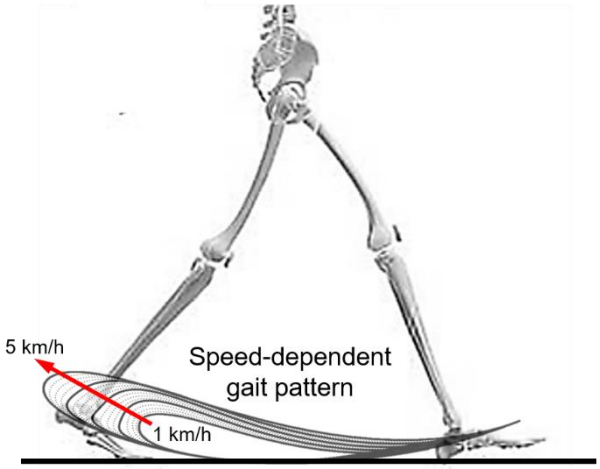

Figure 3.1: Overall goal of the algorithm. The specific target is to produce speed-dependent reference gait patterns in real-time while synchronizing the stance phase of the foot velocity according to the given varying walking speed.

stance phase of the foot velocity according to the given varying walking speed (see Fig. 3.1). To achieve this goal, I first extracted a single gait cycle, reference joint trajectories of discrete speeds from previous work by Koopman et al. [19]. Secondly, I employed Fourier series and profile blending methods to produce spatially and temporally continuous trajectory that interpolates an intermediate point between gait patterns of discrete speeds as a function of normalized time and walking speed. Finally, the stance phase of the foot velocity was synchronized with the given walking speed in real-time based on the gait cycle time estimated by the regression model from a previous study [19]. To validate the proposed algorithm, I simulated changes of gait patterns in two different scenarios with varying walking speed. The simulation results demonstrated that the algorithm can stably produce smooth transition of the joint trajectories in real-time according to the varying

speed in a synchronous manner. I conclude that this method can provide an online speed-dependent reference walking patterns that can be applied to general robotic gait training.

3.2 Methods

3.2.1 Reference Gait Pattern Extraction

A speed-dependent gait prediction algorithm based on a regression model from 15 healthy subjects' data was previously developed and validated by Koopman et al. [19]. This offline algorithm provides time normalized (e.g., 100% gait cycle) reference joint trajectories (including hip flex/extension, abd/adduction, knee flex/extension, and ankle dorsi/plantarflexion) with the input arbitrary walking speed and subject's body-height. I used the predicted joint trajectories from this algorithm as the reference gait patterns. I set my target range of the walking speed to be between 1 and 5 km/h according to the maximum speed limit of the regression model by Koopman et al. [19]. Thus, the joint trajectories of five discrete walking speeds (1, 2, 3, 4, and 5 km/h) were extracted based on the average height of 1.69 m [19], and used them as the reference gait patterns. For the sake of simplicity, I only considered two joints at hip and knee flex/extension in this work. The five reference gait patterns in hip and knee joint plane are illustrated in Fig. 3.3a.

3.2.2 Periodic Joint Trajectory Generation

The next step was to generate a periodic and continuous trajectory as a function of time. To solve this problem, I employed Fourier series to fit each reference gait pattern,

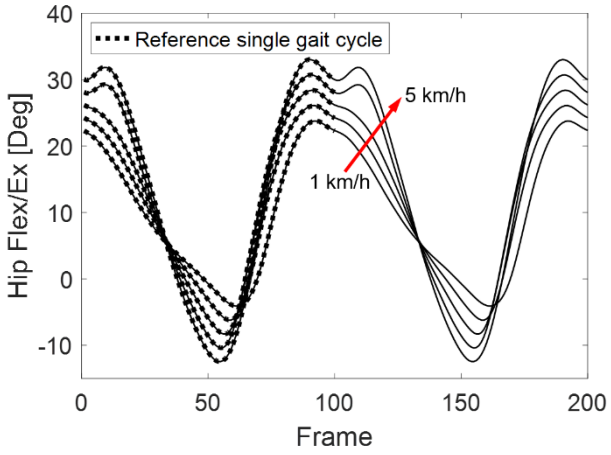

Figure 3.2: Single gait cycle hip flex/extension trajectories of five different walking speeds (dotted lines) and two cycles of the periodic trajectories fitted with Fourier series function (solid line).

similar to the previous gait prediction methods [35], [36]. This method can be used to fit a single gait cycle joint trajectory to a periodic, continuous profile temporally as a function of normalized time frame. For each joint, the Fourier series function was imposed on the i^{th} gait pattern as given by

$$g_i(\tau) = a_{0,i} + \sum_{n=1}^{N} a_{n,i} \cos n\omega_0\tau + \sum_{n=1}^{N} b_{n,i} \sin n\omega_0\tau \qquad (3.1)$$

where $\omega_0 = 2\pi/T$ is the angular frequency, T is the period of gait pattern defined as the normalized final time frame (i.e., $T = 100$), τ is normalized instantaneous time frame, n is the number of sine and cosine functions, i is the walking speed (1, 2, 3, 4, 5 km/h), and $a_{0,i}$, $a_{n,i}$, and $b_{n,i}$ are the Fourier coefficients of i^{th} walking speed. In this work, $N = 10$ sine and cosine functions were sufficient to accurately fit the gait pattern with average root mean square (RMS) difference less than 0.1° (0.03° and 0.05° at hip and knee joint, respectively). It can be observed that the periodic trajectories produced by Fourier series

(solid lines) fit well with the single gait cycle hip flex/extension trajectories (dotted lines) of five different walking speeds (see Fig. 3.2).

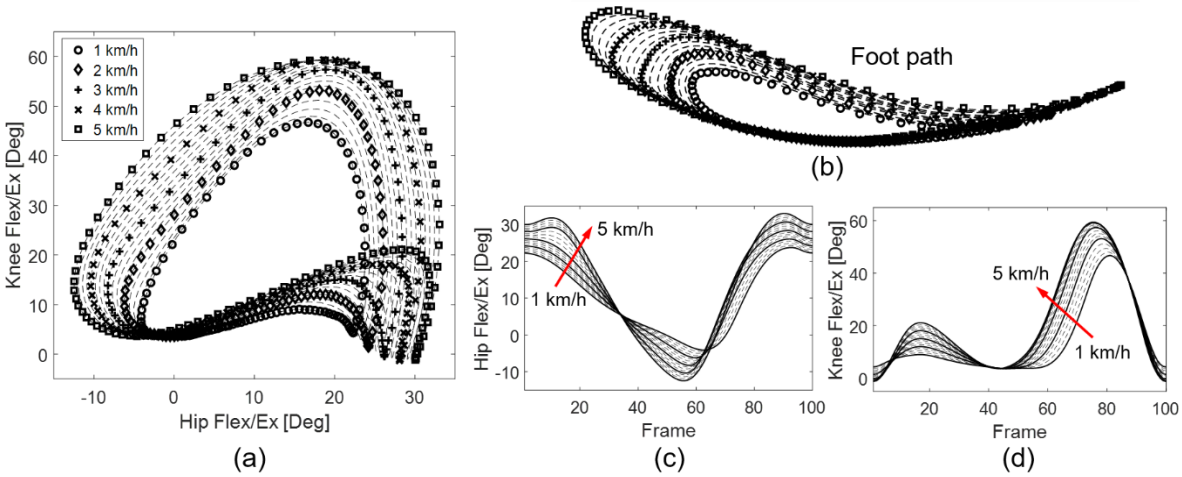

Figure 3.3: Reference gait patterns of 1 to 5 km/h walking speeds (thick markers in (a) and (b), and solid lines in (c) and (d)) overlapped with intermediate gait patterns (dashed lines) produced by the proposed algorithm with speed ratio, r, of 0.25 step, (a) gait patterns in hip and knee flex/extension plane, (b) foot path calculated by imposing joint trajectories to the lower body kinematic model, (c) hip and (d) knee flex/extension joint trajectories in 100% gait cycle.

3.2.3 Speed-dependent Intermediate Gait Patterns

While the Fourier series function generates temporally continuous and periodic trajectory, it does not provide spatial continuity of joint trajectories between different speeds. However, the spatial continuity of gait patterns is another key aspect that is required to achieve the speed-dependent, smooth transition of joint trajectories in real-time. Herein, I describe an approach called profile blending, which is a simple linear combination of two trajectories of different speeds given by

$$g(\tau) = \begin{cases} g_1(\tau), & if\ s < 1 \\ (1-r)g_k(\tau) + r g_{k+1}(\tau), & if\ k \le s < k+1 \\ g_5(\tau), & if\ s \ge 5 \end{cases} \quad (3.2)$$

where $g_k(\tau)$ is the Fourier series function that represents gait pattern of the k^{th} walking speed, s is the given instantaneous walking speed in km/h, k is the integer value between 1 to 4, which indicates reference walking speed in km/h ($1 \le k \le 4,\ \ k \in \mathbb{Z}$), and r is the speed ratio between k and $k+1$, which is defined as the decimal portion of the given online walking speed, s ($r = s - k$). Note that if the given walking speed is between k and $k+1$ km/h, the output trajectory is produced by blending the k^{th} and $k+1^{th}$ gait patterns ($g_k(\tau)$ and $g_{k+1}(\tau)$) according to the speed ratio, r. For instance, if the instantaneous walking speed is given as 2.4 km/h, the algorithm blends 60% of the 2 km/h gait pattern ($g_2(\tau)$) and 40% of the 3 km/h gait pattern ($g_3(\tau)$) to interpolate the intermediate gait pattern of 2.4 km/h. If the given walking speed is below 1 km/h or above 5 km/h, simply the gait pattern of 1km/h or 5km/h is assigned, respectively. As far as the given online walking speed, s, is continuous, which is likely assumption in most walking scenarios, the gait pattern will also be spatially continuous. Figure 3.3 illustrates the intermediate gait patterns with r of 0.25 step overlapped on the reference gait patterns of 1 to 5 km/h walking speeds. The canonical spatial alteration of gait patterns can be observed according to the increased walking speeds between 1 and 5 km/h (dashed lines in Fig. 3.3) with negligibly small average RMS differences of approximately 0.13° and 0.15° at hip and knee joints, respectively, compared to the reference patterns obtained from [19].

3.2.4 Gait Cycle Time Synchronization

The online spatiotemporal transition of speed-dependent gait patterns was produced by the aforementioned Fourier series function and profile blending methods described in the previous subsections. However, the synchronization of the gait cycle time according to the walking speed is not yet achieved, because the Fourier series was imposed on the reference gait patterns with normalized time frame (i.e., 100% gait cycle). Thus, the denormalization to the corresponding gait cycle time is needed to synchronize the gait pattern with the walking speed in terms of absolute time frame. To achieve this, I employed the estimated gait cycle time formula given by

$$CT = 2\sqrt{\frac{SR}{s/3.6}} \tag{3.3}$$

where SR is the step ratio [19], calculated with the linear regression model according to:

$$SR = -0.532 + 0.02 * s + 0.47 * h \tag{3.4}$$

where h is the height of the subject [19]. The estimation of gait cycle time and the coefficients of the linear regression model in Eqs. (3.3) and (3.4) are obtained from [19]. Based on this estimated gait cycle time, the normalized time frame in the Fourier series function was denormalized according to the given walking speed at every instant. This also indicates that the synchronization between the stance phase of foot velocity and the given walking speed is fulfilled.

3.3 Simulation Results

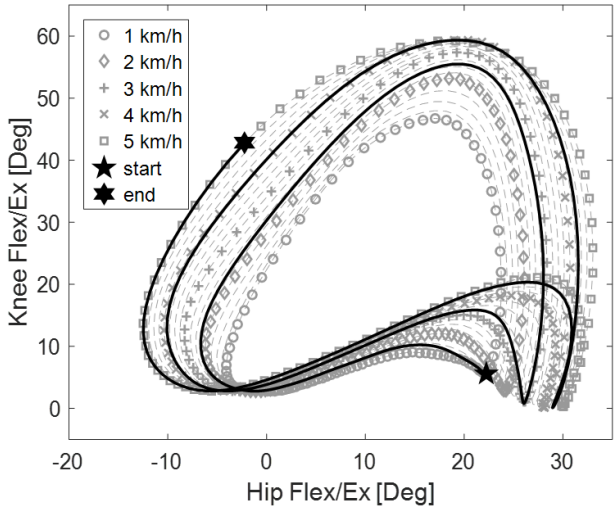

Figure 3.4: The simulation result of Walking Scenario 1. Output joint trajectory (black solid line) on top of reference gait patterns (gray background lines) in hip and knee flex/extension plane. The output trajectory shows smooth and continuous spatial change according to the input walking speed.

The purpose of the simulation was to validate the smooth transition of the reference gait patterns according to the given walking speed in real-time. All simulation algorithms were programmed in MATLAB R2016A (Mathworks Inc., Natick, MA). The spatial and temporal change of gait patterns were evaluated through two different scenarios with arbitrarily given varying walking speeds as described below.

3.3.1 Walking Scenario 1

The first scenario was programmed to demonstrate smooth and continuous transition in gait patterns as speed changes. This was given as a ramp and hold beginning at 1 km/h to 5 km/h in 3 seconds, followed by a 0.3 seconds hold at 5 km/h. Figure 3.4 illustrates the simulation result of output trajectory (black solid line) overlapped on the

reference gait patterns (gray background lines) in the hip and knee flex/extension plane. It can be observed that the algorithm generates smooth and continuous spatial changes in the gait pattern according to the input walking speed.

3.3.2 Walking Scenario 2

The second scenario was planned to evaluate overall spatiotemporal changes as well as the synchronization of the foot velocity with a more complicated varying walking speed. The foot velocity was calculated by imposing the joint trajectories to the lower body

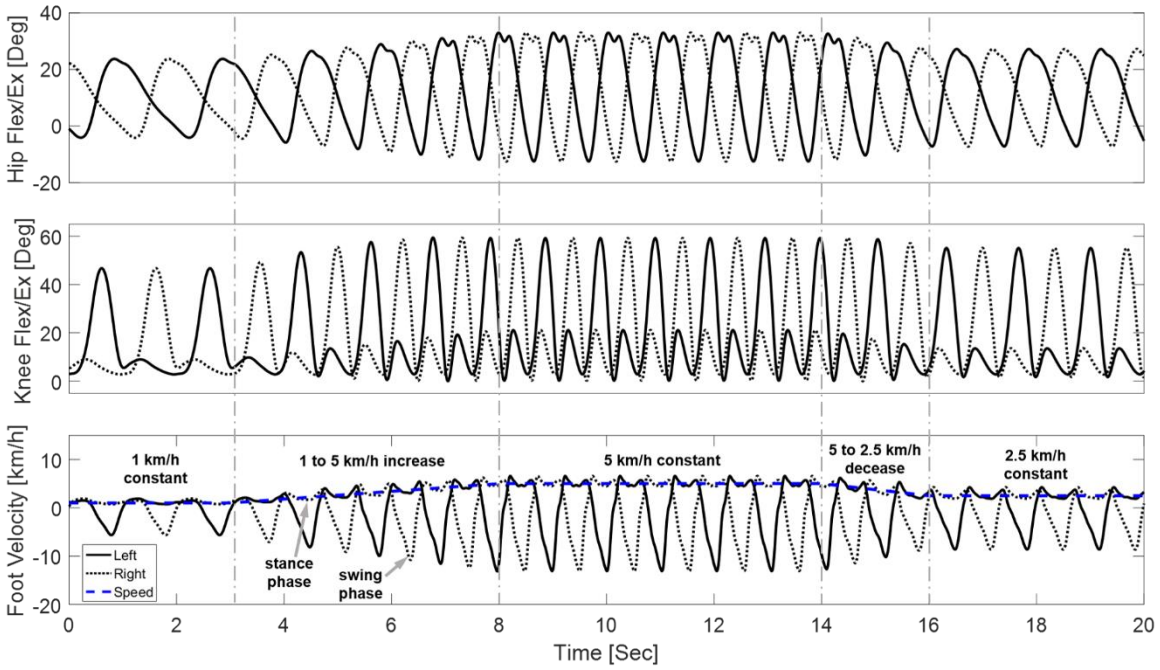

Figure 3.5: The simulation result of Walking Scenario 2. Bilateral (left – solid lines, right – dotted lines) output trajectories of hip (top graph) and knee (middle graph) flex/extension joints, and foot velocities (bottom graph) over time. Note smooth spatial (magnitude in y-axis) and temporal (frequency in x-axis) changes in output trajectories according to the walking speed. The given walking speed (blue dashed line in bottom graph) is overlapped to illustrate synchronicity of stance phase of both foot velocities and varying walking speed.

kinematic model developed with lower limb lengths estimated by body-height [86]. The second walking scenario begins at a constant 1 km/h for 3 seconds, then a ramp up to 5 km/h in a 5 seconds period, followed by a 6 seconds hold at 5 km/h, a ramp down to 2.5 km/h in a 2 seconds period, and finally a 4 seconds hold at 2.5 km/h (see blue dashed line in bottom graph of Fig. 3.5). The output bilateral hip (top graph) and knee (middle graph) flex/extension joint trajectories, and foot velocities overlapped with the given walking speed (bottom graph) in time domain are also shown in Fig 3.5. The trajectories of right side (dotted lines) were calculated by shifting 180° out of phase from the Fourier series function of the left side (solid lines). The smooth and continuous transitions are shown both in hip and knee joint trajectories spatially (magnitude in y- axis) and temporally (frequency in x- axis) according to the given walking speed. It can be also observed that the stance phase of both foot velocities is tracking well with the walking speed (blue dashed line) with mean error of approximately 0.24 km/h.

3.4 Discussion

Providing proper reference joint trajectories to guide natural walking motion is a challenging but fundamental requirement of robotic gait training. In this work, I introduced a novel method for generating online speed-dependent reference gait patterns that can be used for general robotic gait training applications. The major contribution of this work is that the proposed algorithm can generate smooth transitions of reference joint trajectories while synchronizing the foot velocity according to the input varying walking speed (e.g., treadmill speed). The simulation results suggest that the algorithm can become a useful

tool in practice for providing more natural reference walking motions for the robotic gait training as well as other applications such as virtual reality, game programming or animations.

In this work, all ground truth information regarding the reference gait patterns was based on the previously validated prediction algorithm from [19]. According to my simulation results, I found that my algorithm based on reference gait patterns with 1 km/h step can produce reasonably accurate joint trajectories with average RMS difference less than 0.15° compared to those patterns obtained from [19]. This suggests that the proposed method would provide a more realistic walking experience during training of patients with neurological impairments. While only the hip and knee flexion/extension joint trajectories from [19] were demonstrated in this work, this method can easily be expanded to other gait prediction algorithms with additional multi-joints in three dimensional space, provided the canonical gait patterns with different walking speeds.

Another important factor, which is directly related to the safety in robotic gait training, is the synchronization of the foot velocity with the given walking speed. I employed the gait cycle time estimated by the regression model from [19] to obtain time-denormalized joint trajectories, and tested the synchronicity with my lower body kinematic model. According to my simulation results from the second scenario, the mean error between given walking speed (blue dashed line in bottom graph, Fig. 3.5) and calculated foot velocity was approximately 0.24 km/h. This considerable difference may be caused by the prediction error in the regression model [19] and inaccurate anthropometric parameters [86] used for the kinematic model. Despite the error, it can be clearly observed

that the overall trend in the stance phase of the both foot velocities is well synchronized to the given change in walking speed. In future, however, experiment with human subject on a device is needed to validate the practical feasibility of the algorithm for the robotic gait training.

3.5 Conclusions and Future Work

In this work, I introduced a novel approach to establish an algorithm to adapt gait trajectories online based on changes in walking speed. My simulation results showed that the algorithm can generate smooth and continuous transitions between gait patterns according to the varying walking speed in a synchronous manner. I conclude that this algorithm can provide an online speed-dependent reference walking motions that can be applied to general robotic gait training. Future efforts should incorporate anthropometric data into gait pattern estimation and empirically test with human participants.

Chapter 4

Quantifying Dosage of Physical Therapy using Lower Body Kinematics: A Longitudinal Pilot Study on Early Post-Stroke Individuals

4.1 Introduction

The first months following neurological injury such as stroke, known as the subacute stage, are the most critical to sensorimotor recovery of locomotor function [1]. Despite the importance of this initial stage, we lack detailed information of the patient therapy experience, which varies by therapist preference, patients' abilities, and insurance coverage. Meta-analyses suggest that the initial impairment level is the strongest predictor after three months [22], [24]. These results could imply that spontaneous mechanisms dictate recovery, or on the other hand, could imply that our measures of recovery are too coarse to be useful predictors.

Unlike pharmacological interventions, the dosage of physical therapy remains unmeasured or unspecified making assessment of its utility exceedingly difficult [87], [88]. The advent of wearable sensor technology, specifically using accelerometers, has vastly improved our ability to monitor motions in an in/outpatient environment [41], [89]–[91]. In lower limb recovery, the accelerometers were placed on the ankle to track the number of steps during and beyond training sessions [41], [90]. The researchers observed that the number of steps significantly correlated with gait outcome measures [90] and better predicted of functional gait compared to the intensity (heart rate reserve) [41]. While the

number of steps could be an accurate measure of therapy dosage, this finding may also reflect the limitations of the sensor technology. Specifically, with only foot acceleration measured, more detailed information about individual joint motions remain unknown, although are possibly critical to understanding dosage.

Measuring joint kinematics in a clinical environment is challenging due to the limitations on in/outpatient accessibility and mobility. Typical motion capture technology requires a light-controlled, fixed environment and a lengthy setup time. The recent introduction of wireless motion capture based on inertial measurement units (IMUs) provides a flexible, more user-friendly alternative to optical methods [29]. IMUs are portable, low-profile devices composed of accelerometers, gyroscopes and magnetometer measuring linear acceleration, angular velocity and angular orientation relative to earth's magnetic field, respectively. By combining its output, IMUs provide three-dimensional angular motion of individual body segments as well as joint angle trajectories. Recent work has validated the accuracy of these sensors relative to optical motion capture [30]. Importantly, unlike optical motion capture systems, IMUs are minimally obtrusive to therapy with a short setup time and ability to monitor motion within a 20 m radius indoors, making them feasible for inpatient and outpatient studies.

The objective of this observational pilot study is to examine the role of joint kinematics during therapy over the early stage of recovery. To achieve this, I longitudinally monitored full lower body kinematics and heart rate of six post-stroke individuals from the first inpatient gait therapy session until the 12^{th} week of therapy in an outpatient setting. Amount of motion (AoM), the total joint displacements measured from IMU sensors, was

used as our primary dosage of therapy feature. My main functional outcome measure was gait speed recorded during therapy sessions. I expected to find joint motions would be better predictors of recovery than number of steps due to the richer data provided. I also expected to find that training with greater focus on the impaired side would be associated with greater functional improvements [92].

To our knowledge, this work is the first longitudinal study measuring full lower body kinematics during physical therapy sessions on subacute post-stroke individuals. The information gleaned from this study will provide a more nuanced picture of post-stroke recovery during the early stage, leading towards better predictors and an improved understanding of the benefits of physical therapy.

4.2 Methods

4.2.1 Patients

I recruited nine individuals with subacute stroke (<1 month) to participate in this study in accordance with the University of Texas Institutional Review Board and St. David's Medical Center located in Austin, TX. Among nine patients, six individuals were longitudinally monitored for a total of 59 one-hour physical therapy sessions consisting of gait and non-gait activities. Individuals ranged in age and impairment level (see Table 4.1). Inclusion criteria of this study were: ischemic cerebral infarction based on MRI data, hemiparesis, premorbidly independent, within two weeks following injury or as soon as able to participate in gait training determined by the physical therapist. Exclusion criteria

Table 4.1: Demographics and clinical characteristics of participants.

Patient #	P1	P2	P3	P4	P5	P6
Age (years)	61	59	68	68	52	27
Sex	M	M	M	M	F	M
BMI (kg/cm^2)	29.6	25.8	28.7	28.2	25.8	40.5
Affected side	L	L	R	R	L	R
1^{st} recording after admission (days)	15	5	6	7	20	31
Recordings (sessions)	12	7	11	5	12	12
Ankle foot orthosis (used sessions)	-	6	11	-	-	12
Assistive device (used sessions)	1	7	3	5	10	11
Baseline impairment (admission motor FIM score)	18	26	31	22	22	16

BMI – body mass index, FIM – functional independence measure, M – male, F – female, L – left, R – right

include cerebellar damage, prior stroke, stroke-related pain syndromes, or functionally relevant neuromuscular impairments.

Participants were allowed to use any assistive devices including wheelchair, body weight support, walker, cane or ankle foot orthosis (AFO) during sessions if necessary (see Table 4.1). Prior to the first session, the experimenter and therapist explained all the experimental procedures and obtained informed consent. I began monitoring therapy as soon as patients were capable of beginning gait therapy, i.e. as soon as the patients were able to stand with therapist's assistance and ready for walking. Three participants did not complete the full dataset; one participant did not complete the full 12 therapy sessions due to discharge to a different hospital (P2), one could only complete 11 sessions due to lack of insurance coverage (P3), and one was discharged to home therapy (P4). Three participants were excluded from the dataset because two of them were not able to walk before discharge and one discharged before the recording session.

Figure 4.1: Capture of a patient receiving conventional physical therapy while wearing IMU and heart rate (underneath t-shirt) sensors.

4.2.2 Experimental Setup and Protocol

My goal was to consecutively monitor conventional physical therapy sessions with minimal intrusion. I targeted a maximum 12 recording sessions over the course of the first three months throughout the inpatient to outpatient phases. My recording session frequency was greater in the earlier stages of recovery, i.e. two/week for three weeks, one/week for four weeks, then one every other week. For each session, I attached seven commercial IMU motion sensors (XSens, Enschede, The Netherlands) on the pelvis and bilaterally on thighs, shanks and feet. IMUs provide three-dimensional angular motion of each body segment at a sampling rate of 60Hz. Patients also donned a heart rate monitor (Polar Electro, NY) on

the chest to record heart rate sampled at 1 Hz. Data was transmitted wirelessly to a commercial Latitude E5470 laptop (Dell, TX).

The total setup time took approximately 10 to 20 minutes. All setup was performed immediately prior to the normally scheduled physical therapy sessions. After donning sensors, participants were asked to maintain a straight standing position for five seconds to calibrate the system. Therapist assistance was provided for this calibration as necessary. Further recalibrations of the system were conducted during the therapy session if sensor drift was detected. Following calibration, patients performed typical 1-hour training under the supervision of a physical therapist (see Fig. 4.1). The experimenter used a cart to follow the patient and therapist to maintain wireless communication of sensor signals. The experimenter noted all therapy activities. Altogether, the setup time and donning the sensors provided minimal disruption to the typical therapy regimen. Each therapy session incorporated a number of tasks aside from overground walking and body weight supported treadmill training. Sessions included activities of daily living such as transferring to wheelchair and stair climbing, strengthening activities such as an exercise bike and weight bearing, as well as coordination activities such as stepping and balancing. After the session, all sensors were removed from the patient.

4.2.3 Feature Extraction and Outcomes

For each session, all features of therapy dosage and gait outcome measures were extracted from the recorded joint kinematics and heart rate data. Custom software was written in MATLAB (Mathworks, Inc. R2016a, Natick, MA) to calculate the features and

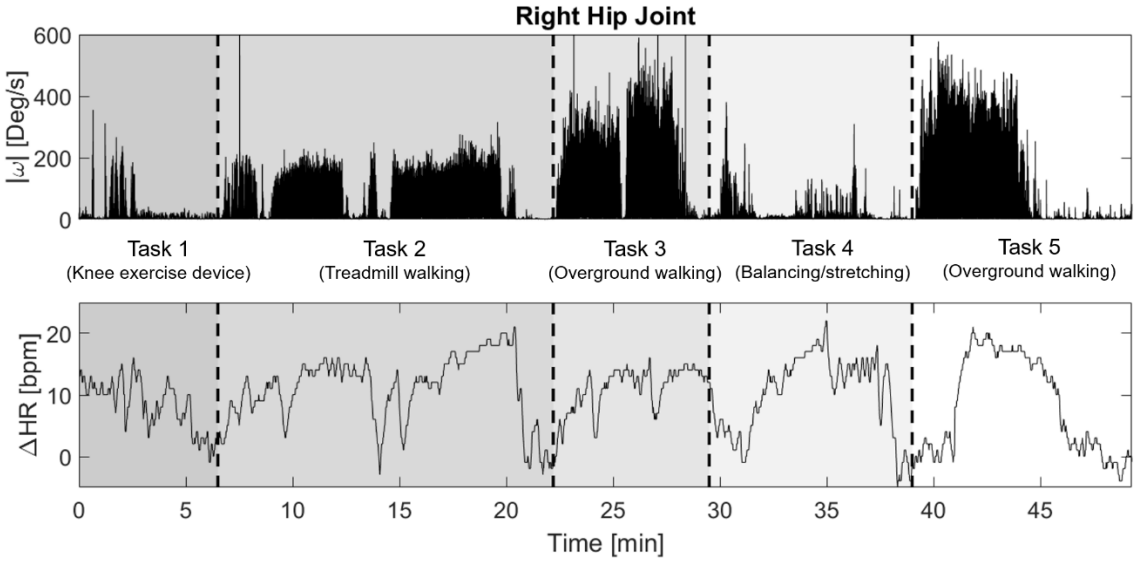

Figure 4.2: Absolute angular velocity, |ω|, at right hip joint obtained from IMU sensors (top graph) and heart rate change, ΔHR, from baseline (bottom graph) during a 1-hour physical therapy session.

outcomes. Figure 4.2 shows an example of recorded data including absolute angular velocity of right hip joint and heart rate change from baseline over a whole 1-hour physical therapy session. IMU data incorporated three-dimensional orientations of all lower body segments as well as joint angle trajectories. Sensor data and notes taken by the experimenter were used to extract the features of therapy dosage and the gait outcomes as described below.

I categorized the features of dosage into amount, intensity and variability consistent with the previous works [41], [93]. The amount was defined in two different ways: the number of steps and the amount of motion (AoM). The number of steps was measured by counting the heel strike events of each foot during the walking portion [94]. AoM was defined as the total angular displacement measured from IMU sensors. AoM at each

individual joint was calculated with the integration of absolute angular velocity at each joint over whole 1-hour session including both gait and non-gait tasks as given by

$$AoM_i = \int_0^T |\omega_i(t)|dt \tag{4.1}$$

where $\omega_i(t)$ is the angular velocity of ith joint, T is the final time of the session, and i represents each joint motion. The joint motions of interest included all three rotations of the pelvis and hip, as well as knee flexion/extension and ankle dorsi/plantarflexion and were defined as individual AoMs. The total AoM was defined as the sum of all joint AoMs. The total AoM was additionally partitioned in gait and non-gait periods (AoM_G and AoM_{NG}, respectively) and by unaffected (AoM_{US}) and affected (AoM_{AS}) sides. Intensity was estimated by the change in heart rate (ΔHR) determined by average heart rate during therapy from the baseline heart rate during rest before the session [95], [96]. Variability was defined as number of tasks performed during the session recorded by the experimenter. Each session was composed of various tasks depending on the patient's ability and therapist's discretion.

The increased gait speed in patients with stroke is known as highly correlated with improvements in functional recovery [42]. Thus I selected gait speed as the main functional outcome measure [41], [93]. In each session, I extracted a portion of therapy with normal, straight walking at a comfortable speed. I then obtained joint angle trajectories and truncated them into single gait cycles from heel strike to heel strike of the left foot [94]. The average distance and time taken by each gait cycle in the sample were extracted by using the lower body kinematic model with the lower limb lengths estimated by the

anthropometric data based on height [97]. The average gait speed was then calculated by dividing average distance by the time taken by each gait cycle.

4.2.4 Statistical Analysis

R version 3.4.1 (2017 The R foundation for Statistical Computing) was used for the statistical analysis. Linear mixed regression model was used to test the relationship between features of therapy dosage and average gait speed as a gait performance measure with significance level, $\alpha = 0.05$. All features of dosage including AoM (total, partial or individual), step number, ΔHR, number of tasks performed were standardized and used as fixed effects and the subject was used as random effect of the mixed model. For the evaluation of better or best indicator of gait performance, I used comparison tools for mixed model including Akaike information criteria (AIC), Bayesian information criteria (BIC) and coefficient of determination (R^2) [98]. To compare the difference in AoM between unaffected and affected sides, I used paired t-test with significance level of $\alpha = 0.05$.

4.3 Results

4.3.1 Overall Dosage of Therapy

I first examined how the extracted features representing therapy dosage correlate with gait speed. Figures 4.3A and 4.3B illustrate changes over time in features of therapy dosage and the functional outcome, gait speed, respectively, for all six patients. I used linear mixed regression models on these data for the statistical analysis. The results

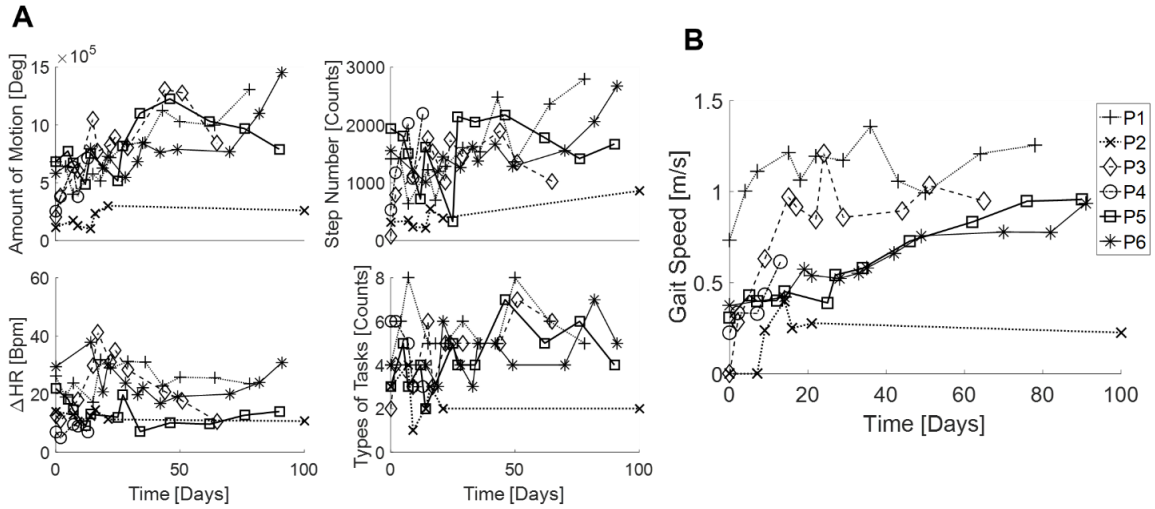

Figure 4.3: A Changes in features of therapy dosage over time (top left) total amount of motion, (top right) step number, (bottom left) average change in heart rate from baseline, (bottom right) types of tasks performed. B Changes in outcome measure of average gait speed over time.

indicated all the independent variables were significantly correlated with gait speed, including total AoM (p<0.01), step number (p<0.01), types of tasks performed (p<0.01), ΔHR (p<0.05), and time (p<0.01). According to the goodness-of-fit measures, total AoM (R^2 =32.1%) revealed the greatest explained variance followed by time (R^2 =15.5%), step number (R^2 =14.1%), types of tasks performed (R^2 =8.0%) and ΔHR (R^2 =5.8%) with consistent trends in AIC and BIC (smallest AIC and BIC for total AoM and greatest for ΔHR). These results are summarized in Table 4.2.

4.3.2 Amount of Motion during Gait and Non-Gait Periods

I divided AoM into gait (AoM_G) and non-gait (AoM_{NG}) portions for each whole 1-hour therapy session to analyze the differential effects of gait on recovery. On average, 45.5% of the duration of the therapy session was dedicated to gait training, and 75.3% of

Table 4.2: p-values and goodness-of-fit measures of linear mixed models with features of therapy dosage and average gait speed.

	Fixed Effects	β [95% CI]	R^2	AIC	BIC
Dosage of therapy features	AoM_{Total}	0.534 [0.366, 0.703]***	32.1%[a]	105.9	114.3
	$Time$	0.413 [0.276, 0.549]***	15.5%	108.9	117.2
	$Steps$	0.374 [0.196, 0.552]***	14.1%[a]	121.6	129.9
	$Tasks$	0.275 [0.083, 0.468]**	8.0%	129.6	137.9
	ΔHR	0.237 [0.003, 0.470]*	5.8%	133.4	141.8
AoM during gait and non-gait period	AoM_G	0.473 [0.305, 0.641]***	24.9 %[a]	111.3	119.6
	AoM_{NG}	0.097 [-0.085, 0.279]	0.8 %	136.4	144.7
	AoM_G AoM_{NG}	0.507 [0.343, 0.671]*** 0.173 [0.029, 0.318]*	32.1 %[a]	107.5	117.9

AoM_{Total} – total amount of motion, ΔHR– heart rate change, AoM_G – amount of motion during gait, AoM_{NG} – amount of motion during non-gait, CI – confidence interval, AIC – Akaike Information Criterion, BIC – Bayesian Information Criterion, *** $p<0.001$, ** $p<0.01$, * $p<0.05$

[a]Note that models with AoM_{Total} and *AoM* with both gait and non-gait portions (AoM_G and AoM_{NG}) best represent the data as opposed to *AoM* during gait only (AoM_G) and step number.

the total AoM during a therapy session occurred during walking. Table 4.2 shows the results of models with AoM_G and AoM_{NG}. AoM_G demonstrated a significant association with gait speed (p<0.01) whereas AoM_{NG} alone did not (p=0.29). However, the model including both AoM_G and AoM_{NG} showed both parameters significantly correlated with gait speed (p<0.01 for AoM_G and p<0.05 for AoM_{NG}). Further, the variance accounted for the latter model (32.1%) was higher than AoM_G alone (R^2 =24.9%) and AoM_{NG} alone (R^2 =0.8%). I also compared AoM_G alone with step number. While they both revealed significant associations with gait speed (both p<0.01), the variance explained by AoM_G (R^2 =24.9%) was greater than step number (R^2 =14.1%). Additional correlation analyses demonstrated stronger association between AoM_G and step number (r = 0.93) than total AoM with step number (r = 0.83).

Table 4.3: p-values and goodness-of-fit measures of linear mixed models with partial and individual AoMs and average gait speed.

	Fixed Effects	β [95% CI]	R^2	AIC	BIC
AoM of US/AS	AoM_{US}	0.536 [0.364, 0.708]***	32.9%	106.9	115.2
	AoM_{AS}	0.503 [0.337, 0.668]***	27.8%	107.9	116.2
AoM of individual joints at pelvis	$AoM_{Pel,tilt}$	0.531 [0.343, 0.718]***	30.6%	111.1	119.4
	$AoM_{Pel,oblq}$	0.500 [0.319, 0.681] ***	27.4%	112.1	120.4
	$AoM_{Pel,ro}$	0.429 [0.234, 0.623] ***	19.0%	120.2	128.5
AoM of individual joints at US	$AoM_{hip,abd}$	0.547 [0.371, 0.723] ***	31.2%	106.9	115.2
	$AoM_{hip,ie}$	0.383 [0.184, 0.583] ***	16.5%	124.0	132.3
	$AoM_{hip,fe}$	0.457 [0.266, 0.647] ***	24.8%	117.8	126.2
	$AoM_{knee,fe}$	0.509 [0.353, 0.665] ***	29.2%	104.5	112.8
	$AoM_{ankle,pdf}$	0.470 [0.301, 0.639] ***	24.1%	111.9	120.2
AoM of individual joints at AS	$AoM_{hip,abd}$	0.427 [0.252, 0.603] ***	19.8%	117.0	125.3
	$AoM_{hip,ie}$	0.403 [0.223, 0.582] ***	16.7%	119.6	127.9
	$AoM_{hip,fe}$	0.451 [0.276, 0.626] ***	23.5%	114.9	123.2
	$AoM_{knee,fe}$	0.520 [0.364, 0.675] ***	28.1%	103.4	111.7
	$AoM_{ankle,pdf}$	0.484 [0.320, 0.648] ***	26.0%	109.3	117.6

US – unaffected side, *AS* – affected side, *Pel* – pelvis, *oblq* – obliquity, *ro* – rotation, *abd* – abd/adduction, *ie* – int/external rotation, *fe* – flex/extension, *pdf* – plantar/dorsiflexion. Note better representation of data on unaffected side compared to affected side. Also, joints with various ranges of motion (knee, hip abduction, pelvic tilt) represent data best on joint level (see discussion section).

4.3.3 Amount of Motion at Individual Joints

I additionally observed how specific joint motions were correlated with functional gait recovery. Because joint AoMs were not independent (average r = 0.86), I modeled each joint motion alone instead of multiple joint AoMs. Results are presented in Table 4.3. All individual joints were significantly correlated with the average gait speed (p<0.01). Goodness-of-fit measures varied between R^2 =16.5 – 31.2%, the greatest at hip abduction/adduction and smallest at hip internal/external rotation, both of the unaffected sides.

Table 4.4: Paired t-test between AoM of unaffected/affected sides.

	ΔAoM [95% CI]	p-value
$AoM_{US/AS}$	22911° [-4659, 50481]	0.09
$AoM_{hip,abd}$	-867° [-3154, 1420]	0.37
$AoM_{hip,ro}$	-5112° [-14125, 3901]	0.20
$AoM_{hip,fe}$	5536° [-3582, 14654]	0.18
$AoM_{knee,fe}$	10870° [-1199, 22939]	0.07
$AoM_{ankle,pdf}$	12484° [2592, 22376]	< 0.05*

$\Delta AoM = AoM_{US} - AoM_{AS}$

4.3.4 Amount of Motion between Unaffected/Affected Sides

Next I determined the degree to which the motion on the affected and unaffected sides corresponded to recovery. Both AoM_{US} and AoM_{AS} were significantly correlated with functional gait recovery (both p<0.01, see Table 4.3). However, the goodness-of-fit measures demonstrated slightly greater explained variance in AoM_{US} (R^2 =32.9%) compared to AoM_{AS} (R^2 =27.8%) with similar trends in AIC and BIC. Secondly, paired t-tests were used to evaluate absolute differences between AoM_{US} and AoM_{AS} as well as individual joints (i.e., hip flexion/extension, abduction/adduction, internal/external rotation, knee flexion/extension and ankle plantar/dorsi-flexion) of bilateral legs (see Table 4.4). There were no significant differences between AoM_{US} and AoM_{AS}, and individual joints (all p>0.05) except for ankle plantar/dorsiflexion with greater AoM at unaffected side (p<0.05).

4.4 Discussion

The “dosage” that physical therapy provides would be one of the most fundamental but least understood phenomena in rehabilitation. In this study, I took the novel approach

measuring therapy using portable lower limb motion capture. Additionally, I longitudinally recorded therapy sessions during both inpatient and outpatient phases in order to measure as early and extensively as possible. My main finding was that the amount of motion (AoM) was a better predictor of gait speed than the number of steps, spontaneous recovery (i.e. time), intensity measured by heart rate change or the types of tasks performed. This result and the additional findings outlined in this study suggest that wearable sensors can become a valuable tool for better understanding dosage of therapy received and the efficacy of rehabilitation training.

Several early studies attempted to quantify dosage of therapy by observing duration or number of repetitions in task-specific movements [87], [88], [99], [100]. More recent studies measured overall limb motions using accelerometers and concluded that the number of steps was associated with improved gait recovery [41], [90], [101]. However, I hypothesized that richer data involving joint motions would reveal greater nuance and thus result in a more accurate correlate of recovery. I observed that the AoM was substantially better associated with recovery (32.1% of variance) than number of steps (14.1% of variance). This result suggests that obtaining joint kinematics during therapy results in a useful predictor of recovery. Since this was an observational study, I cannot conclude whether inducing greater AoM will result in improved recovery. Yet I speculate that this relationship would likely be found given the greater walking outcomes in the high intensity therapy group compared to the control group who received conventional therapy [41].

It is possible that the high correlation of AoM with gait speed is due to the simple observation that walking faster results in greater joint motion. My results suggest that this

is not the case. I separated the AoM during gait (AoM_G) from AoM during activities other than gait (AoM_{NG}, e.g. transfers, stretching/balancing, exercise bike, etc.). If gait speed was primarily a reflection of the amount of motion during gait of a therapy session, we would expect the highest correlation between AoM_G and gait speed. On the contrary, the model that accounted for the greatest variance in gait speed included both AoM_G and AoM_{NG} (Table 4.2), suggesting that the motions during non-gait tasks were important in explaining recovery. This corresponds with previous finding that the exercise dose including both gait and non-gait training in the early stage is an important indicator of walking speed [102]. Further, while AoM_G correlated strongly with step number (r = 0.93), total AoM was not as strong (r = 0.83) despite being a better predictor of gait recovery than step number. Thus, these results indicate that AoM provides valuable information not included in step number.

In addition to AoM, other features including time, step number, change in heart rate, and types of tasks were also significantly correlated with gait speed. These results are consistent with previous works [21], [41], [101]. The correlations of these parameters indicate that they may also be useful predictors for recovery. However, the finding that time (R^2 =15.5%) explained more variance than the other variables including step number (R^2 =14.1%) suggests that these features may have limited value in predicting improvements in gait speed compared to spontaneous recovery.

While recording kinematics of all seven lower body segments provides a rich kinematic dataset, it is possible we could get similar predictive value from fewer sensors given that all individual joint AoMs significantly associated with gait speed (all p<0.01, see Table 4.3). I found the greatest explained variance in unaffected side hip

abduction/adduction (R^2 =31.2%) followed by pelvic tilt (R^2 =30.6%), and bilateral knee flexion/extension of the unaffected (R^2 =29.2%) and affected (R^2 =28.1%) sides. It should be noted that bilateral knees had the lowest AIC and BIC in contrast to the R^2 values. Although not completely consistent, the correlation between R^2 and both information criteria (AIC and BIC) were reasonably strong (both r = -0.86) indicating similar trends between goodness-of-fit measures. It is unclear why hip abduction/adduction of the unaffected side appeared to be so influential given that it is not typically a focus of treatment or locomotor function. This result may be related to the strong correlation between range of motion at unaffected side hip abduction/adduction and gait speed in stroke individuals [26]. Further research is needed to investigate this relationship, which may indeed be epiphenomenal. On the other hand, pelvic tilt is highly correlated to gait speed, and its increased range of motion would indicate greater fore/aft balance [103], [104]. The inclusion of knee flexion/extension is expected as this joint has long been believed a key contributor of functional activities including walking [105]. These results would suggest that a single IMU on the pelvis, or an additional one on the unaffected thigh, or measuring knee joint motions could provide similar predictive power as a full lower body suit. Even further, I cannot dispute that a single low-cost gyroscope on the pelvis or other aforementioned locations (i.e., thigh, shank) could also provide reasonably accurate prediction of recovery [106].

I observed that AoM of the unaffected side explained more variance than the affected side (Table 4.3), which was surprising. I assumed that therapeutic principles of forced use, successfully applied to the upper limb [92], would translate to the lower limb.

However, despite no clear difference in the AoM between sides (except for ankle dorsi/plantarflexion likely be explained by restricted motion from AFO, see Table 4.4), the unaffected side accounted for 32.9% of the variance compared to 27.8% of the affected side. This result may be supported by previous studies that found greater correlations between gait speed and selected joint variables (i.e., joint range, moment, power, muscle strength) of the unaffected lower limb than affected side although these studies were conducted on chronic post-stroke individuals [26], [107]. Thus, there is no evidence that the forced use of the lower limb is applied in current gait therapy. However, this result justifies further investigation whether this therapeutic principle of forced use on affected limb will improve better functional recovery.

The purpose of this study is to provide initial evidence that recording gait kinematics during therapy can provide more valuable information than previously measured quantities such as step number. My observations suggest that it can. However, these results come with important caveats. For example, my conclusions are limited to a small sample size only including mildly to moderately impaired individuals who were capable of walking within the initial stage of recovery. Also, my inclusion criteria restricted my sample size, along with the need to recruit patients remaining in the same inpatient institution for outpatient therapy. The average length of inpatient hospital stay in US is approximately 3 weeks [108], and many of the patients were not able to continue the outpatient therapy after discharge (e.g., location, insurance coverage, move to other facilities or receiving home therapy, etc.). Thus, I filtered out many patients during the screening and recruited only those who were likely to continue the outpatient therapy at

the same hospital. Even from those recruited participants, not everyone could complete full 12 recording sessions due to similar reasons. Despite the small sample size, my data still provided clear initial results on the relative importance of several indicators of recovery, offering a glimpse into how therapy can be effectively monitored in the future. However, expanding this work incorporating a larger range of impairment levels, possibly through a network of hospitals, would overcome these hurdles and improve generalizations.

My conclusions are also limited to the assumption that gait speed is the primary measure of functional gait recovery [42]. However, there are other clinical measures of functional recovery such as Functional independence measure (FIM), Berg balance scale or 5X sit-to-stand [109]–[111]. I did not include clinical measures of gait recovery here because these measures were not acquired every therapy session and thus were not helpful in explaining variance. However, future work with a larger cohort could make use of valuable predictors such as clinical outcomes, brain structure, lesion mapping, and others [23], [24].

There were also technical limitations that may have affected my results. IMUs have historically shown inaccuracies compared to optical motion capture [112]. Effects such as drift due to the inhomogeneity of the magnetic field can have deleterious consequences on data collection. I tried to mitigate these issues as much as possible by using an IMU motion capture system specifically designed for capturing kinematics [29], and has been previously validated [30]. This system has proprietary software features that help reduce the effects of sensor drift and claims an accuracy of 1.5° [29]. While our system provides rich data with the ability to monitor patient's motion in real-time, the relatively short

battery life compared to simple accelerometers restricted to measure the activities beyond the therapy sessions. However, the activities in daily life beyond therapy may have affected the patient's recovery especially during outpatient phase. I expect that future advances in IMU technology including prolonged battery life will lead to more accurate and broader data collection. I also hope that the advent of wearable sensors such as wireless flexible electronics can make use of additional physiological information such as ground reaction force and muscle activity to better identify the dosage of therapy [106], [113], [114].

4.5 Conclusions

Despite decades of research on physical therapy, we still lack knowledge of its active factors of effective regimen. In this work I introduced a novel approach of recording lower body kinematics longitudinally during the first three months of therapy post-stroke. I conclude that the amount of joint motion during gait therapy can be an important predictor of recovery (gait speed) in post-stroke individuals, and perhaps more useful than step number. Portable motion capture using inertial measurement units can provide valuable data and greater insight into the therapy experience. These promising initial results justify further research into the dosage of therapy in a larger clinical study.

Chapter 5

Does Kinematic Gait Quality Improve with Functional Gait Recovery? A Longitudinal Pilot Study on Early Post-Stroke Individuals

5.1 Introduction

Restoration of gait and motor recovery following neurological injury such as stroke involves improvements both in functional ability and quality of movements. However, typical clinical outcomes for measuring gait are mostly focused on functional ability such as gait speed [42], timed-up-and-go [43], six minute walk [44], and others; only sparse information on gait quality in the form of symmetry or natural gait patterns are characterized. Disturbances in gait quality are associated with an increased risk of falls [46], greater energy expenditure [27] and may lead long term problems such as learned non-use or use-dependent plasticity and pain [47], [48]. For instance, patients with asymmetric gait have shown greater metabolic energy expenditure from 50% to 67% more than that of body weight-matched healthy controls with same walking speed [49].

The definition of recovery is controversial. In upper extremity studies, most interventions are based on outcome measures related to functionality of the affected limb [115]. Consistent with this philosophy, one of the most effective therapies involves forced use of the affected limb [92]. In terms of gait, the goal is often to restore healthy spatiotemporal symmetry, indicating a recovery on the affected limb [116]. Robotic gait

training is another example attempting to regain symmetric, natural gait patterns of both limbs [12]. On the other hand, an opposing philosophy in recovery is that the more mobile unaffected limb will take over for the reduced functionality of the affected limb. For example, a previous study on chronic post-stroke individuals reported that longer step length in affected side may be represented by relatively greater compensatory action of the unaffected leg [117]. Thus, it is unclear how the affected and unaffected limbs contribute to gait function (speed) during the recovery period after stroke.

Parameters to measure gait quality can be broken down into more than just spatiotemporal characteristics. While spatiotemporal symmetry has been well charted in post-stroke individuals [117]–[119], this parameter is composed of combination of joint motions, or joint kinematics. Post-stroke individuals also exhibit significant asymmetry in joint kinematics with greater inter-individual variability than spatiotemporal characteristics [27]. Typical asymmetry in joint kinematics includes reduced hip extension, knee flexion and ankle dorsi/plantarflexion, and knee hyperextension on impaired side [26], [49], [120]. While these studies have attempted to characterize disturbances in joint kinematics after stroke [27], the majority report instantaneous measurements on chronic patients. There is currently a lack of information regarding how these joint kinematics change over the course of initial (subacute) recovery.

In recent years, limb kinematics, related to end-effector movement in task space (e.g., limb length [28], leg extension angle [121], and foot path area [16]), are suggested to be an important parameters for locomotor function [28] (Figure 5.2, middle). Description of the end-effector (i.e., foot) location is likely more relevant to underlying control of gait.

It may also be a more accurate way to describe gait recovery post-stroke. For instance, Chang et al. suggested that joint kinematics were coordinated with greater variance to preferentially conserve and stabilize the limb kinematics of walking after neuromuscular injury of cats [28]. In humans, however, no evidence exists to show how spatiotemporal characteristics, along with limb or joint kinematics change over the course of early recovery and whether they correspond with gait function. Characterizing how these gait quality parameters change over recovery can help determine how to time interventions to maximize function.

The objective of this observational pilot study is to examine changes in gait quality in terms of spatiotemporal, limb and joint kinematic features over the initial stage of recovery. The primary technical challenge of this endeavor is measuring kinematics in a clinical environment longitudinally. I overcome this problem by using portable, unobtrusive IMU motion capture to measure gait kinematics over the initial recovery stage of 12 weeks. Given that a large variance has been commonly reported in joint kinematics [27], [28], my first hypothesis is that gait quality will remain asymmetric over the course of early recovery, and the asymmetry will be mainly driven by joint kinematics. Second, I expect the impaired side of limb kinematics will preferentially associate with increased gait speed over joint kinematics, reflective of a previous study in cats [28]. Finally, I hypothesize kinematic features of the unaffected side will contribute to the walking function more than affected side due to the residual capacity of greater motor function in the unaffected side [48], [117].

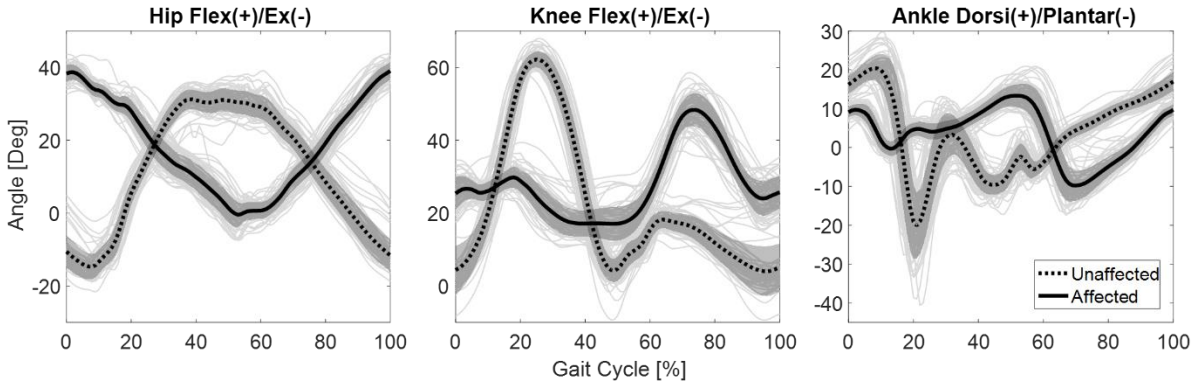

Figure 5.1: Example joint angle trajectories of single gait cycle (left heel strike to heel strike) in sagittal plane (12th session of patient 5), hip flexion/extension (left), knee flexion/extension (middle), and ankle dorsi/plantarflexion (right).

This work will describe a novel characterization of disturbances in gait quality during the early recovery process. The information from this study will justify the importance of gait quality and delineate underlying kinematic mechanism of how patients improve functional recovery with disturbed gait quality throughout the initial stage, providing insight for more effective therapy regimens.

5.2 Methods

Data was collected as described in Chapter 4.

5.2.1 Gait Features and Outcomes

For each session, a normal, straight overground walking at a comfortable speed was sampled to extract features of gait quality and gait outcome measures. Custom software was written in MATLAB (Mathworks, Inc. R2016a, Natick, MA) to calculate the features and outcomes. The joint angle trajectories of the sampled gait portion were truncated and

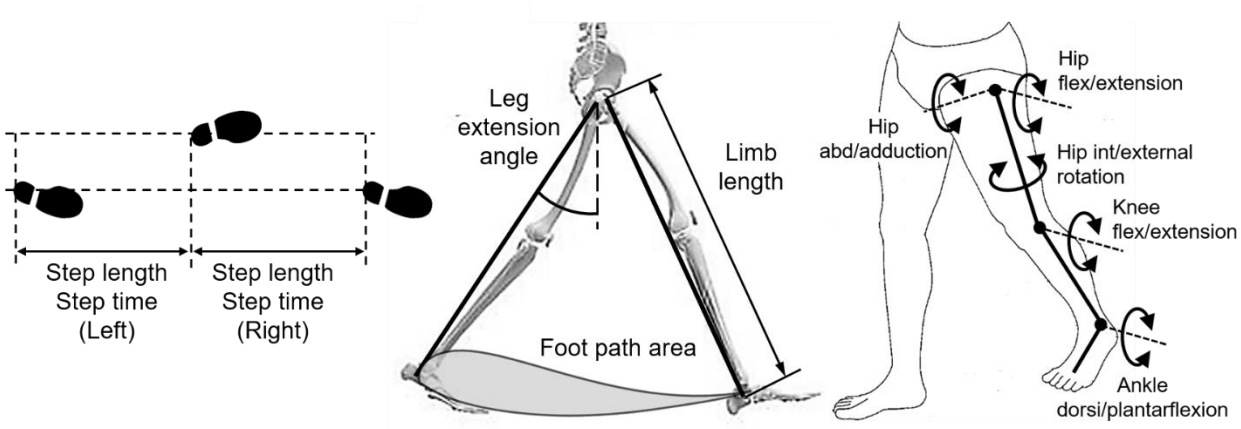

Figure 5.2: Features of gait quality. Spatiotemporal characteristics include step length and step time (left), limb kinematics include leg extension angle, limb length and foot path area (middle), and joint kinematics include range of selected joint motions (right).

normalized into 100% of gait cycle from heel strike to heel strike of the left foot [94]. Figure 5.1 illustrates an example of recorded gait kinematics data from a session including bilateral joint angle trajectories of single gait cycle in sagittal plane. Gait features and outcome measures were extracted by imposing the gait kinematics data into lower body kinematic model with the lower limb lengths estimated by the anthropometric data based on height of each individuals as described below [97].

I categorized gait features into spatiotemporal characteristics, limb and joint kinematics (see Fig. 5.2). Parameters of spatiotemporal characteristics include step length and step time, defined as the linear distance between right and left feet, and the duration of each step, respectively [122] (see Fig. 5.2, left). Limb kinematics is related to end-effector movement in task space, and suggested to be an important parameter for locomotor function [28]. The parameters of limb kinematics incorporate limb length (LL) [28], leg

extension angle (LEA) [121], and foot path area (FPA) [16] defined as the range of linear distance between hip and foot, the angle between a line from hip to the foot and vertical before toe-off, and area of foot pattern from hip in sagittal plane during gait cycle, respectively (see Fig. 5.2, middle). The parameters of joint kinematics are defined as the range of selected joint motions (RoM) including all three rotations of hip, knee flex/extension and ankle dorsi/plantarflexion (Fig. 5.2, right). All features involve affected and unaffected sides, enabling symmetry analysis.

The increased gait speed in patients with stroke is highly correlated to improvements in functional recovery [42]. Thus I selected gait speed as the main functional outcome measure [41], [93]. In each session, the average gait speed was calculated by dividing average distance by the time taken by each gait cycle.

5.2.2 Symmetry Test of Gait Features

5.2.2.1 Overall gait symmetry

Symmetry is a common measure of gait quality [25], [123]. In its simplest form, symmetry is represented by the ratio of stance time on each limb or step length [117]. But one can walk with symmetric spatiotemporal characteristics and still exhibit asymmetric walking (i.e., asymmetric in kinematics). Here I combined all the aforementioned gait parameters into one symmetry measure by employing the combined gait asymmetry metric (CGAM) based on Mahalanobis distance [123]. Mahalanobis distance is a distance measure of a multi-dimensional data point in a data distribution space [124]. Compared to Euclidean distance, the Mahalanobis distance takes covariance of data into account to

standardize the scaling of distance measure in multi-dimensional space. The CGAM uses Mahalanobis distance from ideal symmetry (i.e., zero) to the symmetry ratio obtained from gait parameters. For each session, the symmetry ratio of i^{th} gait parameter was calculated with the symmetry ratio index [123] given by

$$|sr_i| = \frac{|US_i - AS_i|}{0.5(US_i + AS_i)} \tag{5.1}$$

where US_i and AS_i are the i^{th} gait parameter of unaffected and affected sides, respectively, and i represents each gait parameter. Note that the symmetry ratio, $|sr_i| = 0$, with perfect symmetry. The symmetry of spatiotemporal, limb and joint kinematic features was then evaluated with the Mahalanobis distance, D_m, given by

$$D_m = \sqrt{\frac{R * \mathrm{S}^{-1} * R^T}{\sum(\mathrm{S}^{-1})}} \tag{5.2}$$

where $R = [|sr_1|, \cdots, |sr_n|]$ is the vector of symmetry ratios, $\mathrm{S} \in R^{n \times n}$ is the covariance matrix of symmetry ratio data, and n is the number of gait parameters. Normal healthy walking is not perfectly symmetric, but spatially and temporally falls under 6% [125]. Thus, I considered symmetry ratio less than 6% to be "symmetric" walking.

5.2.2.2 Symmetry of individual gait parameters

The symmetry of individual parameters including spatiotemporal characteristics (SL, ST), limb (LL, LEA, FPA) and joint kinematic (RoMs of selected joints) features was then independently analyzed to explore which parameters mainly contributed to gait a/symmetry. The symmetry ratio from Eq. (5.1) was used to evaluate symmetry of individual parameters. Note that with the absolute value in Eq. (5.1), the symmetry ratio

only indicates whether each parameter is symmetric or not, without taking into account the direction of which side is greater. The symmetry ratio less than 6% was defined as "symmetric" walking for individual parameters [125].

5.2.3 Deviation of Gait Parameters

While the symmetry ratio in Eq. (5.1) is an insightful measure of gait symmetry (i.e., which gait parameters are a/symmetric), this does not explain the direction of which side (i.e., unaffected or affected) is more dominant to walking. This information can be observed by simply removing the absolute value from the numerator of symmetry ratio (denoted as sr_i) in Eq. (5.1). Specifically, the positive value of symmetry ratio indicates unaffected side greater than the affected side and the negative value indicates vice versa. Thus, the sign (i.e., positive or negative) and the magnitude of symmetry ratio were used to evaluate which side was more dominant during gait over the overall course of initial recovery (average of all dataset) as well as at the maximum recovery (session at maximum gait speed).

5.2.4 Limb Kinematics vs. Joint Kinematics

The parameters of kinematic features were combined to examine whether the impaired side of limb kinematics is preferentially associated with gait speed over joint kinematics [28]. The Mahalanobis distance was revisited to combine the parameters of limb (LEA, LL, FPA) and joint kinematics (RoMs of selected joints), respectively. While the input data of Mahalanobis distance was symmetry ratio in the symmetry test (i.e.,

CGAM), here I imposed each standardized parameter value into Mahalanobis distance metric to combine each of limb and joint kinematic feature into one value per session. For each side, changes in the Mahalanobis distance of limb and joint kinematics were observed over gait speed, respectively, to examine which kinematic feature is more strongly associated with functional gait recovery.

5.2.5 Statistical Analysis

R version 3.4.1 (2017 The R foundation for Statistical Computing) was used for the statistical analysis. For the analysis, 53 sessions of dataset from total 59 recording sessions were used, excluding the sessions without walking (first two sessions from P2 and first session from P3) and outliers with exaggerated range of motion < 60° at ankle dorsi/ plantarflexion, likely be distorted by magnetic interference of IMUs (8^{th} session of P3, 9^{th} session of P5, 2^{nd} session of P6).

The linear mixed regression model was used to evaluate the relationship between symmetry of gait features and speed as a functional gait measure with significance level $\alpha < 0.05$. For the overall gait symmetry test, the Mahalanobis distances of spatiotemporal, limb and joint kinematic features were standardized and used as dependent variables. For the symmetry test of individual parameters, the symmetry ratio, $|sr_i|$, of each gait parameter was used as a dependent variable. For both tests, gait speed and subject were used as a fixed effect and a random effect of the mixed model, respectively. A one-sided one-sample t-test was used to evaluate the symmetry of overall gait features and individual gait parameters at the maximum functional recovery with significance level of $\alpha < 0.05$.

The symmetry ratio measure at maximum gait speed of each patient was extracted and compared with 6% as the reference of healthy symmetric gait [125].

For the limb vs. joint kinematics test, the linear mixed regression model was used to evaluate the relations between both kinematic features and gait speed with significance level of $\alpha < 0.05$. Coefficient of determination (R^2), Akaike information criteria (AIC), and Bayesian information criteria (BIC) were used to compare goodness-of-fit of the models.

To examine the gait deviation between unaffected and affected sides, one-sided one-sample t-test was applied with significance level of $\alpha < 0.05$. For each parameter, the symmetry ratio without the absolute value (i.e., sr_i) of all sessions and the sessions at maximum gait speed, representing overall recovery phase and maximum functional recovery, respectively, were compared with healthy symmetry threshold of $\pm$6% (i.e., compared with 6% if $sr_{mean} > 0$, and compared with -6% if $sr_{mean} < 0$, where sr_{mean} is average symmetry ratio of each parameter).

Among six participants, I observed two patients (P5 and P6) showing very similar trends of improvements in functional gait recovery (increase in speed with r = 0.91, see Fig. 5.3). Thus, a case study comparing these two patients was conducted to observe whether their gait quality also changed with similar trends. For each gait parameter, I fitted a linear regression model including interaction effect given by

$$sr_i = \beta_0 + \beta_1 Time + \beta_2 Subject + \beta_3 Time * Subject + \varepsilon \quad (5.3)$$

Where symmetry ratio, sr_i, is dependent variable, β_0 is intercept, and ε is the error variable. β_1, β_2 and β_3 are the fixed effect regression coefficients for time, subject and interaction

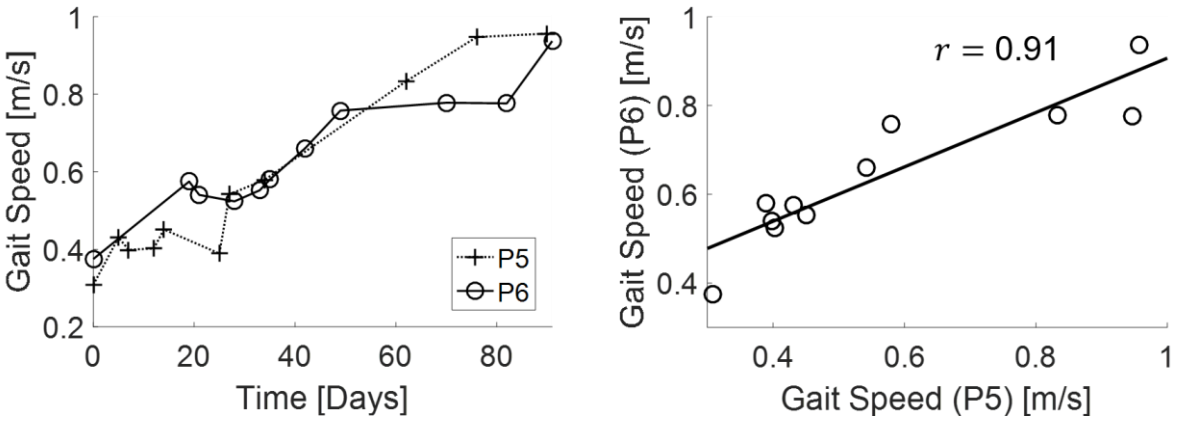

Figure 5.3: Changes in gait speed over the early stage of recovery (left) and correlations in gait speed (right) of patient 5 and 6. Note that the changes in gait speed is showing very similar trend of improvement with correlation of 0.91.

between time and subject, respectively. Herein, the subject was coded as dummy variables, 0 and 1 indicating P5 and P6, respectively. Thus, the difference in slope (i.e., change in symmetry ratio) over time between P5 and P6 was examined by observing the significance of interaction term, β_3.

5.3 Results

5.3.1 Symmetry of Overall Gait Features

I first examined whether the symmetry of spatiotemporal, limb and joint kinematic features improved with gait speed over the initial recovery phase of three months. Figure 5.4 illustrates changes in Mahalanobis distances of spatiotemporal characteristics (left), limb kinematics (middle), and joint kinematics (right) over gait speed, respectively. The results indicated that the symmetry improved significantly in spatiotemporal characteristics

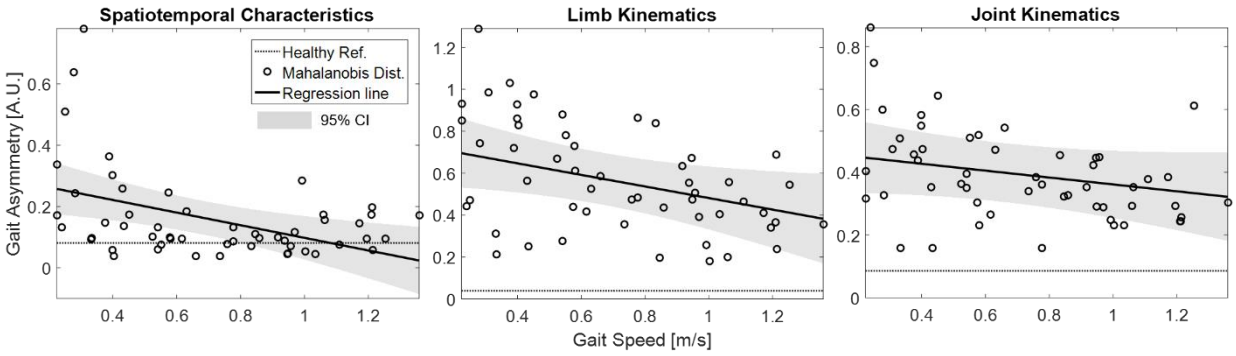

Figure 5.4: Change in overall gait symmetry measures based on combined gait asymmetry metric (CGAM) including spatiotemporal characteristics (left), limb kinematics (middle), and joint kinematics (right) with gait speed. The dotted line is considered as the threshold for symmetric walking. The regression lines are based on linear mixed regression model (Table 5.1).

Table 5.1: p-values of linear mixed regression models with overall gait features based on combined gait asymmetry metric (CGAM) and gait speed, and one-sided one-sample t-test on gait symmetry measure of the maximum gait speed

	Linear mixed regression		One-sided one sample t-test	
	Slope [95% CI]	p-value	D_{max} [95% CI]	p-value
Spatiotemporal	-0.47 [-0.78, -0.15]	< 0.01	0.11 [0.07, inf]	0.14
Limb kinematics	-0.36 [-0.68, -0.04]	< 0.05	0.56 [0.41, inf]	< 0.01
Joint kinematics	-0.25 [-0.59, 0.09]	0.14	0.38 [0.27, inf]	< 0.01

CI – confidence interval, D_{max} – Mahalanobis distance at maximum functional gait recovery (max speed)

(p<0.01) and limb kinematics (p<0.05) whereas joint kinematics (p=0.14) revealed improving trend although not statistically significant. At the session with maximum gait speed, spatiotemporal characteristics (p=0.14) did not reveal significant difference but limb and joint kinematics remained significantly different (asymmetric) from healthy symmetry threshold (both p<0.01). All results are summarized in Table 5.1.

I also examined changes in gait symmetry features over time using linear mixed regression model. However, none of the features including spatiotemporal characteristics

Table 5.2: p-values of linear mixed regression models with symmetry ratio of individual gait parameters and gait speed, and one-sided one-sample t-test on gait symmetry ratio at the maximum gait speed

Gait Features	Parameters	Linear mixed regression		One-sided one sample t-test	
		Slope [95% CI]	p-value	$\lvert sr_{\max} \rvert$ [95% CI]	p-value
Spatiotemporal Characteristics	Step length	-0.33 [-0.60, -0.06]	< 0.05	0.16 [-0.04, inf]	0.08
	Step time	-0.06 [-0.16, 0.04]	0.26	0.07 [0.01, inf]	0.41
Limb kinematics	Leg extension angle	-0.65 [-1.05, -0.24]	< 0.01	0.29 [0.03, inf]	0.07
	Limb length	-0.09 [-0.40, 0.22]	0.55	0.62 [0.29, inf]	< 0.05
	Foot path area	-0.50 [-1.04, 0.04]	0.07	0.87 [0.38, inf]	< 0.05
Joint kinematics	Hip Flex/Ex	-0.15 [-0.30, -0.00]	< 0.05	0.14 [0.06, inf]	< 0.05
	Hip Abd/Add	-0.06 [-0.36, 0.23]	0.68	0.29 [0.03, inf]	0.07
	Hip Int/Ext	-0.02 [-0.27, 0.24]	0.90	0.36 [0.20, inf]	< 0.01
	Knee Flex/Ex	-0.22 [-0.45, 0.00]	0.05	0.27 [0.03, inf]	0.07
	Ankle Dorsi/Plantar	-0.17 [-0.43, 0.08]	0.18	0.30 [0.08, inf]	< 0.05

Flex/Ex – flex/extension, Abd/Add – abd/adduction, Int/Ext – int/external rotation, Dorsi/Plantar – dorsi/plantarflexion, $\lvert sr_{max} \rvert$ – symmetry ratio at maximum functional gait recovery (max speed)

(p=0.12), limb (p=0.61) and joint kinematics (p=0.16) revealed significant trend (see Appendix B.1).

5.3.2 Symmetry of Individual Gait Parameters

According to the overall symmetry test, all gait features revealed improving trends but both limb and joint kinematics remained asymmetric at the maximum gait speed. Thus, I used linear mixed regression model and one-sided one-sample t-test on individual gait parameters independently to further investigate major contributors of overall gait a/symmetry. The results revealed that the symmetry improved significantly at SL (p<0.05), LEA (p<0.01), and hip flex/extension (p<0.05). However, LL and FPA (both p<0.05) from limb kinematics and hip flex/extension (p<0.05), hip int/external rotation (p<0.01) and ankle dorsi/ plantarflexion (p<0.05) from joint kinematics remained significantly different

Table 5.3: p-values and goodness-of-fit measures of linear mixed regression model with both unaffected and affected limb and joint kinematics over gait speed

Side	Kinematic feature	Linear mixed regression			
		Slope [95% CI]	R^2	AIC	BIC
Unaffected side	Limb kinematics	0.53 [0.26, 0.81]***	27.5%	139.7	147.6
	Joint kinematics	0.77 [0.56, 0.97]***	57.6%	111.0	118.8
Affected side	Limb kinematics	0.79 [0.49, 1.10]***	41.9%	131.4	139.2
	Joint kinematics	0.58 [0.35, 0.81]***	33.1%	135.7	143.6

*** $p < 0.001$, R^2– coefficient of determination, AIC – Akaike information criteria, BIC – Bayesian information criteria

(asymmetric) from healthy symmetry threshold (6%) at the maximum gait speed. As expected, both parameters (SL and ST) in spatiotemporal characteristics did not show significant difference from healthy symmetry threshold. All results are summarized in Table 5.2.

5.3.3 Limb Kinematics vs. Joint Kinematics

To examine whether the limb kinematics is more correlated with functional gait recovery over joint kinematics, the Mahalanobis distance was used to combine the parameters of limb and joint kinematic features of each side into one value. Then the linear mixed regression model was used to fit the Mahalanobis distance of each limb and joint kinematics of unaffected and affected sides over gait speed (see Table 5.3). The results revealed that all kinematic features at both sides significantly associated with gait speed (all p<0.001). However, according to the goodness-of-fit measures, the variance accounted for of limb kinematics (R^2=41.9%) was greater than joint kinematics (R^2=33.1%) at the

Table 5.4: p-values of one-sided one-sample t-test to examine deviations of gait parameters between unaffected and affected side based on average gait symmetry ratio over the course of early recovery

Gait Features	Parameters	One-sided one sample t-test	
		sr_{mean} [95% CI]	p-value
Spatiotemporal Characteristics	Step length	-0.12 [-inf, 0.12]	0.32
	Step time	0.01 [-0.06, inf]	0.89
Limb kinematics	Leg extension angle	0.23 [-0.14, inf]	0.20
	Limb length	0.40 [0.24, inf]	< 0.01
	Foot path area	0.83 [0.48, inf]	< 0.01
Joint kinematics	Hip Flex/Ex	0.14 [0.04, inf]	0.09
	Hip Abd/Add	-0.03 [-inf, 0.14]	0.63
	Hip Int/Ext	-0.15 [-inf, -0.07]	< 0.05
	Knee Flex/Ex	0.27 [0.06, inf]	< 0.05
	Ankle Dorsi/Plantar	0.22 [0.03, inf]	0.07

sr_{mean} – average symmetry ratio of all dataset from six patients

affected side, whereas unaffected side showed a greater correlation in joint kinematics (R^2=57.6%) than limb kinematics (R^2=27.5%) with consistent trends in AIC and BIC.

5.3.4 Deviation of Gait Parameters

The deviation between unaffected and affected sides of each gait parameter was observed to examine more dominant side during walking. The results indicated that unaffected side was significantly greater than affected side in LL (p<0.01), FPA (p<0.01), and knee flex/extension (p<0.05), whereas hip int/external rotation (p<0.05) revealed opposite results over the overall recovery phase (average of all sessions). All results are summarized in Table 5.4 (also, symmetry ratio, sr_i, over time plots are illustrated in Appendix B.2). However, none of the gait parameters showed significant difference between sides at the session with maximum gait speed.

Table 5.5: p-values of linear regression model with interaction effect and symmetry ratio at final session of patient 5 and 6

Gait Features	Parameters	p-values of linear regression			sr at final session	
		β_1	β_2	β_3	P5	P6
Spatiotemporal Characteristics	Step length	< 0.05	< 0.01	0.05	-0.08	-0.20
	Step time	0.07	0.06	0.08	0.06	-0.02
Limb kinematics	Leg extension angle	0.44	0.05	0.11	0.67	0.32
	Limb length	0.99	0.42	< 0.01	0.13	-0.82
	Foot path area	0.41	0.11	< 0.05	0.89	-0.56
Joint kinematics	Hip Flex/Ex	0.12	< 0.01	0.49	0.19	-0.20
	Hip Abd/Add	0.89	0.54	0.48	0.02	0.10
	Hip Int/Ext	0.66	0.43	0.26	-0.41	-0.67
	Knee Flex/Ex	0.10	< 0.01	0.07	0.18	-0.17
	Ankle Dorsi/Plantar	0.71	0.13	0.78	0.73	0.43

sr – symmetry ratio, P5 – patient 5, P6 – patient 6, β_1, β_2 and β_3 are the fixed effect regression coefficients for time, subject and interaction between time and subject, respectively.

5.3.5 Case Study: Patient 5 vs. Patient 6

I conducted a case study comparing two patients (P5 and P6) who had very similar trend of improvements in gait speed (see Fig. 5.3) to observe whether their gait quality also changed with similar trends. Table 5.5 shows the linear regression model including interaction effect and the symmetry ratio, sr_i, at the final sessions that compares individual gait parameters between two patients. The results indicated that symmetry ratios at SL, hip and knee flex/extensions were significantly different (all p<0.01 in β_2) and LL (p<0.01) and FPA (p<0.05) revealed significantly different slopes over time between two patients (see β_3), controlling for other fixed effects. Also note that these two patients are showing opposite dominant sides in these kinematic parameters at the final session (see sign and magnitude of symmetry ratios at the final session in Table 5.5). Figure 5.5 illustrates

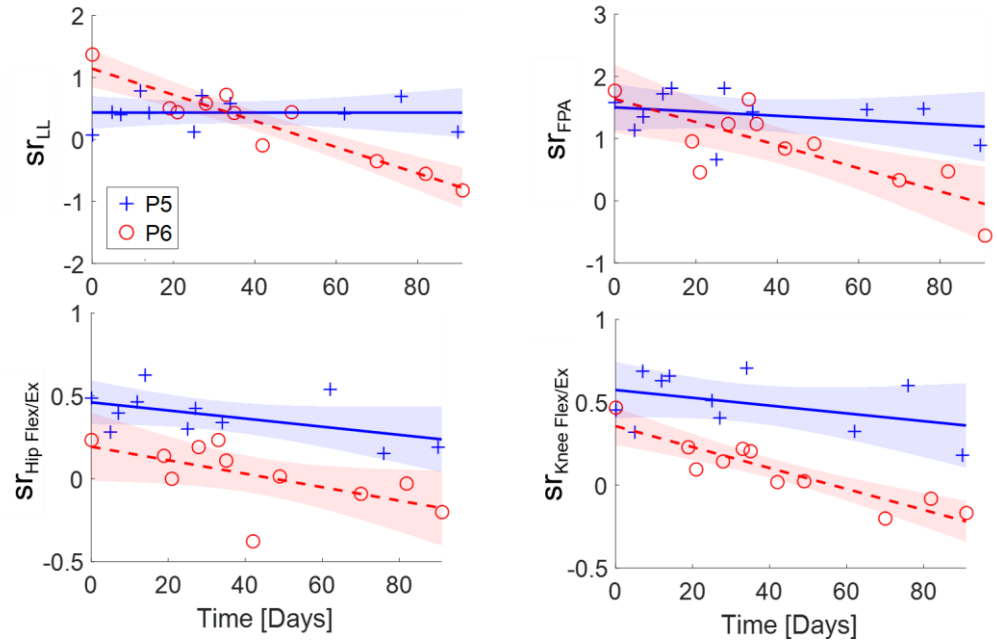

Figure 5.5: Symmetry ratios of limb length (top left), foot path area (top right), hip (bottom left) and knee (bottom right) flex/extensions of patient 5 and 6 over initial stage of recovery. Linear regression models were fitted on both patients' symmetry ratio over time (P5: blue solid line, P6: red dashed line). Note that the changes in symmetry ratio are significantly different between two patients (see also Table 5.5).

changes in symmetry ratio of these kinematic parameters. It can be clearly observed that the trends of change in symmetry ratio between two patients are very different (see Appendix B.3 for other gait parameters over time plots).

5.4 Discussion

Complete locomotor recovery following stroke would require improvements in both functional ability as well as quality of movement. However, typical clinical outcomes focus more on gait function than quality [41], resulting in very little knowledge of how gait quality develops over the course of recovery. My primary goal was to examine the changes

in gait quality in terms of spatiotemporal, limb and joint kinematic features over the early stage of recovery. To achieve this goal, I longitudinally measured full lower body gait kinematics using wearable IMU motion capture over the initial period of three months. My main findings were 1) symmetry of gait quality features overall improved with functional gait recovery, but both limb and joint kinematic features remained asymmetric at the maximum functional recovery, 2) limb kinematics of the impaired side preferentially associated with functional gait recovery over joint kinematics, and 3) the changes in gait quality features exhibited inter-individual variability over the course of early recovery phase. These results justify the importance of gait quality and highlight wearable sensors can become a valuable tool for monitoring detailed disturbances in gait quality, providing insight for more effective therapy strategies.

Gait symmetry is a common measure to characterize disturbances in gait quality [25], [123]. While spatiotemporal symmetry has been increasingly measured and reported in post-stroke individuals [117]–[119], the symmetry in kinematics has not been well charted perhaps due to the difficulties in measuring kinematic data in clinical settings. Based on my longitudinally measured gait kinematics data using wearable IMUs, the spatiotemporal as well as kinematic symmetries were captured and evaluated along with improved gait speed over the course of early recovery. According to the overall gait symmetry test, the results revealed that the symmetry in spatiotemporal characteristics (p<0.01) and limb kinematics (p<0.05) was significantly correlated (towards ameliorating direction) with gait speed and joint kinematics revealed a strong trend of improvement although not statistically significant (p=0.14). This suggests that the symmetry of these

gait features is related to improvements in gait function. This agrees with a previous study that found faster and more symmetric walking showed lower metabolic cost than merely walking faster or more symmetrically [126], providing an important functional implication given the connections between energetic advantages and retaining symmetry along with improvements in gait function.

While the symmetry of overall gait features exhibited improving trend with increased walking speed, only the spatiotemporal characteristics reached symmetry to some degree at the maximum gait speed. This result is contrary to earlier studies that commonly reported asymmetry in spatiotemporal characteristics such as longer swing time or step lengths in the impaired side [27], [117], [119], [125]. This could be related to the limited inclusion criteria of the present study since only the mild to moderately impaired patients who were able to walk before the subacute stage were recruited as participants. Another possible speculation would be a deterioration of spatiotemporal symmetry as the patients enter a chronic phase after having asymmetric gait pattern alterations within and beyond the initial stage of recovery [47], [48]. However, a larger sample size with prolonged data from early to chronic stage needs to be analyzed to make a strong conclusion on this speculation. In kinematics, on the other hand, both limb and joint kinematic features remained significantly asymmetric at the maximum recovery (both $p<0.01$). Overall these results suggest that the symmetry of spatiotemporal characteristics may be associated with greater functional gait recovery compared to limb and joint kinematics.

From the results of overall gait symmetry test, I observed that kinematic features during gait retained asymmetry throughout the period of early recovery. As a next step, I additionally investigated symmetry of individual gait parameters over gait speed to explore which parameters contributed to gait a/symmetry. The results indicated that leg extension angle (p<0.01) and hip flex/extension (p<0.05) were the major kinematic parameters that contributed to improved symmetry over gait speed. This suggests that the leg extension and hip flex/extension are important predictors of functional gait recovery, agreeing with previous studies that found significant correlation of these parameters to propulsive force for walking and gait speed [26], [121]. The positive aspect of these overall results including other non-contributed parameters is that none of the kinematic parameters revealed deteriorating trend of becoming more asymmetric (see slopes in Table 5.2). However, all parameters other than leg extension angle, hip abd/adduction and knee flex/extension remained significantly asymmetric compared to the healthy symmetry threshold (6%) at the maximum gait speed (see Table 5.2). This suggests that there is still a room to improve symmetry on these gait parameters and additional therapeutic efforts need to be made to achieve a complete recovery with symmetric walking.

A previous animal study on cats found that the limb kinematics were preferentially conserved over joint kinematics after peripheral nerve injury [28]. To examine whether this trend translates to post-stroke human subjects, I observed relations of changes in limb and joint kinematics at unaffected and affected sides, respectively, over gait speed. The result revealed that the variance explained by limb kinematics (R^2=41.9%) was greater than joint kinematics (R^2=33.1%) in the affected side, indicating stronger association in limb

kinematics with gait speed over the joint kinematics on impaired side (see Table 5.3). This suggests that post-stroke individuals may use the strategy to preferentially coordinate limb function by compensating joint kinematics during walking, agreeing with the previous study on cats [28], [127]. This greater connection between limb and locomotor functions than joint motion may likely be explained by the deficient capacity of residual function in the individual joints of the impaired side [48]. This also may explain, on the other hand, why the explained variance of joint kinematics (R^2=57.6%) was greater than the limb kinematics (R^2=27.5%) in the unaffected side. I expect these findings will provide a novel insight of which kinematic (i.e., limb or joint) function should more be focused in therapy interventions to maximize both functionality and quality in gait recovery.

While the symmetry analysis provides valuable information of which gait parameters are a/symmetric, this does not indicate which side dominates the gait function. To explore this question, I observed the deviation between unaffected and affected sides at each gait parameter over the overall course of recovery period after stroke (average of all sessions, see Table 5.4). A few gait parameters revealed significant differences between two sides. Limb length (p<0.01), foot path area (p<0.01), and knee flex/extension (p<0.05) were greater in the unaffected side, similar to other previous studies that reported greater contribution of the unimpaired side with chronic post-stroke individuals [26], [117]. Note that all these parameters are related to the sagittal plane kinematics. This suggests that one of the mechanisms for improving gait function (i.e., increased gait speed) may be the relatively greater compensatory sagittal plane behavior of these parameters in the unaffected side [117]. On the other hand, hip int/external rotation was the only joint that

showed greater range of motion in the affected side. An earlier study also reported that the impaired side of this joint was significantly correlated with gait speed on chronic patients [26]. Note that this hip joint motion in transverse plane is not a key contributor of locomotor function. Thus, this may represent the development of compensatory action since there is no reason to have a greater motion in the impaired side of this joint during gait.

A great inter-individual variability in motor recovery is commonly reported in previous studies. Indeed, my data also indicated that there is a large variance in improvements between patients. According to the overall gait symmetry test over time, none of the features showed significant trends. Also, none of the gait parameters revealed significant differences between unaffected and affected sides at the maximum recovery. Given that the significant trends were observed in the symmetry tests in overall and individual gait parameters over functional recovery (speed), the lack of observed differences are coming from the great variance between patient-to-patient (see Appendix B.1 and B.2). A clear example of great inter-individual variability was demonstrated through a case study between P5 and P6. While these two patients had very similar trends of improvements in gait speed (see Fig. 5.3), distinct differences in changes in symmetry were observed in a number of gait parameters including step length (p<0.01), limb length (p<0.01), foot path area (p<0.05), hip (p<0.01) and knee (p<0.01) flex/extensions. In all of these parameters with statistical significance, P5 tended to invariably use more in the unaffected side, whereas P6 initially started with greater in the unaffected side, but proceeded towards the opposite direction over the course of three months (see regression lines in Fig 5.5). Note that these kinematic parameters of two patients are showing opposite

dominant sides at the final session (see sign and magnitude of symmetry ratio, sr, at the final session in Table 5.5). This indicates that post-stroke individuals may attempt different strategies to achieve gait function and adapt to different ways of moving inter-individually (e.g., compensations) as described in [48]. This also suggests that the functional gait measures alone may not be sufficient to fully characterize the gait impairment after stroke.

The purpose of this observational pilot study was to monitor changes in gait quality over the initial recovery phase by measuring full lower body gait kinematics using wearable IMU motion capture. This study suggests initial evidence that observing gait quality can provide diverse aspects of gait recovery that can characterize detailed information of abnormal walking. However, although I have found some strong trends from my data, the results need to be interpreted with an important proviso. This pilot study is limited to a small sample size of six patients with a restricted range of impairment (only post-stroke individuals who were able to walk before initial stage of three months). Despite these drawbacks, my initial findings were based on longitudinally measured data with rich kinematic information highlighting the importance of monitoring gait quality. However, future work including additional physiological measures such as neuromuscular/kinetic (e.g., electromyography, ground reaction force) or imaging (e.g., brain structure, lesion mapping) data will help to fully clarify the underlying mechanism of disturbances in gait quality. I expect this study will justify more expanded research on gait quality with a larger post-stroke population for more reliable generalization and will help to provide better insight for more effective therapy regimens.

Another important advance of this work is the novel approach providing a methodology to track gait quality by measuring joint kinematics over the course of the initial recovery stage, the most critical phase. However, measuring joint kinematics are relatively more sensitive to errors than other conventional gait measures such as gait speed or spatiotemporal characteristics. Typical deleterious effects on data collection, especially with IMUs, include drift due to interference of magnetic field and offset error caused by sensor misalignment, and these effects may have influenced my results. However, to mitigate this issues, I used an IMU motion capture system specifically developed for measuring gait kinematics [29]. In addition, I carefully selected gait kinematic measures that are relatively more reliable (e.g., symmetry, range of motion, etc.) although less detailed than other precise measures addressing full waveforms of kinematic trajectories (e.g., root-mean-square error, Fourier transform, etc.). Nevertheless, I was able to observe some strong and interesting trends with these measures. However, I expect further advances in motion capture technology will help to measure more accurate kinematics data and will allow to observe more precise kinematic features, providing more detailed and reliable results of characterizing post-stroke gait.

5.5 Conclusions

Regaining complete gait recovery following stroke should involve improvements in functional ability as well as quality of movement. However, traditional clinical outcomes for measuring gait are mostly focused on functional ability. The main goal of this study was to investigate how gait quality in terms of spatiotemporal, limb and joint kinematics

changes over the subacute stage of recovery. To achieve this, I measured full lower body kinematics using portable IMU motion capture. I observed that post-stroke individuals exhibited disturbances in gait quality throughout the course of initial recovery while improving gait function. I conclude that observing gait quality will provide more detailed information characterizing disturbances in post-stroke gait. These initial results justify further research on monitoring gait quality with a larger clinical study and suggest wearable sensors can become a valuable tool for characterizing detailed disturbances in gait quality, providing insight for more effective training regimens.

Chapter 6

Conclusions and Future Work

In this dissertation, I have sought to explore novel approaches to overcome substantial problems in gait rehabilitation including financial burden and lack of information on effective therapy regimen with following stated research aims: (1) design of an affordable, adaptable robotic gait trainer that maintains key therapeutic principles, (2) development of an online algorithm for producing speed-dependent reference joint trajectories that can be used for general robotic gait training, (3) quantify dosage of therapy and (4) examine changes in gait quality over the course of early recovery phase by longitudinally monitoring lower body kinematics of subacute post-stoke individuals.

My first two aims made several contributions to the field of rehabilitation robotics. In Chapter 2, I introduced a novel concept of an individual-specific robotic gait trainer intended to reduce the cost without sacrificing beneficial aspects of gait training. The future development of this low-cost device will proliferate robotic training to new markets including resource-limited hospitals, outpatient clinics, patients' homes and also to many research labs. More access to such beneficial training may result in more intensive therapy and greater compliance with training regimens, ultimately producing better outcomes per patient at lower costs. In Chapter 3, I presented a novel method for establishing an online algorithm that can produce a continuous, speed-dependent reference gait patterns, generalizable to most robotic gait trainers and exoskeletons. Specifically, the method can generate smooth transitions in gait trajectories in a synchronous manner with arbitrarily

given varying walking speed. Ultimately, I expect such trajectory-specific training will help individuals suffering from neurological impairments to improve gait function as well as gait quality by providing a more ecological and realistic walking experience during the training.

Then, my third and fourth aims made contributions to the field of neurological physical therapy for subacute post-stroke individuals. For these aims, I longitudinally measured full lower body kinematics during physical therapy sessions using a portable, unobtrusive IMU motion capture device over the course of early recovery. In Chapter 4, I attempted to quantify dosage of therapy based on amount of kinematic joint motion during physical therapy sessions and found that this measure can be a useful predictor of functional gait recovery. I expect these initial results will provide a more nuanced picture of post-stoke recovery during the early stage, leading towards an improved understanding of the benefits of physical therapy. In Chapter 5, I examined changes in gait quality in terms of spatiotemporal, limb and joint kinematic features over the initial stage of recovery. My results indicated that post-stroke individuals retained disturbances in kinematic gait quality throughout the course of early recovery while improving gait function. I expect the findings from this aim will enlighten the importance of gait quality and justify further research on improving gait quality with a larger clinical study. Overall these aims will suggest that wearable sensors can become a valuable tool for better understanding dosage of therapy received and monitoring detailed kinematic gait quality, providing insight for more effective therapy regimens.

There are several ways in which the studies in this dissertation could be further improved. First, additional effort can be made on the amount of motion as a dosage of therapy feature. My results revealed strong correlations between the amount of motion and improved gait speed, indicating that this feature can be a useful predictor of functional gait recovery. However, this does not infer that the amount of motion can be a biomarker of recovery. To explore more on this feature, further research can examine 1) whether the amount of motion at initial period can predict the final level of recovery and 2) whether greater amount of motion can improve better functional recovery.

Secondly, therapeutic principle of forced use (constraint-induced movement therapy), successfully applied to the upper limb [92], may be tested on lower limb. One of my initial hypotheses was that this forced use would translate to the physical therapy on lower limb. However, my data indicated that this principle was not applied with current physical therapy sessions (see Table 4.4). Thus, a randomized controlled trial can be conducted as a future work to test whether the forced use on the affected lower limb can improve better functional recovery.

Third, gait quality features could be adopted to categorize patients' different walking strategies. While the subacute post-stroke individuals exhibited overall improving trend in gait symmetry with improved functional recovery, great inter-individual variability was observed with residual asymmetry especially in kinematic parameters at their maximum functional recovery. Indeed, my case study on two patients who had very similar trend of improved gait function (see Fig. 5.3) demonstrated completely different trend of changes in gait quality measures. Thus, future study can investigate patient-specific care

depending on the type of patient's behavioral strategy characterized with such gait quality measures described in this dissertation.

Finally, one solution for increasing therapy dose as well as improving quality of movement can be training with robots. In recent decades, rehabilitation robots were developed and applied in practice to increase the patient throughput and provide training with natural movements. While some studies report that there exists no evidence showing robotic training is more effective than conventional therapy [61]–[63], we may have overlooked the effect of robotic therapy. For instance, one evidence of improving quality of movement through robotic training could be a study on powered exoskeleton providing a virtual force field of an arbitrary gait pattern on healthy subjects [128]. The researchers found that this feedback control strategy altered users' after-effects towards the desired training pattern. The observation that users adapted to an arbitrary gait pattern suggests that changing kinematic gait pattern (e.g., improving quality of movement) is possible on human subjects. Thus, future work can include training with a robot based on various control paradigms and examine the after-effects though the movement quality measures such as introduced in this dissertation.

Appendices

Appendix A

Kinematics of Jansen Mechanism

The kinematics of Jansen mechanism in Eq. (2.1) can be solved as follow. Given the link length, $L_1 - L_{12}$, and input crank angle, θ_2, the goal is to find all other joint angles, $\theta_3 - \theta_{12}$ and joint positions, $P_1 - P_E$ (see Fig. 2.3).

From upper four-bar mechanism, $L_1L_2L_3L_4$, the joint angles θ_3 and θ_4 can be calculated as given by

$$\theta_3 = 2\tan^{-1}\left(\frac{-E-\sqrt{E^2-4DF}}{2D}\right) \tag{A.1}$$

$$\theta_4 = 2\tan^{-1}\left(\frac{-B-\sqrt{B^2-4AC}}{2A}\right) \tag{A.2}$$

where

$$A = -K_1 - K_2\cos\theta_2 + K_3 + \cos\theta_2;\ B = -2\sin\theta_2 \tag{A.3}$$

$$C = K_1 - (K_2+1)\cos\theta_2 + K_3;\ D = K_5 - K_1 + K_4\cos\theta_2 + \cos\theta_2 \tag{A.4}$$

$$E = -2\sin\theta_2;\ F = K_1 + (K_4-1)\cos\theta_2 + K_5 \tag{A.5}$$

and

$$K_1 = \frac{L_4}{L_1};\ K_2 = \frac{L_4}{L_3};\ K_3 = \frac{L_1^2-L_2^2+L_3^2+L_4^2}{2L_1L_3} \tag{A.6}$$

$$K_4 = \frac{L_4}{L_2};\ K_5 = \frac{L_3^2-L_4^2-L_1^2-L_2^2}{2L_1L_2}. \tag{A.7}$$

From lower four-bar mechanism, $L_1L_7L_8L_4$, the joint angles θ_7 and θ_8 can be calculated as given by

$$\theta_7 = 2\tan^{-1}\left(\frac{-E+\sqrt{E^2-4DF}}{2D}\right) \tag{A.8}$$

$$\theta_8 = 2\tan^{-1}\left(\frac{-B+\sqrt{B^2-4AC}}{2A}\right) \tag{A.9}$$

where

$$A = -K_1 - K_2\cos\theta_2 + K_3 + \cos\theta_2;\ B = -2\sin\theta_2 \tag{A.10}$$

$$C = K_1 - (K_2+1)\cos\theta_2 + K_3;\ D = K_5 - K_1 + K_4\cos\theta_2 + \cos\theta_2 \tag{A.11}$$

$$E = -2\sin\theta_2;\ F = K_1 + (K_4-1)\cos\theta_2 + K_5 \tag{A.12}$$

and

$$K_1 = \frac{L_4}{L_1};\ K_2 = \frac{L_4}{L_8};\ K_3 = \frac{L_1^2-L_7^2+L_8^2+L_4^2}{2L_1L_8} \tag{A.13}$$

$$K_4 = \frac{L_4}{L_7};\ K_5 = \frac{L_8^2-L_4^2-L_1^2-L_7^2}{2L_1L_7}. \tag{A.14}$$

From the coupler, $L_3L_5L_6$, the joint angles θ_5 and θ_6 can be calculated by

$$\theta_5 = 2\tan^{-1}\left(\frac{-B-\sqrt{B^2-4AC}}{2A}\right) \tag{A.15}$$

$$\theta_6 = 2\tan^{-1}\left(\frac{-E-\sqrt{E^2-4DF}}{2D}\right) \tag{A.16}$$

where

$$A = K_1 + \cos\theta_4;\ B = -2\sin\theta_4 \tag{A.17}$$

$$C = K_1 - \cos\theta_4;\ D = K_2 + \cos\theta_4 \tag{A.18}$$

$$E = -2\sin\theta_4;\ F = K_2 - \cos\theta_4 \tag{A.19}$$

and

$$K_1 = \frac{L_6^2-L_3^2-L_5^2}{2L_3L_5};\ K_2 = \frac{L_6^2+L_3^2-L_5^2}{2L_3L_6}. \tag{A.20}$$

From the parallelogram mechanism, $L_6L_8L_9L_{10}$, the joint angle θ_9 can be calculated as given by

$$\theta_9 = 2\tan^{-1}\left(\frac{-B+\sqrt{B^2-4AC}}{2A}\right) \tag{A.21}$$

where

$$A = K_1 + K_2 + K_4;\ B = -2K_3;\ C = K_4 - K_2 + K_1 \tag{A.22}$$

and

$$K_1 = \frac{L_{10}^2 - L_8^2 - L_9^2 - L_6^2}{2L_6L_8L_9};\ K_2 = \frac{1}{L_6}\cos\theta_8 - \frac{1}{L_8}\cos\theta_6 \tag{A.23}$$

$$K_3 = \frac{1}{L_6}\sin\theta_8 - \frac{1}{L_8}\sin\theta_6;\ K_4 = \frac{1}{L_9}(\cos\theta_6\cos\theta_8 + \sin\theta_6\sin\theta_8). \tag{A.24}$$

From the parallelogram mechanism, $L_6L_8L_9L_{10}$, the joint angle θ_{10} can be calculated as given by

$$\theta_{10} = 2\tan^{-1}\left(\frac{-E-\sqrt{E^2-4DF}}{2D}\right) \tag{A.25}$$

where

$$D = K_1 + K_2 + K_4;\ E = -2K_3;\ F = K_4 - K_2 + K_1 \tag{A.26}$$

and

$$K_1 = \frac{L_9^2 - L_6^2 - L_8^2 - L_{10}^2}{2L_6L_8L_{10}};\ K_2 = \frac{1}{L_8}\cos\theta_6 - \frac{1}{L_6}\cos\theta_8 \tag{A.27}$$

$$K_3 = \frac{1}{L_8}\sin\theta_6 - \frac{1}{L_6}\sin\theta_8;\ K_4 = \frac{1}{L_{10}}(\cos\theta_6\cos\theta_8 + \sin\theta_6\sin\theta_8). \tag{A.28}$$

From the rigid foot-link, $L_9L_{11}L_{12}$, the joint angles θ_{11} and θ_{12} can be calculated as given by

$$\theta_{11} = 2\tan^{-1}\left(\frac{-E-\sqrt{E^2-4DF}}{2D}\right) \quad \text{(A.29)}$$

$$\theta_{12} = 2\tan^{-1}\left(\frac{-B-\sqrt{B^2-4AC}}{2A}\right) \quad \text{(A.30)}$$

where

$$A = K_1 + \cos\theta_9;\ B = -2\sin\theta_9 \quad \text{(A.31)}$$

$$C = K_1 - \cos\theta_9;\ D = K_2 + \cos\theta_9 \quad \text{(A.32)}$$

$$E = -2\sin\theta_9;\ F = K_2 - \cos\theta_9 \quad \text{(A.33)}$$

and

$$K_1 = \frac{L_{11}^2 - L_9^2 - L_{12}^2}{2L_9L_{12}};\ K_2 = \frac{L_{11}^2 + L_9^2 - L_{12}^2}{2L_9L_{11}}. \quad \text{(A.34)}$$

Finally, the joint positions, $P_1 - P_E$ can be calculated as given by

$$P_1 = L_1\cos\theta_2 + jL_1\sin\theta_2 \quad \text{(A.35)}$$

$$P_2 = P_1 + L_2\cos\theta_3 + jL_2\sin\theta_3 = P_3 + L_3\cos\theta_4 + jL_3\sin\theta_4 \quad \text{(A.36)}$$

$$P_3 = L_1 + j0 \quad \text{(A.37)}$$

$$P_4 = P_3 + L_6\cos\theta_6 + jL_6\sin\theta_6 = P_2 + L_5\cos\theta_5 + jL_5\sin\theta_5 \quad \text{(A.38)}$$

$$P_5 = P_1 + L_7\cos\theta_7 + jL_7\sin\theta_7 = P_3 + L_8\cos\theta_8 + jL_8\sin\theta_8 \quad \text{(A.39)}$$

$$P_6 = P_4 + L_{10}\cos\theta_{10} + jL_{10}\sin\theta_{10} = P_5 + L_9\cos\theta_9 + jL_9\sin\theta_9 \quad \text{(A.40)}$$

$$P_E = P_5 + L_{11}\cos\theta_{11} + jL_{11}\sin\theta_{11} = P_6 + L_{12}\cos\theta_{12} + jL_{12}\sin\theta_{12}. \quad \text{(A.41)}$$

Appendix B

Symmetry Ratio Plots

B.1 Symmetry of Overall Gait Features over Time

The Mahalanobis distance was used to observe overall gait symmetry. The overall gait symmetry including spatiotemporal, limb and joint kinematic features over time plots are depicted in Fig B.1.

B.2 Deviation of Gait Parameters over Time and Gait Speed

The deviation between unaffected and affected sides of each parameter can be determined by the symmetry ratio without the absolute value from Eq. (5.1). Here, the changes in symmetry ratio (i.e., sr_i) over time and speed plots of individual gait parameters are illustrated in Figs. B.2 (spatiotemporal characteristics), B.3 (limb kinematics), and B.4 (joint kinematics). Note that positive value of symmetry ratio indicates unaffected side greater than the affected side and the negative value indicates vice versa.

B.3 Case Study: Patient 5 vs. Patient 6

The symmetry ratio, sr_i, of individual gait parameters over time plots of patient 5 and 6 are illustrated in Figs. B.5 (spatiotemporal characteristics), B.6 (limb kinematics), and B.7 (joint kinematics).

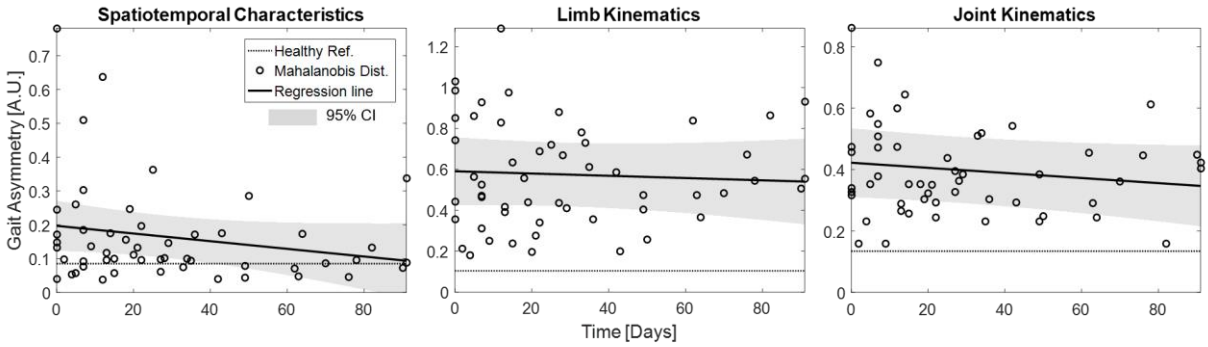

Figure B.1: Change in gait symmetry measures of spatiotemporal characteristics (left), limb kinematics (middle), and joint kinematics (right) over time. The dotted line is considered as the threshold for symmetric walking. The regression lines are based on linear mixed regression model. Note that the all trends are not strong compare to gait symmetry over gait speed plots (see Fig. 5.4).

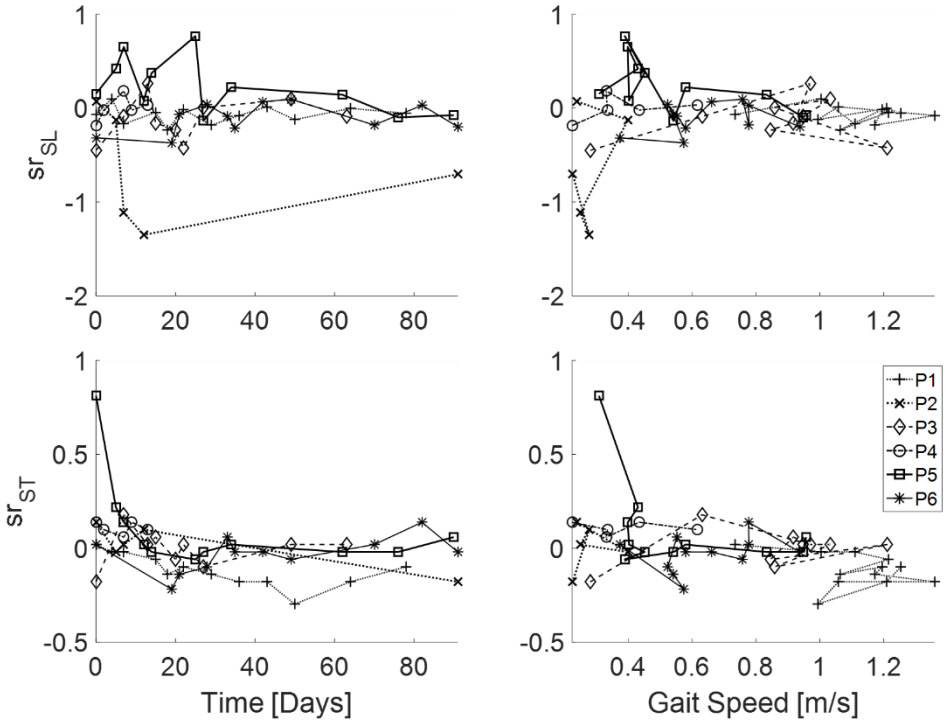

Figure B.2: Change in symmetry ratio of spatiotemporal parameters over time (left column) and gait speed (right column) for all six patients. Step length (top row) and step time (bottom row).

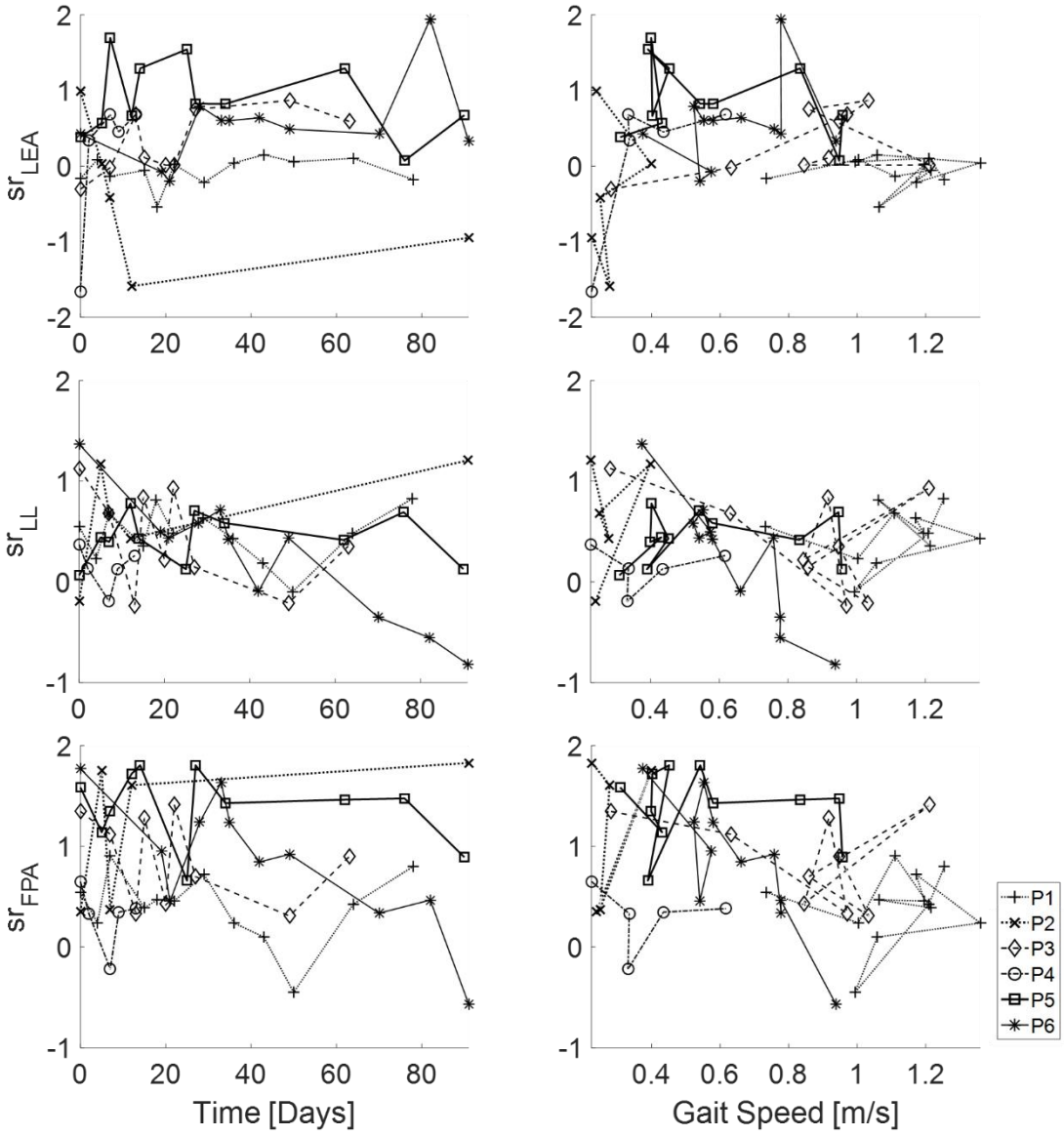

Figure B.3: Change in symmetry ratio of limb kinematic parameters over time (left column) and gait speed (right column) for all six patients. Leg extension angle (top row), limb length (middle row) and foot path area (bottom row).

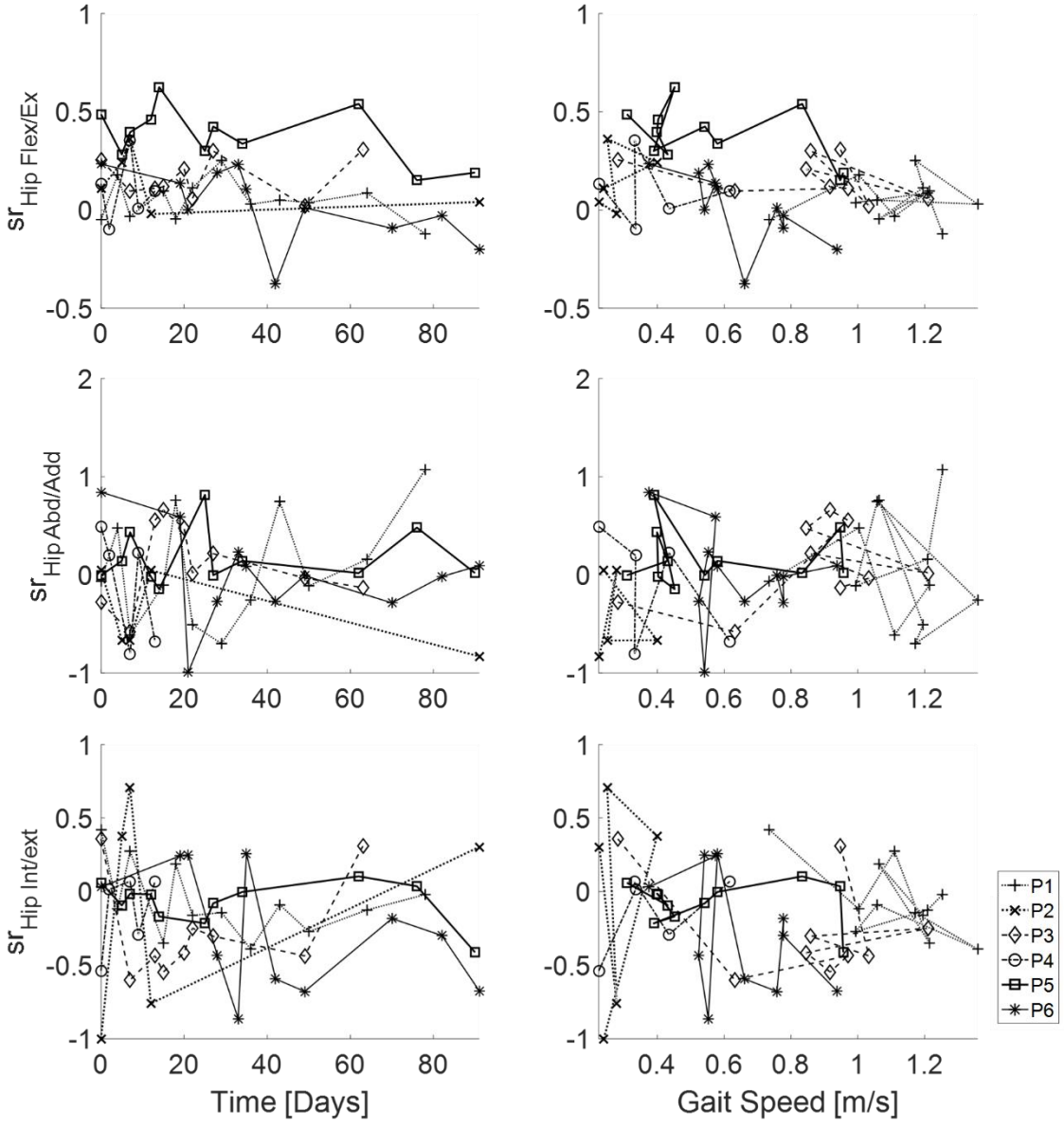

Continued on next page,

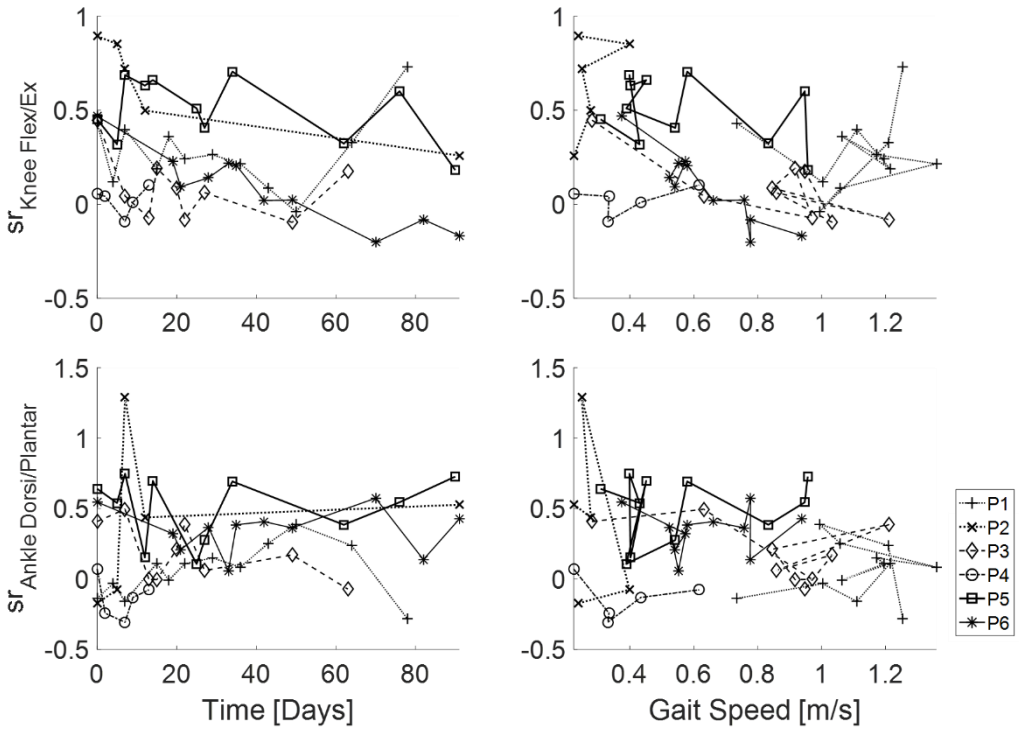

Figure B.4: Change in symmetry ratio of joint kinematic parameters over time (left column) and gait speed (right column) for all six patients. Hip flex/extension (top row), hip abd/adduction (second row), hip int/external rotation (third row), knee flex/extension (fourth row), and ankle dorsi/plantarflexion (bottom row).

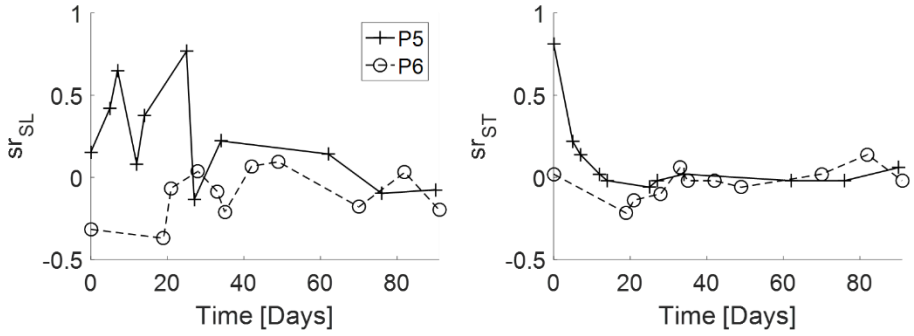

Figure B.5: Change in symmetry ratio of spatiotemporal parameters over time (P5: patient 5 and P6: patient 6). Step length (left) and step time (right).

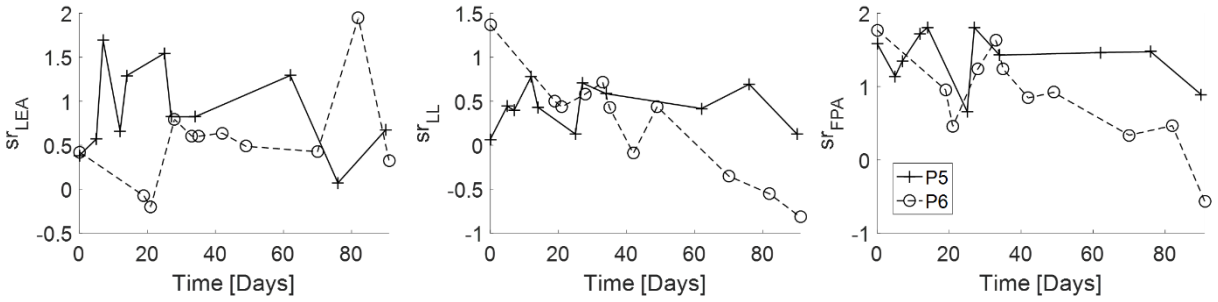

Figure B.6: Change in symmetry ratio of limb kinematic parameters over time (P5: patient 5 and P6: patient 6). Leg extension angle (left), limb length (middle) and foot path area (right).

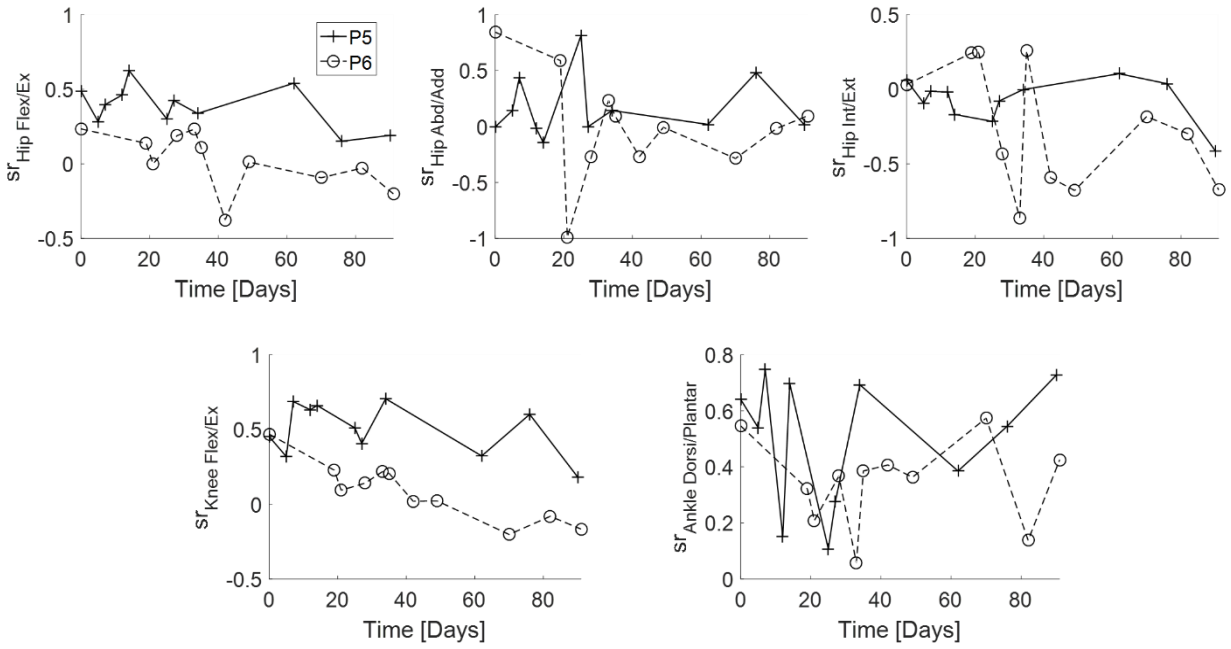

Figure B.7: Change in symmetry ratio of joint kinematic parameters over time (P5: patient 5 and P6: patient 6). Hip flex/extension (top left), hip abd/adduction (top middle), hip int/external rotation (top right), knee flex/extension (bottom left), and ankle dorsi/plantarflexion (bottom right).

Bibliography

[1] H. S. Jørgensen, H. Nakayama, H. O. Raaschou, and T. S. Olsen, "Recovery of walking function in stroke patients: the Copenhagen Stroke Study," *Arch. Phys. Med. Rehabil.*, vol. 76, no. 1, pp. 27–32, 1995.

[2] D. Mozaffarian *et al.*, "Executive Summary: Heart Disease and Stroke Statistics-2016 Update: A Report From the American Heart Association.," *Circulation*, vol. 133, no. 4, p. 447, 2016.

[3] C. for Medicare, M. S. 7500 S. B. Baltimore, and M. Usa, "Overview," 21-Dec-2018. [Online]. Available: https://www.cms.gov/Medicare/billing/therapyServices/index.html. [Accessed: 06-Apr-2019].

[4] K. M. Godwin, J. Wasserman, and S. K. Ostwald, "Cost associated with stroke: outpatient rehabilitative services and medication," *Top. Stroke Rehabil.*, vol. 18, no. sup1, pp. 676–684, 2011.

[5] S. Dodini, "Report on the Economic Well-Being of US Households in 2015," in *2016 Fall Conference: The Role of Research in Making Government More Effective*, 2016.

[6] J. Cubanski, G. Casillas, and A. Damico, "Poverty among seniors: An updated analysis of national and state level poverty rates under the official and supplemental poverty measures," *Kais. Fam. Found.*, 2015.

[7] A. M. Cox, C. McKevitt, A. G. Rudd, and C. D. Wolfe, “Socioeconomic status and stroke,” *Lancet Neurol.*, vol. 5, no. 2, pp. 181–188, 2006.

[8] J. J. Shen and E. L. Washington, “Disparities in outcomes among patients with stroke associated with insurance status,” *Stroke*, vol. 38, no. 3, pp. 1010–1016, 2007.

[9] R. Bonita and R. Beaglehole, “Stroke Prevention in Poor Countries Time for Action,” *Stroke*, vol. 38, no. 11, pp. 2871–2872, 2007.

[10] B. Norrving and B. Kissela, “The global burden of stroke and need for a continuum of care,” *Neurology*, vol. 80, no. 3 Supplement 2, pp. S5–S12, 2013.

[11] E. T. Whittaker, A treatise on the analytical dynamics of particles and rigid bodies. *Cambridge University Press*, 1988.

[12] G. Colombo, M. Joerg, R. Schreier, and V. Dietz, “Treadmill training of paraplegic patients using a robotic orthosis,” *J. Rehabil. Res. Dev.*, vol. 37, no. 6, p. 693, 2000.

[13] J. Mehrholz, B. Elsner, C. Werner, J. Kugler, and M. Pohl, “Electromechanical-assisted training for walking after stroke,” *Cochrane Libr.*, 2013.

[14] K. Y. Nam, H. J. Kim, B. S. Kwon, J. W. Park, H. J. Lee, and A. Yoo, “Robot-assisted gait training (Lokomat) improves walking function and activity in people with spinal cord injury: a systematic review,” *J. Neuroengineering Rehabil.*, vol. 14, no. 1, p. 24, 2017.

[15] M. Patrick, “Overview: Assessing hospital companies’ capital expenditures, in An investor’s guide to the US hospital Industry PART 11 OF 16,” *Market Realist*, 16-Nov-2014.

[16] S. K. Banala, S. H. Kim, S. K. Agrawal, and J. P. Scholz, "Robot assisted gait training with active leg exoskeleton (ALEX)," *IEEE Trans. Neural Syst. Rehabil. Eng.*, vol. 17, no. 1, pp. 2–8, 2009.

[17] R. Riener, L. Lunenburger, S. Jezernik, M. Anderschitz, G. Colombo, and V. Dietz, "Patient-cooperative strategies for robot-aided treadmill training: first experimental results," *IEEE Trans. Neural Syst. Rehabil. Eng.*, vol. 13, no. 3, pp. 380–394, 2005.

[18] J. L. Emken, R. Benitez, and D. J. Reinkensmeyer, "Human-robot cooperative movement training: learning a novel sensory motor transformation during walking with robotic assistance-as-needed," *J. NeuroEngineering Rehabil.*, vol. 4, no. 1, p. 8, 2007.

[19] B. Koopman, E. H. F. Van Asseldonk, and H. Van der Kooij, "Speed-dependent reference joint trajectory generation for robotic gait support," *J. Biomech.*, vol. 47, no. 6, pp. 1447–1458, 2014.

[20] X. Wu, D. X. Liu, M. Liu, C. Chen, and H. Guo, "Individualized Gait Pattern Generation for Sharing Lower Limb Exoskeleton Robot," *IEEE Trans. Autom. Sci. Eng.*, no. 99, pp. 1–12, 2018.

[21] G. Kwakkel, B. Kollen, and J. Twisk, "Impact of time on improvement of outcome after stroke," *Stroke*, vol. 37, no. 9, pp. 2348–2353, Sep. 2006.

[22] F. Coupar, A. Pollock, P. Rowe, C. Weir, and P. Langhorne, "Predictors of upper limb recovery after stroke: a systematic review and meta-analysis," *Clin. Rehabil.*, vol. 26, no. 4, pp. 291–313, 2012.

[23] S. Prabhakaran *et al.*, "Inter-individual variability in the capacity for motor recovery after ischemic stroke," *Neurorehabil. Neural Repair*, vol. 22, no. 1, pp. 64–71, 2008.

[24] M. C. Smith, W. D. Byblow, P. A. Barber, and C. M. Stinear, "Proportional recovery from lower limb motor impairment after stroke," *Stroke*, vol. 48, no. 5, pp. 1400–1403, 2017.

[25] S. Viteckova, P. Kutilek, Z. Svoboda, R. Krupicka, J. Kauler, and Z. Szabo, "Gait symmetry measures: A review of current and prospective methods," *Biomed. Signal Process. Control*, vol. 42, pp. 89–100, 2018.

[26] C. M. Kim and J. J. Eng, "Magnitude and pattern of 3D kinematic and kinetic gait profiles in persons with stroke: relationship to walking speed," *Gait Posture*, vol. 20, no. 2, pp. 140–146, 2004.

[27] B. Balaban and F. Tok, "Gait Disturbances in Patients With Stroke," *PM&R*, vol. 6, no. 7, pp. 635–642, 2014.

[28] Y. H. Chang, A. G. Auyang, J. P. Scholz, and T. R. Nichols, "Whole limb kinematics are preferentially conserved over individual joint kinematics after peripheral nerve injury," *J. Exp. Biol.*, vol. 212, no. 21, pp. 3511–3521, 2009.

[29] M. Paulich, M. Schepers, N. Rudigkeit, and G. Bellusci, "Xsens MTw Awinda: Miniature Wireless Inertial-Magnetic Motion Tracker for Highly Accurate 3D Kinematic Applications," Xsens Technologies Report, 2018.

[30] J. T. Zhang, A. C. Novak, B. Brouwer, and Q. Li, "Concurrent validation of Xsens MVN measurement of lower limb joint angular kinematics," *Physiol. Meas.*, vol. 34, no. 8, p. N63, 2013.

[31] Y. Yun, H. C. Kim, S. Y. Shin, J. Lee, A. D. Deshpande, and C. Kim, “Statistical method for prediction of gait kinematics with Gaussian process regression,” *J. Biomech.*, vol. 47, no. 1, pp. 186–192, 2014.

[32] J. Mehrholz and M. Pohl, “Electromechanical-assisted gait training after stroke: a systematic review comparing end-effector and exoskeleton devices,” *J. Rehabil. Med.*, vol. 44, no. 3, pp. 193–199, 2012.

[33] I. Díaz, J. J. Gil, and E. Sánchez, “Lower-limb robotic rehabilitation: literature review and challenges,” *J. Robot.*, vol. 2011, 2011.

[34] C. Glackin *et al.*, “Gait trajectory prediction using Gaussian process ensembles,” in *Humanoid Robots (Humanoids), 2014 14th IEEE-RAS International Conference on*, 2014, pp. 628–633.

[35] N. B. Melo, C. E. Dorea, P. J. Alsina, and M. V. Araujo, “Joint trajectory generator for powered orthosis based on gait modelling using PCA and FFT,” *Robotica*, vol. 36, no. 3, pp. 395–407, 2018.

[36] S. Ren, W. Wang, Z. G. Hou, X. Liang, J. Wang, and L. Peng, “Anthropometric Features Based Gait Pattern Prediction Using Random Forest for Patient-Specific Gait Training,” in *International Conference on Neural Information Processing*, 2018, pp. 15–26.

[37] D. Aoyagi, W. E. Ichinose, S. J. Harkema, D. J. Reinkensmeyer, and J. E. Bobrow, “A robot and control algorithm that can synchronously assist in naturalistic motion during body-weight-supported gait training following neurologic injury,” *IEEE Trans. Neural Syst. Rehabil. Eng.*, vol. 15, no. 3, pp. 387–400, 2007.

[38] J. L. Emken, S. J. Harkema, J. A. Beres-Jones, C. K. Ferreira, and D. J. Reinkensmeyer, “Feasibility of manual teach-and-replay and continuous impedance shaping for robotic locomotor training following spinal cord injury,” *IEEE Trans. Biomed. Eng.*, vol. 55, no. 1, pp. 322–334, 2008.

[39] H. Vallery, E. H. Van Asseldonk, M. Buss, and H. Van Der Kooij, “Reference trajectory generation for rehabilitation robots: complementary limb motion estimation,” *IEEE Trans. Neural Syst. Rehabil. Eng.*, vol. 17, no. 1, pp. 23–30, 2009.

[40] R. P. Van Peppen, G. Kwakkel, S. Wood-Dauphinee, H. J. Hendriks, P. J. Van der Wees, and J. Dekker, “The impact of physical therapy on functional outcomes after stroke: what’s the evidence?,” *Clin. Rehabil.*, vol. 18, no. 8, pp. 833–862, 2004.

[41] T. G. Hornby *et al.*, “Variable Intensive Early Walking Poststroke (VIEWS): A Randomized Controlled Trial,” *Neurorehabil. Neural Repair*, vol. 30, no. 5, pp. 440–450, Jun. 2016.

[42] J. K. Tilson *et al.*, “Meaningful gait speed improvement during the first 60 days poststroke: minimal clinically important difference,” *Phys. Ther.*, vol. 90, no. 2, pp. 196–208, 2010.

[43] D. Podsiadlo and S. Richardson, “The timed ‘Up & Go’: a test of basic functional mobility for frail elderly persons,” *J. Am. Geriatr. Soc.*, vol. 39, no. 2, pp. 142–148, 1991.

[44] P. L. Enright, “The six-minute walk test,” *Respir. Care*, vol. 48, no. 8, pp. 783–785, 2003.

[45] J. K. Tilson *et al.*, “Meaningful gait speed improvement during the first 60 days poststroke: minimal clinically important difference,” *Phys. Ther.*, vol. 90, no. 2, pp. 196–208, 2010.

[46] V. Weerdesteyn, M. de Niet, H. J. van Duijnhoven, and A. C. Geurts, “Falls in individuals with stroke,” *J. Rehabil. Res. Dev.*, vol. 45, no. 8, pp. 1195–1214, 2008.

[47] M. F. Levin, J. A. Kleim, and S. L. Wolf, “What do motor ‘recovery’ and ‘compensation’ mean in patients following stroke?,” *Neurorehabil. Neural Repair*, vol. 23, no. 4, pp. 313–319, 2009.

[48] T. A. Jones, “Motor compensation and its effects on neural reorganization after stroke,” *Nat. Rev. Neurosci.*, vol. 18, no. 5, p. 267, 2017.

[49] S. M. Woolley, “Characteristics of gait in hemiplegia,” *Top. Stroke Rehabil.*, vol. 7, no. 4, pp. 1–18, 2001.

[50] J. F. Veneman, R. Ekkelenkamp, R. Kruidhof, F. C. T. Van der Helm, and H. Van der Kooij, “Design of a series elastic-and Bowden cable-based actuation system for use as torque-actuator in exoskeleton-type training,” in *9th International Conference on Rehabilitation Robotics, 2005. ICORR 2005.*, 2005, pp. 496–499.

[51] S. Hesse and D. Uhlenbrock, “A mechanized gait trainer for restoration of gait,” *J. Rehabil. Res. Dev.*, vol. 37, no. 6, pp. 701–708, 2000.

[52] H. Schmid, S. Hesse, R. Benhardt, and J. Kruger, “Haptic walker-A Novel HaPtic Foot Device ACM,” *Transacitons Appl. Percept.*, vol. 2, no. 2, pp. 166–180, 2005.

[53] S. Freivogel, J. Mehrholz, T. Husak-Sotomayor, and D. Schmalohr, “Gait training with the newly developed ‘LokoHelp’-system is feasible for non-ambulatory

patients after stroke, spinal cord and brain injury. A feasibility study," *Brain Inj.*, vol. 22, no. 7–8, pp. 625–632, 2008.

[54] J. Mehrholz and M. Pohl, "Electromechanical-assisted gait training after stroke: a systematic review comparing end-effector and exoskeleton devices," *J. Rehabil. Med.*, vol. 44, no. 3, pp. 193–199, 2012.

[55] S. Hesse *et al.*, "Treadmill training with partial body weight support compared with physiotherapy in nonambulatory hemiparetic patients," *Stroke*, vol. 26, no. 6, pp. 976–981, 1995.

[56] M. Pohl *et al.*, "Repetitive locomotor training and physiotherapy improve walking and basic activities of daily living after stroke: a single-blind, randomized multicentre trial (DEutsche GAngtrainerStudie, DEGAS)," *Clin. Rehabil.*, vol. 21, no. 1, pp. 17–27, 2007.

[57] S. Hesse, C. Werner, D. Uhlenbrock, S. V. Frankenberg, A. Bardeleben, and B. Brandl-Hesse, "An electromechanical gait trainer for restoration of gait in hemiparetic stroke patients: preliminary results," *Neurorehabil. Neural Repair*, vol. 15, no. 1, pp. 39–50, 2001.

[58] C. Werner, S. Von Frankenberg, T. Treig, M. Konrad, and S. Hesse, "Treadmill training with partial body weight support and an electromechanical gait trainer for restoration of gait in subacute stroke patients a randomized crossover study," *Stroke*, vol. 33, no. 12, pp. 2895–2901, 2002.

[59] A. Mayr, M. Kofler, E. Quirbach, H. Matzak, K. Fröhlich, and L. Saltuari, "Prospective, blinded, randomized crossover study of gait rehabilitation in stroke

patients using the Lokomat gait orthosis," *Neurorehabil. Neural Repair*, vol. 21, no. 4, pp. 307–314, 2007.

[60] C. D. M. Simons, E. H. F. van Asseldonk, J. I. Folkersma, J. van den Hoek, M. Postma, and J. H. Buurke, "First clinical results with the new innovative robotic gait trainer LOPES," 2009.

[61] B. Husemann, F. Müller, C. Krewer, S. Heller, and E. Koenig, "Effects of locomotion training with assistance of a robot-driven gait orthosis in hemiparetic patients after stroke a randomized controlled pilot study," *Stroke*, vol. 38, no. 2, pp. 349–354, 2007.

[62] S. H. Peurala, I. M. Tarkka, K. Pitkänen, and J. Sivenius, "The effectiveness of body weight-supported gait training and floor walking in patients with chronic stroke," *Arch. Phys. Med. Rehabil.*, vol. 86, no. 8, pp. 1557–1564, 2005.

[63] K. P. Westlake and C. Patten, "Pilot study of Lokomat versus manual-assisted treadmill training for locomotor recovery post-stroke," *J. Neuroengineering Rehabil.*, vol. 6, no. 1, p. 1, 2009.

[64] Robotics business review, "Healthcare Robotics: 2014," 2014.

[65] S. Freivogel, D. Schmalohr, and J. Mehrholz, "Improved walking ability and reduced therapeutic stress with an electromechanical gait device," *J. Rehabil. Med.*, vol. 41, no. 9, pp. 734–739, 2009.

[66] J. A. Beres-Jones and S. J. Harkema, "The human spinal cord interprets velocity-dependent afferent input during stepping," *Brain*, vol. 127, no. 10, pp. 2232–2246, 2004.

[67] V. Dietz, G. Colombo, and L. Jensen, “Locomotor activity in spinal man,” *The lancet*, vol. 344, no. 8932, pp. 1260–1263, 1994.

[68] Y. Laufer, R. Dickstein, Y. Chefez, and E. Marcovitz, “The effect of treadmill training on the ambulation of stroke survivors in the early stages of rehabilitation: a randomized study,” *J. Rehabil. Res. Dev.*, vol. 38, no. 1, p. 69, 2001.

[69] R. F. Macko *et al.*, “Treadmill exercise rehabilitation improves ambulatory function and cardiovascular fitness in patients with chronic stroke a randomized, controlled trial,” *Stroke*, vol. 36, no. 10, pp. 2206–2211, 2005.

[70] V. Dietz, “Proprioception and locomotor disorders,” *Nat. Rev. Neurosci.*, vol. 3, no. 10, pp. 781–790, 2002.

[71] B. Jansen, E. L. Doubrovski, and J. C. Verlinden, “Animaris Geneticus Parvus: Design of a complex multi-body walking mechanism,” *Rapid Prototyp. J.*, vol. 20, no. 4, pp. 311–319, 2014.

[72] D. A. Cunningham, P. A. Rechnitzer, M. E. Pearce, and A. P. Donner, “Determinants of self-selected walking pace across ages 19 to 66,” *J. Gerontol.*, vol. 37, no. 5, pp. 560–564, 1982.

[73] R. L. Norton, Design of machinery: an introduction to the synthesis and analysis of mechanisms and machines. *McGraw-Hill Professional*, 2004.

[74] A. Ravindran, G. V. Reklaitis, and K. M. Ragsdell, Engineering optimization: methods and applications. *John Wiley & Sons*, 2006.

[75] K. Kora, J. Stinear, and A. McDaid, “Design, Analysis, and Optimization of an Acute Stroke Gait Rehabilitation Device,” *J. Med. Devices*, vol. 11, no. 1, p. 014503, 2017.

[76] C. Y. Jung, J. Choi, S. Park, J. M. Lee, C. Kim, and S. J. Kim, “Design and control of an exoskeleton system for gait rehabilitation capable of natural pelvic movement,” in *2014 IEEE/RSJ International Conference on Intelligent Robots and Systems*, 2014, pp. 2095–2100.

[77] G. Morone *et al.*, “Robot-assisted gait training for stroke patients: current state of the art and perspectives of robotics,” *Neuropsychiatr. Dis. Treat.*, vol. 13, p. 1303, 2017.

[78] E. H. F. van Asseldonk, J. F. Veneman, R. Ekkelenkamp, J. H. Buurke, F. C. T. van der Helm, and H. van der Kooij, “The Effects on Kinematics and Muscle Activity of Walking in a Robotic Gait Trainer During Zero-Force Control,” *IEEE Trans. Neural Syst. Rehabil. Eng.*, vol. 16, no. 4, pp. 360–370, Aug. 2008.

[79] A. Duschau-Wicke, J. von Zitzewitz, A. Caprez, L. Lunenburger, and R. Riener, “Path control: a method for patient-cooperative robot-aided gait rehabilitation,” *IEEE Trans. Neural Syst. Rehabil. Eng.*, vol. 18, no. 1, pp. 38–48, 2010.

[80] R. Riener, “Technology of the Robotic Gait Orthosis Lokomat,” in *Neurorehabilitation Technology*, V. Dietz, T. Nef, and W. Z. Rymer, Eds. Springer London, 2012, pp. 221–232.

[81] A. Q. Tan and Y. Y. Dhaher, “Evaluation of lower limb cross planar kinetic connectivity signatures post-stroke,” *J. Biomech.*, vol. 47, no. 5, pp. 949–956, 2014.

[82] Y. Stauffer *et al.*, “The WalkTrainer—a new generation of walking reeducation device combining orthoses and muscle stimulation,” *IEEE Trans. Neural Syst. Rehabil. Eng.*, vol. 17, no. 1, pp. 38–45, 2009.

[83] H. Yano, K. Kasai, H. Saitou, and H. Iwata, “Development of a gait rehabilitation system using a locomotion interface,” *J. Vis. Comput. Animat.*, vol. 14, no. 5, pp. 243–252, 2003.

[84] D. C. Kerrigan, M. K. Todd, U. Della Croce, L. A. Lipsitz, and J. J. Collins, “Biomechanical gait alterations independent of speed in the healthy elderly: evidence for specific limiting impairments,” *Arch. Phys. Med. Rehabil.*, vol. 79, no. 3, pp. 317–322, 1998.

[85] J. L. Lelas, G. J. Merriman, P. O. Riley, and D. C. Kerrigan, “Predicting peak kinematic and kinetic parameters from gait speed,” *Gait Posture*, vol. 17, no. 2, pp. 106–112, 2003.

[86] D. A. Winter, *Biomechanics and motor control of human movement*. John Wiley & Sons, 2009.

[87] C. English, J. Bernhardt, M. Crotty, A. Esterman, L. Segal, and S. Hillier, “Circuit class therapy or seven-day week therapy for increasing rehabilitation intensity of therapy after stroke (CIRCIT): a randomized controlled trial,” *Int. J. Stroke*, vol. 10, no. 4, pp. 594–602, 2015.

[88] C. E. Lang *et al.*, “Observation of amounts of movement practice provided during stroke rehabilitation,” *Arch. Phys. Med. Rehabil.*, vol. 90, no. 10, pp. 1692–1698, 2009.

[89] M. A. Urbin, R. R. Bailey, and C. E. Lang, "Validity of body-worn sensor acceleration metrics to index upper extremity function in hemiparetic stroke," *J. Neurol. Phys. Ther. JNPT*, vol. 39, no. 2, p. 111, 2015.

[90] T. G. Hornby *et al.*, "Feasibility of focused stepping practice during inpatient rehabilitation poststroke and potential contributions to mobility outcomes," *Neurorehabil. Neural Repair*, vol. 29, no. 10, pp. 923–932, 2015.

[91] T. D. Klassen, J. A. Semrau, S. P. Dukelow, M. T. Bayley, M. D. Hill, and J. J. Eng, "Consumer-based physical activity monitor as a practical way to measure walking intensity during inpatient stroke rehabilitation," *Stroke*, vol. 48, no. 9, pp. 2614–2617, 2017.

[92] S. L. Wolf *et al.*, "Effect of constraint-induced movement therapy on upper extremity function 3 to 9 months after stroke: the EXCITE randomized clinical trial," *Jama*, vol. 296, no. 17, pp. 2095–2104, 2006.

[93] C. L. Holleran, D. D. Straube, C. R. Kinnaird, A. L. Leddy, and T. G. Hornby, "Feasibility and potential efficacy of high-intensity stepping training in variable contexts in subacute and chronic stroke," *Neurorehabil. Neural Repair*, vol. 28, no. 7, pp. 643–651, 2014.

[94] J. A. Zeni Jr, J. G. Richards, and J. S. Higginson, "Two simple methods for determining gait events during treadmill and overground walking using kinematic data," *Gait Posture*, vol. 27, no. 4, pp. 710–714, 2008.

[95] M. B. Gilman, "The use of heart rate to monitor the intensity of endurance training," *Sports Med.*, vol. 21, no. 2, pp. 73–79, 1996.

[96] R. M. Carney, K. E. Freedland, P. K. Stein, J. A. Skala, P. Hoffman, and A. S. Jaffe, "Change in heart rate and heart rate variability during treatment for depression in patients with coronary heart disease," *Psychosom. Med.*, vol. 62, no. 5, pp. 639–647, 2000.

[97] D. A. Winter, Biomechanics and motor control of human movement. *John Wiley & Sons*, 2009.

[98] S. Nakagawa and H. Schielzeth, "A general and simple method for obtaining R2 from generalized linear mixed-effects models," *Methods Ecol. Evol.*, vol. 4, no. 2, pp. 133–142, 2013.

[99] G. Kwakkel *et al.*, "Effects of augmented exercise therapy time after stroke a meta-analysis," *Stroke*, vol. 35, no. 11, pp. 2529–2539, 2004.

[100] K. R. Lohse, C. E. Lang, and L. A. Boyd, "Is more better? Using metadata to explore dose–response relationships in stroke rehabilitation," *Stroke*, vol. 45, no. 7, pp. 2053–2058, 2014.

[101] T. G. Hornby, J. L. Moore, L. Lovell, and E. J. Roth, "Influence of skill and exercise training parameters on locomotor recovery during stroke rehabilitation," *Curr. Opin. Neurol.*, vol. 29, no. 6, pp. 677–683, 2016.

[102] K. Scrivener, C. Sherrington, and K. Schurr, "Amount of exercise in the first week after stroke predicts walking speed and unassisted walking," *Neurorehabil. Neural Repair*, vol. 26, no. 8, pp. 932–938, 2012.

[103] J. Crosbie, R. Vachalathiti, and R. Smith, "Age, gender and speed effects on spinal kinematics during walking," *Gait Posture*, vol. 5, no. 1, pp. 13–20, 1997.

[104] S. W. Saunders, A. Schache, D. Rath, and P. W. Hodges, “Changes in three dimensional lumbo-pelvic kinematics and trunk muscle activity with speed and mode of locomotion,” *Clin. Biomech.*, vol. 20, no. 8, pp. 784–793, 2005.

[105] P. J. Rowe, C. M. Myles, C. Walker, and R. Nutton, “Knee joint kinematics in gait and other functional activities measured using flexible electrogoniometry: how much knee motion is sufficient for normal daily life?,” *Gait Posture*, vol. 12, no. 2, pp. 143–155, 2000.

[106] D. T. P. Fong and Y. Y. Chan, “The use of wearable inertial motion sensors in human lower limb biomechanics studies: a systematic review,” *Sensors*, vol. 10, no. 12, pp. 11556–11565, 2010.

[107] C. M. Kim and J. J. Eng, “The relationship of lower-extremity muscle torque to locomotor performance in people with stroke,” *Phys. Ther.*, vol. 83, no. 1, pp. 49–57, 2003.

[108] M. Camicia, H. Wang, M. DiVita, J. Mix, and P. Niewczyk, “Length of stay at inpatient rehabilitation facility and stroke patient outcomes,” *Rehabil. Nurs.*, vol. 41, no. 2, pp. 78–90, 2016.

[109] K. J. Ottenbacher, Y. Hsu, C. V. Granger, and R. C. Fiedler, “The reliability of the functional independence measure: A quantitative review,” *Arch. Phys. Med. Rehabil.*, vol. 77, no. 12, pp. 1226–1232, Dec. 1996.

[110] L. Blum and N. Korner-Bitensky, “Usefulness of the Berg Balance Scale in Stroke Rehabilitation: A Systematic Review,” *Phys. Ther.*, vol. 88, no. 5, pp. 559–566, May 2008.

[111] S. L. Whitney, D. M. Wrisley, G. F. Marchetti, M. A. Gee, M. S. Redfern, and J. M. Furman, “Clinical Measurement of Sit-to-Stand Performance in People With Balance Disorders: Validity of Data for the Five-Times-Sit-to-Stand Test,” *Phys. Ther.*, vol. 85, no. 10, pp. 1034–1045, Oct. 2005.

[112] W. H. K. De Vries, H. E. J. Veeger, C. T. M. Baten, and F. C. T. Van Der Helm, “Magnetic distortion in motion labs, implications for validating inertial magnetic sensors,” *Gait Posture*, vol. 29, no. 4, pp. 535–541, 2009.

[113] M. Sathiyanarayanan and S. Rajan, “MYO Armband for physiotherapy healthcare: A case study using gesture recognition application,” in *Communication Systems and Networks (COMSNETS), 2016 8th International Conference on*, 2016, pp. 1–6.

[114] A. Muro-De-La-Herran, B. Garcia-Zapirain, and A. Mendez-Zorrilla, “Gait analysis methods: An overview of wearable and non-wearable systems, highlighting clinical applications,” *Sensors*, vol. 14, no. 2, pp. 3362–3394, 2014.

[115] S. Barreca, S. L. Wolf, S. Fasoli, and R. Bohannon, “Treatment interventions for the paretic upper limb of stroke survivors: a critical review,” *Neurorehabil. Neural Repair*, vol. 17, no. 4, pp. 220–226, 2003.

[116] S. L. Patterson, M. M. Rodgers, R. F. Macko, and L. W. Forrester, “Effect of treadmill exercise training on spatial and temporal gait parameters in subjects with chronic stroke: a preliminary report,” *J. Rehabil. Res. Dev.*, vol. 45, no. 2, p. 221, 2008.

[117] C. K. Balasubramanian, M. G. Bowden, R. R. Neptune, and S. A. Kautz, “Relationship between step length asymmetry and walking performance in subjects

with chronic hemiparesis," *Arch. Phys. Med. Rehabil.*, vol. 88, no. 1, pp. 43–49, 2007.

[118] K. K. Patterson, W. H. Gage, D. Brooks, S. E. Black, and W. E. McIlroy, "Evaluation of gait symmetry after stroke: a comparison of current methods and recommendations for standardization," *Gait Posture*, vol. 31, no. 2, pp. 241–246, 2010.

[119] K. K. Patterson, A. Mansfield, L. Biasin, K. Brunton, E. L. Inness, and W. E. McIlroy, "Longitudinal changes in poststroke spatiotemporal gait asymmetry over inpatient rehabilitation," *Neurorehabil. Neural Repair*, vol. 29, no. 2, pp. 153–162, 2015.

[120] J. Perry and J. M. Burnfield, "Gait analysis: normal and pathological function," 1992.

[121] C. L. Peterson, J. Cheng, S. A. Kautz, and R. R. Neptune, "Leg extension is an important predictor of paretic leg propulsion in hemiparetic walking," *Gait Posture*, vol. 32, no. 4, pp. 451–456, 2010.

[122] R. Verma, K. N. Arya, P. Sharma, and R. K. Garg, "Understanding gait control in post-stroke: implications for management," *J. Bodyw. Mov. Ther.*, vol. 16, no. 1, pp. 14–21, 2012.

[123] T. Ramakrishnan, C. A. Lahiff, and K. B. Reed, "Comparing Gait with Multiple Physical Asymmetries Using Consolidated Metrics," *Front. Neurorobotics*, vol. 12, p. 2, 2018.

[124] R. De Maesschalck, D. Jouan-Rimbaud, and D. L. Massart, “The mahalanobis distance,” *Chemom. Intell. Lab. Syst.*, vol. 50, no. 1, pp. 1–18, 2000.

[125] C. M. Kim and J. J. Eng, “Symmetry in vertical ground reaction force is accompanied by symmetry in temporal but not distance variables of gait in persons with stroke,” *Gait Posture*, vol. 18, no. 1, pp. 23–28, 2003.

[126] L. N. Awad, J. A. Palmer, R. T. Pohlig, S. A. Binder-Macleod, and D. S. Reisman, “Walking speed and step length asymmetry modify the energy cost of walking after stroke,” *Neurorehabil. Neural Repair*, vol. 29, no. 5, pp. 416–423, 2015.

[127] J. M. Bauman and Y. H. Chang, “Rules to limp by: joint compensation conserves limb function after peripheral nerve injury,” *Biol. Lett.*, vol. 9, no. 5, p. 20130484, 2013.

[128] S. H. Kim, S. K. Banala, E. A. Brackbill, S. K. Agrawal, V. Krishnamoorthy, and J. P. Scholz, “Robot-assisted modifications of gait in healthy individuals,” *Exp. Brain Res.*, vol. 202, no. 4, pp. 809–824, 2010.

Vita

Sung Yul Shin received the degree of Bachelor of Science in mechanical design engineering from Korea Polytechnic University, Siheung, South Korea, in 2009 and the degree of Master of Science in robotics engineering from University of Science and Technology (UST), Daejeon, Korea, in 2011. From 2011 to 2014, he was a Researcher with the Center for Bionics, Korea Institute of Science and Technology (KIST), Seoul, Korea. In Fall 2014, he entered the Mechanical Engineering graduate program at The University of Texas at Austin. From 2014 to 2019, he was employed as a graduate research assistant in Rewire Lab.

Contact Email: syshin0228@utexas.edu

This dissertation was typeset with Microsoft Word by the author.